



**Pétrogenèse et potentiel économique de la Formation d'Obatogamau, région de  
Chibougamau, Sous-province de l'Abitibi**

**par Adrien Boucher**

**Mémoire présenté à l'Université du Québec à Chicoutimi en vue de l'obtention du grade de  
Maître en Géologie et génie géologique**

Québec, Canada

## RÉSUMÉ

Les grands ensembles de basaltes présents dans les ceintures de roches vertes archéennes forment des séquences volcaniques de grande très étendue. Ces unités revêtent également une importance économique en raison de leur association commune avec des systèmes minéralisés tels que les sulfures massifs volcanogènes (SMV) et les gisements d'or orogénique. Ces ensembles sont généralement considérés comme homogènes bien que leur hétérogénéité soit peu testée. Les niveaux felsiques qu'ils peuvent contenir sont notamment peu documentés. Parmi ces ensembles de basaltes, certaines unités sont riches en mégacristaux de plagioclase et sont associées spatialement à des suites intrusives anorthositiques dans lesquels les mégacristaux se seraient formés avant l'émission des laves. Le nombre d'exemples appuyant cette hypothèse reste cependant faible et les conditions de formation des mégacristaux sont peu documentées. Outre l'hétérogénéité de ces ensembles et l'origine des mégacristaux de plagioclase, la source mantellique de ces laves est également débattue ; parfois assimilée à un manteau appauvri et parfois assimilée à un manteau plus primitif.

La présente maîtrise se penche sur la Formation d'Obatogamau située dans la région de Chibougamau au sein de la Sous-province de l'Abitibi. Cette formation correspond à un large ensemble de basaltes à mégacristaux de plagioclases en association spatiale avec plusieurs suites intrusives anorthositique. Elle a de plus, été relativement peu étudiée, avec un âge mal contraint et un potentiel économique très peu défini. L'étude visait donc à questionner ces aspects en plus de l'hétérogénéité de la séquence, de l'origine des mégacristaux et de la source mantellique des laves. Elle se base sur une étude de la chimie et de la pétrogenèse des laves après une campagne d'échantillonnage menée sur une zone restreinte où la Formation d'Obatogamau présente une bonne exposition en surface.

D'après les données de chimie roche totale, la Formation d'Obatogamau apparaît extrêmement homogène avec l'essentiel des laves correspondant à des basaltes et basaltes andésitiques riches en fer et la plupart des quelques roches plus différencierées située dans la partie supérieure de la séquence de laves. En outre, la chimie des éléments traces indique une source mantellique faiblement appauvrie pour la majorité des laves mafiques. La forte homogénéité de la séquence de laves pourrait indiquer d'importants taux d'effusions limitant les effets de différenciation magmatique ce qui semble être confirmé par les résultats de modélisation pétrogénétique obtenus à l'aide de l'algorithme MELTS. Une unité felsique, probablement volcanique, a été échantillonnée dans un but de datation U-Pb sur zircon, donnant un âge de

$2726,2 \pm 1,6$  Ma similaire aux âges connus pour la Formation de Waconichi, sus-jacente à la Formation d’Obatogamau. Il n’est cependant pas possible d’exclure totalement la possibilité que cette unité soit un filon-couche lié à la Formation de Waconichi.

L’ensemble de ces résultats suggère une mise en place rapide de la Formation d’Obatogamau, potentiellement sur une durée inférieure à quelques Ma, ce qui impliquerait un écart d’âge important avec les quelques unités sous-jacentes connues. Les observations réalisées sur le terrain indiquent un nombre limité d’épisodes de quiescence volcanique, matérialisés par des niveaux volcano-sédimentaires de faible épaisseur, cohérent avec une mise en place rapide de la séquence de lave et des taux d’effusion importants. Ceci impliquerait des conditions non favorables aux minéralisations de type SMV dans le secteur d’étude.

Les observations pétrographiques et la chimie des amphiboles indique cependant que les laves du secteur étudié présentent un faciès métamorphique situé à la transition entre les schistes verts et les amphibolites suggérant des conditions favorables pour la génération de fluides métamorphiques. Cela pourrait indiquer un contexte favorable pour les minéralisations de type orogéniques à conditions que des conduits structuraux aient pu permettre la circulation et la canalisation de tels fluides.

L’étude des mégacristaux de plagioclase a montré un fort degré de recristallisation qui n’a pas permis d’établir de lien avec les suites intrusives anorthositiques du secteur. Les données de chimie roche totale suggèrent toutefois que certaines coulées à mégacristaux de plagioclase aient pu remobiliser des cumulats d’oxydes de fer-titane, connus pour cristalliser au sein des suites intrusives anorthositiques.

## TABLE DES MATIÈRES

RÉSUMÉ.....	ii
TABLE DES MATIÈRES .....	iv
REMERCIEMENTS .....	vii
INTRODUCTION GÉNÉRALE.....	1
Introduction .....	1
Problématique générale .....	2
Constat .....	8
Problématique spécifique .....	9
Objectifs du projet .....	13
PRÉSENTATION DE L'ARTICLE .....	15
Contribution des auteurs .....	15
PÉTROGÉNÈSE ET POTENTIEL ÉCONOMIQUE DE LA FORMATION D'OBATOGAMAU, RÉGION DE CHIBOUGAMAU, SOUS-PROVINCE DE L'ABITIBI.....	18
Résumé traduit.....	18
Abstract.....	20
Introduction .....	21
Geological Setting .....	24
Abitibi Subprovince .....	24
Chibougamau Area .....	26
Fieldwork and Sampling.....	29

Methodology .....	33
Whole rock chemistry .....	33
Processing of whole rock analyses .....	34
Mineral chemistry .....	37
U-Pb geochronology .....	39
Results .....	40
Whole rock chemistry .....	40
Hydrothermal alteration .....	43
Magmatic differentiation modelling .....	44
Petrography and Thermobarometry .....	45
U-Pb geochronology .....	46
Interpretation and Discussion .....	46
Fractional crystallisation .....	47
Age and eruption rate .....	50
Magmatic sources .....	52
Economic potential .....	55
Conclusions .....	59
Acknowledgements .....	60
References .....	61
Appendix .....	79
A1 .....	79
Figures .....	82
Tables.....	101

CONCLUSION GÉNÉRALE .....	108
RÉFÉRENCES .....	115
MATÉRIEL SUPPLÉMENTAIRE.....	123

## REMERCIEMENTS

Je tiens d'abord à remercier les directeurs du projet, Lucie Mathieu et Réal Daigneault pour leur encadrement, leurs encouragements et leur patience. Je tiens également à remercier Pierre Bedeaux pour ses conseils, notamment sur le terrain, et les discussions de longue haleine que nous avons pu avoir, permettant aux réflexions menées atour du projet de mûrir jusqu'au stade actuel. J'aimerai remercier le professeur Michael Hamilton pour la préparation et l'analyse des grains de zircon ainsi que le traitement des données ayant permis l'obtention de l'âge présenté dans cette étude. Je tiens à remercier les professeurs Paul Bédard, Sarah Jane Barnes, Edward Sawyer et Michael Higgins d'avoir bien voulu répondre à mes questions lorsque je suis venu les solliciter, ainsi que les professeurs Pierre Cousineau et Bruno Lafrance d'avoir pris sur leur temps pour venir partager leur expertise et leurs interprétations sur le terrain. J'aimerai remercier Patrick Houle pour le partage de ses précieuses connaissances sur la géologie de la région de Chibougamau ainsi que l'appui logistique qu'il a pu fournir à l'équipe *Metal Earth* lors des deux étés passés sur le terrain.

J'aimerai également remercier les assistants Antoine Brochu, Mike Bellemare, Laura-Pier Perron-Desmeules, Maryse Desrochers pour leur sérieux et dévouement lors des travaux menés sur le terrain durant le premier été de terrain. J'aimerai aussi remercier les assistants Belalahy Brandy Marcel, Nesrine Mokchah, Yohannes Yacouba Degnan et Mathieu Robin pour leur travail assidu lors du second été de terrain.

Je tiens à remercier David Noël, Dany Savard, Audrey Lavoie de l'UQAC ainsi que Jonathan Tremblay, d'IOS services géoscientifiques pour leur disponibilité et leur aide lors de la préparation et de l'analyse d'échantillons. Je tiens également à remercier Carl Guillemette, Marc Choquette et Suzie Côté de l'Université Laval pour l'acquisition des cartographies chimiques  $\mu$ XRF et les réponses qu'ils ont fourni à mes questions.

Enfin, j'aimerais remercier mes camarades de maîtrise, à savoir Youssouf Ahmadou Youssoufou, Marie Kieffer, Julien Huguet, Baptiste Madon, Floriane Guillevic et Quentin Fayard pour leur soutien tout au long de ce projet et leur capacité à supporter ma prodigieuse aptitude à la râlerie.

## INTRODUCTION GÉNÉRALE

### Introduction

Le présent document vise à présenter les résultats obtenus dans le cadre d'un projet de maîtrise en sciences de la Terre mené au sein de l'Université du Québec à Chicoutimi.

Les résultats sont présentés sous la forme d'un article rédigé en anglais et soumis à une revue scientifique ; la Revue Canadienne des Sciences de la Terre. Le projet a été mené sous la direction de la Professeure Lucie Mathieu et la codirection du Professeur Réal Daigneault dans le cadre du programme de recherche *Metal Earth*, piloté par l'Université Laurentienne. Le but de ce programme de recherche est de déterminer les caractéristiques et processus clés qui ont un impact sur la distribution des métaux dans les ceintures de roches vertes archéennes qui présentent des caractéristiques géologiques similaires et des quantités de gisements très différentes.

Le projet de maîtrise s'inscrit dans l'un des quatre volets du projet *Metal Earth*, le volet recherche à l'échelle du transect, qui vise à documenter la géologie de secteurs de quelques 10-100 km<sup>2</sup> ayant également fait l'objet de levés géophysiques. Ce projet de maîtrise porte sur la Formation d'Obatogamau, une unité volumineuse constituée de laves mafiques et située dans la région de Chibougamau, Québec.

## Problématique générale

Les roches étudiées sont des roches métamorphiques et, par soucis de simplification, le préfixe « méta » est omis pour tous les types de roches archéennes mentionnés dans le texte. Plus de 50% du volume de la croûte continentale terrestre s'est formé avant la fin de l'Archéen (voir Laurent et al. 2014 et références incluses). Les cratons archéens sont principalement constitués de trois ensembles lithologiques :

- Les ceintures plutono-métamorphiques, qui sont des assemblages de roches sédimentaires et de roches intrusives qui sont principalement des intrusions de type tonalite-trondhjemite-granodiorite –TTG ;
- Les ceintures de roches vertes, qui correspondent à des roches supra-crustales (c.-à-d. roches sédimentaires et roches volcaniques) recoupées par des intrusions (de type TTG principalement) ;
- Des plutons plus riches en K que les TTG, qui sont de faible volume et qui recoupent les deux premiers ensembles et font parties des dernières étapes de formation des cratons archéens.

Les ceintures de roches vertes, telles que celles observées dans la Sous-province de l'Abitibi, Canada, sont une composante essentielle des cratons qui ont une grande importance économique. Ce sont des assemblages de roches supra-crustales qui se sont majoritairement mises en place sur le plancher océanique et qui sont dominées par des ensembles volcaniques mafiques-ultramafiques à felsiques et par des roches

sédimentaires (Dimroth et al. 1982, Condie 1989, Daigneault et al. 2002). La majorité des roches magmatiques se sont formées pendant la période synvolcanique, qui est caractérisée par la mise en place de gros volumes importants de magmas. Ces magmas forment des laves de composition mafique à felsique et d'affinité tholéïitique à claco-alcaline ainsi que des intrusions qui correspondent à des complexes sub-volcaniques (Dimroth et al. 1982, Mueller et al. 1989). La période synvolcanique est suivie par les périodes syn- et post-tectoniques, qui sont caractérisées par la mise en place de plus petits volumes de magmas d'affinité calco-alcaline à alcaline pendant et après une période de déformation et d'érosion (Moyen et al. 2003, Laurent et al. 2014). Un grand nombre d'intrusions, qui sont principalement de type TTG, est également mis en place durant la totalité de ces épisodes magmatiques (Sage et al. 1996, Laurent et al. 2014). Les ensembles volcaniques archéens sont les hôtes de nombreuses minéralisations de types sulfures massifs volcanogènes (SMV) et or orogénique formées pendant les périodes synvolcaniques et syntectoniques, respectivement.

Les roches volcaniques mafiques constituent une part importante des ceintures de roches vertes archéennes (Condie 1989). Les basaltes sous-marins peuvent former de grandes unités, qui se sont généralement mises en place sur le plancher océanique et sont observables sur plus de 100 kilomètres de distance. Certaines coulées peuvent être individualisées sur des dizaines de km (Dimroth et al. 1982). Ces basaltes sont généralement considérés comme ayant été produits par la fusion partielle d'un manteau relativement enrichi, ce qui les distingue des basaltes des rides médio-océaniques actuelles qui proviennent du manteau appauvri (Condie 2005, Bédard 2006, Herzberg et

al. 2010, Moyen et Laurent 2018). La nature de ce manteau enrichi fait l'objet de plusieurs hypothèses. Il s'agit soit : 1) d'un manteau primitif ayant subi peu d'extraction de croûte et/ou qui a été homogénéisé par une convection vigoureuse (Condie 2005, Moyen et Laurent 2018) ; ou 2) d'un manteau appauvri qui aurait été ré-enrichi par l'introduction de croûte dans le manteau par, par exemple, un processus de délamination (Wyman 1999, Bédard et al. 2006).

Plusieurs modèles sont proposés pour expliquer la formation des ceintures de roches vertes (Dimroth et al. 1982, Polat et Kerrich 2001, Thurston 2002, Windley 2017, Polat et al. 2018b). Ces modèles s'appuient, entre autres, sur notre compréhension du mode de mise en place des unités basaltiques. Les principaux modèles sont : 1) le modèle horizontal de type « tectonique des plaques » (Wyman 1999, Polat et Kerrich 2001, Daigneault et al. 2002, Polat et al. 2006) ; et 2) le modèle verticaliste de sagduction présenté sous forme d'inversion/retournement de croûte ou du manteau lithosphérique (Hamilton 1998, Bédard 2006, Bédard et al. 2013).

Les unités de basaltes forment majoritairement des plaines de lave issues d'un volcanisme fissural. Ces unités sont des empilements de coulées de laves homogènes et d'épaisseurs généralement constantes (Dimroth et al. 1982). Alternativement, ces accumulations de coulées de laves pourraient correspondre à de grands complexes volcaniques centraux interdigités entre eux (Dimroth et al. 1982, Mueller et al. 1989, Scott et al. 2002). Ces morphologies volcaniques (p.ex. présence ou absence de volcan central) restent toutefois difficiles à distinguer en raison de la faible densité

d'affleurement et de la déformation, notamment du plissement, qui affectent les ceintures de roches vertes.

La chimie des basaltes des ceintures de roches vertes est globalement caractérisée par une affinité tholéïtique et des ratios d'éléments à fort effet de champ (*high field strength elements – HFSE*) différents de ceux des laves de type N-MORB (*normal- mid-ocean ridge basalt*) qui correspondent aux basaltes post-archéens des ridges médio-océaniques (Condie 2005, Moyen et Laurent 2018). En effet, si les basaltes archéens sont majoritairement d'affinité tholéïtique (magmas pauvres en éléments alcalins, faiblement oxydés, et présentant un pic d'enrichissement en fer important lors de la différenciation), ils présentent des contenus en éléments traces indiquant qu'ils proviennent du manteau primitif. En outre, les magmas parentaux des basaltes archéens présentent des ratios Fe/Mg et des ratios Al/(Mg+Fe) plus élevés et plus faibles, respectivement, que ceux des magmas parentaux des N-MORB (Cattel et Taylor 1990, Hamilton 2007). Ils contiennent également moins de titane que les N-MORB (Hamilton 2007). Les grands épanchements de basaltes archéens sont considérés comme relativement homogènes d'un point de vue chimique et pétrologique, et l'hétérogénéité potentielle de ces séquences reste peu documentée. Ces séquences volcaniques sont constituées de coulées caractérisées par un faible ratio longueur/épaisseur qui correspondent à des faciès massifs et coussinés, qui sont les plus communs, ainsi que quelques brèches de coulées. Ces coulées présentent une vésicularité généralement faible qui pourrait indiquer une profondeur de mise en place (sous l'eau) importante (Dimroth et al. 1982, Mueller et al. 1989). D'un point de vue économique, ces épanchements

basaltiques peuvent présenter une association spatiale avec des minéralisations de type SMV et or orogénique. Les SMV sont généralement associés aux épisodes de quiescence dans le volcanisme. Ces épisodes de quiescence peuvent être matérialisés par la présence de niveaux sédimentaires épiclastiques ou de roches volcaniques felsiques intercalés entre les coulées de laves mafiques. Ces niveaux peuvent être difficiles à identifier sur le terrain en raison de leur faible épaisseur, ce qui conduit à un faible nombre d'occurrences documentées.

Une partie des grands épanchements tholéïitiques archéens est riche en mégacristaux de plagioclase. Les basaltes à mégacristaux montrent couramment une association spatiale avec de larges intrusions archéennes, généralement litées (aussi appelés intrusions litées ou suites intrusives litées), qui contiennent des niveaux anorthositiques (Phinney et al. 1988, Ashwal 2010, Ashwal et Bybee 2017). Cette association spatiale est majoritairement observée et documentée dans la Province de Supérieur et au Groenland, où se trouvent les plus grandes concentrations connues de suites intrusives litées archéennes tholéïitiques présentant des niveaux anorthositiques (Ashwal et Bybee 2017). Les mégacristaux de plagioclase observés dans les intrusions, les coulées de basalte associées et les filons-couches gabbroïques qui les accompagnent sont sub-arrondis et pseudohexagonaux (Phinney et al. 1988, Ashwal et Bybee 2017). Leurs tailles varient de 0.5 à 30 cm. Ils présentent une composition très calcique proche du pôle anorthite ( $An_{80}$  en moyenne) et ont une composition chimique relativement uniforme avec une bordure (jusqu'à 200  $\mu\text{m}$  d'épaisseur) généralement plus sodique ( $An_{60-70}$  en moyenne) que le cœur du minéral, et ceci est comparable à la composition

des phénocristaux de plagioclase tabulaires observés dans la matrice des coulées de lave (Phinney et al. 1988). Cette différence de composition entre cœur et bordure indiquerait un déséquilibre de composition entre les plagioclases contenus dans la matrice des laves et les mégacristaux de plagioclase, qui se seraient formés en profondeur puis auraient développé une surcroissance en équilibre chimique avec leur matrice pendant le refroidissement de la coulée de lave.

D'une manière générale, l'association spatiale entre les suites intrusives litées à niveaux anorthositiques et les laves et dykes mafiques d'affinité tholéitique qui contiennent des mégacristaux de plagioclase, combinée aux similitudes chimiques observées entre les mégacristaux des coulées de lave et les suites intrusives à niveaux anorthositiques, permet de proposer un lien génétique entre ces différents types de roches magmatiques (Phinney et al. 1988, Ashwal 2010, Ashwal et Bybee 2017, Polat et al. 2018). Phinney et collaborateurs (1988), Phinney et Morrison (1990), Polat et collaborateurs (2009) et Polat et collaborateurs (2018) proposent tous une mise en place à faible profondeur des suites intrusives archéennes anorthositiques, et une partie de ces suites intrusives pourrait donc correspondre à des chambres magmatiques de sub-surface qui auraient alimenté des éruptions (c.-à-d. des complexes sub-volcaniques). Les mégacristaux de plagioclase sont souvent interprétés comme flottant dans la partie supérieure de la chambre en raison de leur densité plus faible que celle du magma mafique (Warren 1990, Namur et al. 2011, Ashwal et Bybee 2017), ce qui facilite leur mobilisation lors des éruptions volcaniques. Aussi, les mégacristaux se seraient formés par refroidissement lent à des températures proches du liquidus et auraient effectué leur

croissance en interagissant avec des magmas plus mafiques injectés dans la chambre ou des magmas provenant des niveaux profonds d'une chambre animée de mouvements de convection (Polat et al. 2018). Les conditions de formation des mégacristaux restent toutefois peu documentées, ce qui ne permet pas de préciser le lien entre chambre et coulées, ni de comprendre l'architecture volcanique associée.

## Constat

Les grands épanchements de basaltes tholéïtiques à mégacristaux de plagioclase observés dans les ceintures de roches vertes archéennes sont peu documentés et leur potentiel économique est méconnu. En effet, les points suivants demandent à être éclaircis :

- Ces basaltes présentent une homogénéité apparente qui demande à être confirmée par des études géochimiques détaillées. Les fins niveaux de roches felsiques intercalés entre les coulées sont également peu documentés et leur origine est mal comprise ;
- Les conditions de formation des mégacristaux de plagioclase observés dans les basaltes ainsi que leur origine (leur chambre source) restent mal contraintes ;
- Les caractéristiques de la source mantellique de ces basaltes, et notamment le caractère primitif ou ré-enrichi de cette source, sont encore débattues, ce qui complique l'étude des processus géodynamiques archéens ;

- Le niveau de connaissance du potentiel économique que présentent ces formations pour les minéralisations de type SMV dépend directement de la compréhension de leur stratigraphie et de leur association avec des sources de chaleur (intrusions magmatiques).

## Problématique spécifique

La ceinture de roches vertes de l’Abitibi est la plus grande ceinture de roches vertes archéennes au monde (Card 1990). Cela en fait un lieu idéal pour étudier la formation des ceintures de roches vertes, dont les coulées de basaltes sont l’un des principaux constituants (Wyman 1999).

Les coulées de lave de la Formation d’Obatogamau occupent une superficie importante dans la région de Chibougamau-Chapais. Elles sont reconnues depuis le front de la Province de Grenville à l’est et s’étendent sur plus de 100 km vers l’Ouest jusque dans le secteur de Desmaraisville (Allard et Gobeil 1984, Mueller et al. 1989). La grande étendue spatiale de cette formation et la facilité d’accès en font une cible idéale pour documenter les ensembles de basaltes archéens contenant des mégacristaux de plagioclase. L’épaisseur totale de la Formation d’Obatogamau est d’environ 3-4 km selon Leclerc et al. (2008) mais varie de façon importante en carte. La Formation d’Obatogamau est constituée de basaltes massifs et coussinés, ainsi que de filons-

couches gabbroïques co-magmatiques qui représenteraient moins de 10% du volume de la séquence (Cimon 1977). La formation comprend également de fins niveaux de roches volcanoclastiques et de laves de composition andésitique (Leclerc et al. 2017) à rhyolitique (Cimon 1977). La partie mafique de la Formation d'Obatogamau comprend, dans le secteur cartographié par Cimon (1977), trois membres informels définis sur la base des proportions de mégacristaux de plagioclase. Les membres inférieur et supérieur contiennent peu de mégacristaux de plagioclase, respectivement moins de 3% et moins de 1%. Le membre intermédiaire, quant à lui, peut contenir jusqu'à 15% de mégacristaux. La Formation d'Obatogamau est également connue pour être spatialement associée avec plusieurs intrusions litées à niveaux anorthositiques comme, par exemple, la Suite Intrusive du Lac Doré et celle de la Rivière Opawica, qui ont été proposés comme étant génétiquement liés aux coulées de lave et comme étant la source des mégacristaux de plagioclase (Allard 1976, Midra 1989, Bédard et al. 2009, Polat et al. 2017).

Le Groupe de Roy, dont la stratigraphie a été récemment révisée, comprend la majeure partie de l'assemblage volcanique de la région de Chibougamau (Leclerc et al. 2011, Leclerc et al. 2017 et références incluses). Il est constitué de deux cycles volcaniques qui comprennent deux formations chacun. Avant révision, ces formations étaient, de la base au sommet, les formations d'Obatogamau et de Waconichi pour le cycle volcanique 1, ainsi que la Formation de Gilman et la Formation de Blondeau pour le cycle volcanique 2. Les formations d'Obatogamau et de Gilman présentent des compositions majoritairement mafiques. Les formations de Waconichi et de Blondeau,

quant à elles, passent de compositions mafiques à felsiques depuis leur base vers leur sommet. Lors de leur révision de la stratigraphie du Groupe de Roy, Leclerc et collaborateurs (2008, 2011) ont corrélé la base de la Formation de Gilman (ancienne base du cycle 2), le Membre de David, avec le sommet de la Formation d'Obatogamau sur la base de considérations géochimiques et géochronologiques. En outre, ces auteurs proposent de renommer le sommet de la Formation de Gilman sous le nom de Formation de Bruneau (nouvelle base du cycle 2). La nouvelle stratigraphie comprend donc le cycle volcanique 1, constitué des formations d'Obatogamau et de Waconichi, et le cycle volcanique 2, constitué des formations de Bruneau, de Blondeau et de Bordeleau (Leclerc et al. 2017).

La Formation d'Obatogamau n'a pas été datée directement. Elle est plus ancienne que la Formation de Waconichi datée à 2726-2730 Ma (Mortensen 1993, Leclerc et al. 2011, David et al. 2012). La Formation d'Obatogamau est plus récente que la Formation andésitique de Chrissie, qui précède le Groupe de Roy et pour laquelle un âge de  $2791,4 \pm 3,7$  Ma a été obtenu (Charbonneau et al. 1991, David et al. 2011), et que la Formation rhyodacitique des Vents, considérée initialement comme faisant partie de la Formation d'Obatogamau (Potvin 1991) mais maintenant considérée comme prédatant le Groupe de Roy (Leclerc et al. 2017). La Formation des Vents avait été datée initialement par Mortensen (1993) qui lui attribuait un âge de  $2759 \pm 1,6$  Ma (les âges obtenus les plus anciens sont de  $2805 \pm 1,4$  Ma, mais la majorité des zircons ont été considérés comme des xénocristaux par l'auteur), puis a de nouveau été datée à  $2798,7 \pm 0,7$  Ma par Davis et collaborateurs (2014). Cet âge est de  $> 60$  Ma plus ancien que celui

de la Formation de Waconichi. Ainsi, la période de mise en place de la Formation d'Obatogmau est mal contrainte et s'est produite après ~2.76 Ga et avant ~2.73 Ga.

L'architecture volcanique de la Formation d'Obatogamau est peu documentée et deux modèles viennent expliquer la formation de la plaine de lave : Picard et Piboule (1986) proposent une mise en place par le biais d'une grande fissure alimentant le volcanisme, tandis que Mueller et collaborateurs (1989), quant à eux, proposent que cette formation corresponde à des volcans boucliers à faible relief, sur la base des variations latérales des faciès volcaniques (laves massives, coussinées, brèches de coulées) observées sur le terrain.

La source des magmas des coulées de lave de la Formation d'Obatogamau est rapprochée par Picard et Piboule (1986) d'une source mantellique appauvrie (de type N-MORB) qui présenterait toutefois quelques similitudes avec les E-MORB (*enriched – mid-ocean ridge basalt*), qui correspondent aux basaltes de plateaux ou « points chauds » actuels. Les laves mafiques de la Formation d'Obatogamau sont décrites comme majoritairement basaltiques et ayant une affinité tholéïitique (Ludden et al. 1984, Leclerc et al. 2011). Les laves coussinées les plus évoluées sont des andésites (Ludden et al. 1984). Cependant, le contexte de formation et la chimie des unités felsiques répertoriées par Cimon (1977) au sein de la séquence ne sont pas documentées.

D'un point de vue économique, des niveaux minéralisés en sulfures semi-massifs à massifs ont été décrits dans la Formation d'Obatogamau par Cimon (1977). De

nombreux indices d'or orogénique ont également été répertoriés par Dion et Simard (1999). Cependant, le potentiel de la Formation d'Obatogamau pour les minéralisations de type SMV n'a jamais été évalué et peu de travaux se sont penchés sur le potentiel de la formation d'Obatogamau pour les minéralisations orogéniques.

## Objectifs du projet

Afin de répondre aux objectifs du projet, il est nécessaire de raffiner la compréhension de la Formation d'Obatogamau. Par conséquent, cinq objectifs ont été retenus sur la base des questions en suspens :

- Objectif 1 : déterminer les signatures géochimiques et pétrologiques de la Formation d'Obatogamau et documenter les variations spatiales de ces signatures si elles sont présentes afin de mieux appréhender le système magmatique associé ;
- Objectif 2 : obtenir une meilleure caractérisation de la source mantellique des coulées de lave de la Formation d'Obatogamau ;
- Objectif 3 : documenter au mieux les conditions de formation des mégacristaux de plagioclase observés dans les coulées de lave et tenter de déterminer s'il existe un lien génétique entre la Formation d'Obatogamau (ou une partie de la Formation) et l'une des suites intrusives litées anorthositiques du secteur étudié ;

- Objectif 4 : réaliser des datations U-Pb sur les niveaux volcaniques felsiques observés dans le but de mieux contraindre la ou les périodes de mise en place de la Formation d'Obatogamau ;
- Objectif 5 : évaluer, pour le secteur d'étude sélectionné, le potentiel économique de la Formation d'Obatogamau pour les minéralisations de type SMV en lien avec l'environnement volcanique observé et amener, dans la mesure du possible, des éléments pouvant indiquer si un contexte favorable pour les minéralisations de type or orogénique est présent.

## PRÉSENTATION DE L'ARTICLE

**Titre anglais du manuscrit :** Petrogenesis and economic potential of the Obatogamau Formation, Chibougamau area, Abitibi Subprovince.

**Journal :** Revue Canadienne des Sciences de la Terre.

**Statut :** soumis, en révision.

**Auteurs :** Adrien Boucher<sup>1</sup>, Lucie Mathieu<sup>1</sup>, Michael Hamilton<sup>2</sup>, Pierre Bedeaux<sup>1</sup> et Réal Daigneault<sup>1</sup>

<sup>1</sup>Centre d'Études sur les Ressources Minérales, Département des Sciences Appliquées, Université du Québec à Chicoutimi, Chicoutimi, Québec G7H 2B1.

<sup>2</sup>Jack Satterly Geochronology Laboratory, Department of Earth Sciences, University of Toronto, 22 Russell St., Toronto, ON, Canada M5S 3B1

## Contribution des auteurs

Premier auteur : Adrien Boucher

- Échantillonnage

- Cartographie et descriptions de terrain.
- Traitement et interprétation des données (hors géochronologie), observations pétrographiques, analyses MEB.
- Rédaction de l'article et du mémoire.

Second auteur : Lucie Mathieu

- Direction du projet.
- Aide à l'interprétation générale des données.
- Aide à la rédaction et correction du manuscrit.

Troisième auteur : Michael Hamilton

- Séparation, tri et préparation des grains de zircon utilisés pour les analyses géochronologiques.
- Analyses des grains et interprétation préliminaire des données.
- Correction du manuscrit, rédaction de l'annexe portant sur le détail de la méthodologie employée pour les analyses géochronologiques.

Quatrième auteur : Pierre Bedeaux

- Aide à l'interprétation des données de terrain.
- Aide à l'interprétation des données acquises sur amphibole et chlorite.
- Correction du manuscrit.

Cinquième auteur : Réal Daigneault

- Codirection du projet.
- Correction du manuscrit.

# PÉTROGENÈSE ET POTENTIEL ÉCONOMIQUE DE LA FORMATION D'OBATOGAMAU, RÉGION DE CHIBOUGAMAU, SOUS-PROVINCE DE L'ABITIBI

**Mots clés :** Ceinture de roches vertes, Sous-province de l'Abitibi, Stratigraphie, Géochimie des plaines de lave, Volcanologie, Géochronologie, Potentiel économique, Sulfures massifs volcanogènes (SMV).

## Résumé traduit

Les empilements de laves mafiques sont des constituants essentiels des ceintures de roches vertes archéennes. Elles présentent un intérêt économique en raison des quantités importantes de minéralisation d'or et de métaux de bases qu'elles contiennent principalement sous forme de systèmes synvolcaniques de sulfures massifs volcanogènes (SMV) et de systèmes syntectoniques d'or orogénique. Déchiffrer la pétrogénèse de ces unités mafiques est également essentiel pour notre compréhension de l'évolution géodynamique précoce des ceintures de roches vertes. Cette étude se focalise sur la pétrogénèse et le potentiel économique d'un des plus anciens et des plus épais empilements de coulées de laves mafiques observés dans la Sous-province néoarchéenne de l'Abitibi, c.-à-d. la Formation d'Obatogamau, située dans la région de Chibougamau,

Canada. La Formation d'Obatogamau, non datée, s'étend sur plus de 100 km en direction E-O et est principalement constituée de basaltes et basaltes andésitiques, avec ou sans mégacristaux de feldspath. À l'aide de datations U-Pb sur zircon, cette étude tente de fournir un premier âge direct pour la Formation d'Obatogamau ( $2726,2 \pm 1,6$  Ma), qui est similaire à l'âge des unités sus-jacentes. Les données de chimie roche-totale montrent que la chimie des roches mafiques tholéïtiques riches en fer est fortement homogène. En outre, les résultats de modélisation pétrogénétique qui suggèrent des effets limités de différenciation. L'ensemble de ces résultats permet de proposer que la Formation d'Obatogamau se soit mise en place rapidement, potentiellement en quelques Ma, et impliquerait un écart d'âge important avec les unités volcaniques plus anciennes sous-jacentes. D'importants taux d'effusion sont cohérents avec de courts épisodes de quiescence volcanique déduits des observations de terrain, ce qui suggère des conditions non optimales pour les systèmes SMV. La pression et la température du pic de métamorphisme déduit de la chimie des amphiboles, cependant, suggèrent des conditions favorables pour la génération de fluides métamorphiques et la zone d'étude pourrait être prospective pour les minéralisations de type or orogénique à condition que des conduits structuraux aient permis la canalisation de tels fluides.

## Petrogenesis and economic potential of the Obatogamau Formation, Chibougamau area, Abitibi Subprovince

**Keywords:** Greenstone belt, Abitibi Subprovince, Stratigraphy, Lava plain geochemistry, Volcanology, Geochronology, Economic potential, Volcanogenic massive sulphides (VMS).

### Abstract

Mafic lava flow piles are essential components of Archean greenstone belts. They present an economic significance as they host significant amount of gold and base metals mineralisation, mostly as synvolcanic volcanogenic massive sulphides systems (VMS) and syntectonic orogenic gold systems. Understanding the petrogenesis of these mafic units is also essential to our comprehending of the early geodynamic evolution of greenstone belts. This study focuses on the petrogenesis and economic potential of one of the oldest and thickest pile of mafic lava flows observed in the Neoarchean Abitibi Subprovince, i.e., the Obatogamau Formation, Chibougamau area, Canada. The undated Obatogamau Formation extends over more than 100 km in the E-W direction and is mostly made of basalts and basaltic andesites, with or without feldspar megacrysts. Using zircon U-Pb dating, this study attempts to provide a first direct age for the Obatogamau Formation ( $2726.2 \pm 1.6$  Ma), which is similar to the age of the overlaying

unit. Whole rock chemistry data shows that the chemistry of the Fe-rich tholeiitic mafic rocks is highly homogeneous. Besides, petrogenetic modelling points to limited effects of differentiation. All these results allow us to propose that the Obatogamau Formation emplaced rapidly, possibly within a few Ma, and imply a significant age gap between the Obatogamau Formation and the underlaying older volcanic units. High effusion rates are consistent with the short episodes of volcanic quiescence deduced from field observations, thus pointing to non-optimal conditions for VMS systems. The pressure and temperature of peak metamorphism deduced from amphibole chemistry, however, point to favorable conditions for the release of metamorphic fluids in the study area which may be prospective for orogenic gold mineralisation provided that structural conduits allowed for the channeling of such fluids.

## Introduction

Precambrian mafic lava flow units host a large amount of gold and base metals mineralisation. In addition, basalts are major constituents of greenstone belts and are thus essential to unravel the early evolution of the Archean crust. These mafic flows correspond to mantle-derived melts that formed oceanic crusts and/or plateaus, which evolved into cratons through debated geodynamic processes, e.g., subduction, sagduction and subcretion (Herzberg and Rudnick 2012, Mints 2017, Bédard 2018, Moyen and Laurent 2018). Understanding the petrogenesis and stratigraphy of Archean

mafic lava flows and related mineralisation is essential to unravel the evolution and economic potential of greenstone belts. Basalts can also be used to gain insights into the chemistry of the Precambrian mantle and to shed light on the debated geodynamic processes that lead to melt extraction in the early Earth (Wyman 1999, Polat and Kerrich 2001, Condie 2005, Gibson et al. 2007, Kerrich et al. 2008, Thurston et al. 2008, Condie et al. 2016).

The most voluminous mafic units are lava plains that likely result from fissure volcanism (Dimroth et al. 1982, Picard and Piboule 1986, Mueller et al. 1989, Scott et al. 2002). These are generally viewed as monotonous successions of tholeiitic lava flows formed by sustained eruption and as the result of, for example, plume-related magmatism (Rey et al. 2003, Gerya et al. 2015). However, detailed studies, such as those carried on the Kinojévis Group in the southern Abitibi greenstone belt, have revealed more complex depositional histories and prolonged episodes of volcanic quiescence between older assemblages and overlaying flows (Ayer et al. 2002, Thurston et al. 2008). Such stratigraphic investigation has important implication for our understanding of the origin of greenstone belts, but also has economic applications, as prolonged episodes of volcanic quiescence are favorable to volcanogenic massive sulphides (VMS) mineralising processes.

The Abitibi Subprovince is one of the largest and best preserved greenstone belt in the world and is host to numerous gold and base metal deposits (Card 1990), making it ideal to investigate the origin and metal endowment of Neoarchean supracrustal units.

Within the northeastern corner of the belt, the Obatogamau Formation is an extensive pile of mafic flows that is exposed with varying thickness in the Chibougamau area. This undated formation lies within a 30-60 Ma age gap between rocks that are amongst the oldest (2759-2798 Ma) in the Abitibi Subprovince and the 2726-2730 Ma overlaying intermediate to felsic rocks-dominated Waconichi Formation (Mortensen 1993, Legault 2003, Thurston et al. 2008, David et al. 2011, 2012, Leclerc et al. 2011, 2017, Davis et al. 2014). The defining characteristic of the Obatogamau Formation is the presence of feldspar megacrysts in part of the mafic flows. This formation has been the subject of limited scientific investigation and exploration efforts with respect to its size (Cimon 1977, Allard and Gobeil 1984, Ludden et al. 1984, Picard and Piboule 1986, Daigneault and Allard 1990, Leclerc et al. 2011, 2017, Polat et al. 2018b). Indeed, the distribution of feldspar megacrysts, the chemistry of the sequence, the real thickness of the pile, and the occurrence of potentially prolonged episodes of volcanic quiescence are poorly documented, which hinder evaluation of its potential for VMS or orogenic gold mineralisation.

This study focuses on the mafic lava flow sequence of the Obatogamau Formation, as exposed in the Chibougamau area, in order to comment on the source, magmatic evolution and economic potential of one of the oldest part of the Abitibi greenstone belt. This study employs a combination of field observations, whole rock chemistry, petrogenetic modelling, and mineral chemistry to assess the origin of the lava pile and the potential distribution of synvolcanic (VMS) and post-volcanic (orogenic gold) hydrothermal systems. Metamorphic conditions in conjunction with fault systems

are critical for orogenic gold style of mineralisation (Phillips and Powell 2010). Therefore, this study uses mineral chemistry, besides to field work, in order to constrain the metamorphic grade in the study area. One should note, however, that this study was conducted on a small portion of the Obatogamau Formation. Therefore, the economic considerations presented here may not be projectable to the whole formation.

## Geological Setting

### Abitibi Subprovince

The study area is located in the northeastern corner of the Neoarchean Abitibi Subprovince, Superior Province, Canada. Bedrock exposures comprise voluminous mafic to felsic volcanic rocks, topped and interbedded with sedimentary rocks, and that are intruded by intermediate to felsic batholiths, smaller multiphase plutons and small-volume intrusions (plugs). The main period of magmatic activity is referred to as the synvolcanic period, during which most of the volcanic rocks, deep water sedimentary rocks, as well as the subvolcanic intrusive complexes and deeper intrusions of the tonalite-trondhjemite-granodiorite (TTG) suite, formed (Dimroth et al. 1982, Mueller and Donaldson 1992, Sage et al. 1996, Chown et al. 2002, Laurent et al. 2014). The synvolcanic period is followed by the syn- and post-tectonic periods, which are characterized by erosion, sedimentation, deformation and alkaline magmatism (Mueller

and Donaldson 1992, Chown et al. 2002, Moyen et al. 2003, Beakhouse et al. 2011, Laurent et al. 2014).

The Abitibi greenstone belt was divided into northern and southern volcanic zones based on stratigraphy and location of major structures such as the Cadillac-Larder Lake and Destor-Porcupine Manneville fault zones (Ludden et al. 1986, Chown et al. 1992). These northern and southern zones display contrasting styles of ultramafic to mafic magmatism. For example, both zones are made of thick mafic volcanic successions, whereas komatiites are most abundant in the southern zone (Dimroth et al. 1982, Daigneault et al. 2004), and uncommon in the northern zone, e.g., Chibougamau area. In this area, only large volume of intrusive bodies such as the three differentiated sills of the Cummings Intrusive Suite (total thickness of 1.2 - 2.5 km), which extend over 160 km in the E-W direction (Duquette 1976, Mortensen 1993, Bédard et al. 2009), display ultramafic rocks (cumulates) at their base. In addition, large anorthosite-bearing synvolcanic layered intrusions, such as the Bell River Intrusive Suite and the Lac Doré Intrusive Suite (LDIS), are only observed in the northern zone (Dimroth et al. 1982, Ludden et al. 1986, Chown et al. 1992, Maier et al. 1996, Daigneault et al. 2004, Bédard et al. 2009). In addition, most volcanic rocks and synvolcanic plutons in the northern zone formed at 2735-2705 Ma, before their counterparts of the southern zone, formed at 2715-2697 Ma (Ludden et al. 1986, Chown et al. 1992, Daigneault et al. 2004, Thurston et al. 2008).

The Abitibi Subprovince is renowned for its numerous gold deposits, which are mostly observed in the southern zone along major faults, such as the Cadillac-Larder Lake and the Destor-Porcupine Manneville fault zones (Daigneault et al. 2002, Bateman et al. 2008). Most gold deposits are orogenic gold mineralisation formed during the syntectonic period, such as the Lamaque-Sigma deposit (Taner and Trudel 1991).

The belt also hosts many volcanogenic massive sulphides (VMS) deposits, which can be gold-rich, such as the Lemoine deposit in the Chibougamau area (Mercier-Langevin et al. 2014). These VMS form clusters around paleo-heat sources (i.e., sub-volcanic intrusive complexes), such as the Flavrian Pluton in the southern part of the belt and the Bell River Intrusive Suite (Matagami mining camp) in the northern zone (Hannington et al. 2003, Ross et al. 2014). Thus, and contrarily to orogenic gold deposits, VMS systems are abundant in both the southern and northern zones.

### **Chibougamau Area**

The supracrustal rocks of the Chibougamau area (Fig. 1) were deformed (large-scale folds and faults) and metamorphosed (greenschist to amphibolite facies) during the Kenoran orogeny (Daigneault et al. 1990), but the prefix ‘meta’ is omitted in this manuscript. The youngest units are exposed in the core of E-W-trending synclines, while the cores of anticlines are occupied by large-volume intrusive bodies, such as TTG suites and anorthosite-bearing layered intrusions (Daigneault et al. 1990). In addition, some of the oldest volcanic rocks of the Abitibi Subprovince are preserved along the margin of

batholiths (Thurston et al. 2008). In the Chibougamau area, these older units include the  $2791.4 \pm 3.7$  Ma andesite-dominated Chrissie Formation (Charbonneau et al. 1991, David et al. 2011) and the  $2798.7 \pm 0.7$  Ma Des Vents Formation (Davis et al. 2014, Leclerc et al. 2017). Early interpretations described the Des Vents Formation as a felsic member interbedded with the mafic lavas of the Obatogamau Formation (Mueller et al. 1989, Potvin 1991), which has a crystallisation age of  $2759.0 \pm 1.6$  Ma and contains up to 2805 Ma old inherited zircon grains (Mortensen 1993). The Chrissie and Des Vents formations are topped by the Roy and Opémisca groups that are dominated by volcanic and sedimentary rocks, respectively. In the study area (Fig. 1), these volcanic units are wrapped around the Eau Jaune Complex and the Lapparent Intrusive Suite.

The Roy Group is made of two mafic to felsic volcanic cycles (Allard 1976, Daigneault and Allard 1990, Leclerc et al. 2011, 2017). Volcanic cycle 1 consists of the undated mafic to intermediate lava flows pile of the Obatogamau Formation, topped by the 2730-2726 Ma, mafic to felsic lava flows and volcanoclastic units of the Waconichi Formation (Mortensen 1993, Legault 2003, Leclerc et al. 2011, David et al. 2012). The Waconichi Formation is the main VMS-bearing unit of the Chibougamau area, e.g., the Lemoine deposit (Mercier-Langevin et al. 2014). Volcanic cycle 2 is made of mafic to intermediate lava flows ( $2724.4 \pm 1.2$  Ma Bruneau Formation; Davis et al. 2014), sedimentary and volcanoclastic units ( $< 2721 \pm 3$  Ma Blondeau Formation; Leclerc et al. 2012), felsic volcanic and volcanoclastic rocks (Scorpio Formation; Charbonneau et al. 1991), and volcano-sedimentary rocks (Bordeleau Formation). The Roy Group is unconformably overlain by the ca  $< 2700$  Ma sedimentary rocks of the Opémisca Group

(Picard and Piboule 1986, Daigneault and Allard 1990, David et al. 2007, Leclerc et al. 2011, 2012, 2017).

The Obatogamau Formation, on which this study focuses, is a thick (generally 3-4 km, locally thicker) volcanic unit of volcanic cycle 1. It is essentially made of mafic to intermediate lava flows and co-magmatic gabbro sills, which may contain cm-long feldspar megacrysts. This formation is recognized over 150 km in the E-W direction and has been considered either as a lava plain or as a cluster of low relief shield volcanoes (Cimon 1977, Allard and Gobeil 1984, Mueller et al. 1989, Daigneault and Allard 1990, Charbonneau et al. 1991). Three members were identified in the stratotype section, which is located east of the Muscocho Syncline (Fig. 2a), on the basis of their megacrysts contents (Cimon 1977, Leclerc et al. 2017). The lower, intermediate and upper members contain 1-3%, 20% and < 1% of feldspar megacrysts, respectively. The mafic flows are locally interbedded with intermediate to felsic units (Cimon 1977, Leclerc et al. 2017). In addition, the upper part of the Obatogamau Formation is interbedded with the Waconichi Formation (Daigneault and Allard 1990, Leclerc et al. 2011, 2017), pointing to coeval magmatic systems and/or to chemically stratified magma chambers. The rocks of the Obatogamau Formation have basaltic-andesitic compositions and tholeiitic affinities (Ludden et al. 1984, Picard and Piboule 1986, Leclerc et al. 2011, 2017). The mantle source of these units is slightly depleted and has been compared to the sources of both normal- and enriched-mid ocean ridge basalt (N- and E-MORB), as well as basalts related to hot spots and back-arc basins (Ludden et al. 1984, Picard and Piboule 1986, Polat et al. 2018a). The rocks of volcanic cycle 1 are contemporaneous of

the  $2728.3 \pm 1.2$  Ma LDIS, a layered intrusion emplaced in the Obatogamau (David Member) and Waconichi formations (Allard 1976, Daigneault and Allard 1990, Mortensen 1993, Leclerc et al. 2011, Arguin et al. 2018).

The most voluminous part of the LDIS is made up of anorthositic gabbro cumulates (Allard 1976, Daigneault and Allard 1990). The main mineral observed in these rocks is a cm-long calcic plagioclase generally pseudomorphed by the greenschists facies in an assemblage of epidote+albite±white mica. Two other layered anorthosite-bearing intrusions are known in the study area, i.e., the Rivière Opawica Intrusive Suite and the Lac de la Chaleur Intrusive Suite (Durocher 1979, Midra 1989, Daigneault and Allard 1990). Both the LDIS and the Rivière Opawica Intrusive Suite have been interpreted as comagmatic with the Obatogamau Formation (Midra 1989, Polat et al. 2018a).

## Fieldwork and Sampling

The main study area is located along a SW-NE profile, west of the Muscocho Syncline (Fig. 2a), where the Obatogamau Formation is exposed from its stratigraphic base to top and where road access is available. There, the Obatogamau Formation is in contact with the Waconichi and Chrissie formations to the N and SW, respectively, and has an apparent thickness of 7 km. Whether this is representative of stratigraphic thickness

related to the proximity to an emission center or sequence duplication by fault systems could not be demonstrated clearly. Indeed, no major faults were observed on the field, but these could have been missed due to outcrops scarcity. The studied volcanic units have been deformed and metamorphosed to the conditions of the greenschist facies during regional N-S shortening prior to craton stabilisation (Kenoran orogeny; Daigneault et al. 1990). The bedding and the main foliation planes tend to wrap around the Eau Jaune Complex (Fig. 1 and 2a). These structures dip steeply and are oriented NW-SE in the main study area, and the younging direction is to the NE (Daigneault et al. 1990).

The main study area contains rocks of the Obatogamau and Chrissie formations according to recent interpretations (SIGÉOM 2019). However, in the field, half of the visited outcrops mapped as the Chrissie Formation correspond to megacrysts-bearing mafic flows (Fig. 2). Hence, as the occurrence of feldspar megacryst is the defining characteristic of the Obatogamau Formation, we consider these rocks as part of the Obatogamau Formation and question the extend of the Chrissie Formation as interpreted by the Ministère de l'Énergie et des Ressources Naturelles du Québec (MERN). Modifying this map would, however, require dedicated mapping that is beyond the scope of this paper.

Outcrop distribution is uneven along the studied profile, with outcrop scarcity near the stratigraphic top of the sequence. The main lithologies observed in the field are pillowed (most abundant) to massive, aphyric or megacrysts-bearing, mafic lava flows,

and some occasional intrusive facies (gabbro sills). The observed distribution of feldspar megacrysts in the sequence (Fig. 2b; supplemental material S1-2) is akin to what has been described for the stratotype section described by Cimon (1977). Indeed, the flows outcropping in the central part of the studied profile contain up to 15% megacrysts (30% observed on one occasion) and the flows near the base and top of the profile contain < 5% megacrysts and 0% (aphyric) megacrysts, respectively.

Some outcrops display thin (15 cm to a few meters thick) sedimentary horizons interbedded with mafic lava flows and that may indicate of episodes of volcanic quiescence (Fig. 3 and 4a). Their abundance may have been underestimated because of outcrop scarcity. These sedimentary horizons are made of mudstone, that may contain significant amounts of graphite, and chert horizons. In addition, markers of weak hydrothermal alteration (sericitization and silicification) are ubiquitous in the mafic flows in the area, with locally stronger alteration near the occurrence of detrital and chemical horizons. Low concentrations of sulphides (pyrrhotite and/or pyrite ± chalcopyrite-sphalerite-galena) are ubiquitous in the sediments and flows alike. In the latter, they tend to form small pockets that are commonly observed rimming pillows along with quartz accumulations. This synvolcanic alteration is overprinted by quartz-carbonate veinlets and veins related to hydrothermal systems coeval with the main deformation event (syn- to late- tectonic periods).

East of the studied traverse (outcrop n°57, Fig. 2a and 4b), a felsic unit interbedded with mafic flows (Fig. 3 and 4b) was sampled for geochronological

investigation. This unit is completely aphanitic and appears highly siliceous, displaying a chert-like texture. It is transposed in a shear zone, along with mafic lava flows. Locally high concentrations of vesicles in the mafic flows highlight the volcanic bedding before deformation and point to a probable stratigraphic concordance of the felsic with the mafic flows with folding of the volcanic bedding (Fig. 4b). The texture and concordance of this unit lead us to think that this unit is volcanic and to designate it as such. However, there is no evidence allowing us to completely rule out the possible intrusive nature of this unit.

This felsic unit is located a few km below the stratigraphic top of the Obatogamau Formation (Fig. 2), and could therefore be located at a mid-section level in the lava flows pile. The mafic flows in contact with the felsic unit are megacrysts-bearing. Similar flows are abundant in the intermediate part of the Obatogamau Formation but relatively rare otherwise, especially in the upper part of the pile (Fig. 2b and 4b). This tends to corroborate the mid-section location of this felsic unit.

Other samples were collected along the main profile (for the most part) for whole rock and petrographic analyses. Forty-five samples were collected in the megacrysts-bearing ( $n=19$ ) and aphyric ( $n=18$ ) mafic flows, coarse-grained mafic rocks ( $n=6$ ) and felsic volcanic unit ( $n=2$ , correspond to the unit sampled for geochronological investigation). Whether the coarse-grained mafic rocks correspond to the core of thick lava flows or gabbro sills could not always be determined due to limited exposure. Some megacrysts-bearing mafic flows contain  $< 1\%$  megacrysts and may have been mistaken

for aphyric mafic flows. The mining company IAMGOLD Corp. provided one additional sample of megacrysts-bearing mafic flow, from a drill core located SE of the Eau Jaune Complex. Sample coordinates are provided in the electronic supplemental material S1-1, S1-2 S4-1, and S4-2.

## Methodology

### Whole rock chemistry

Forty-three samples were prepared for whole rock analysis (supplement material S1-1). Three duplicates, as well as the LK-NIP-1 and ORCA-1 reference materials from Geoscience Laboratories (Geo Labs, Ontario Geological Survey), were analysed to assess analytical reproducibility. Feldspar megacrysts were removed from 11 of the 19 megacrysts-bearing mafic flow samples in order to evaluate how feldspar megacrysts impact on whole rock chemistry. For the same purpose, sample n°151A1, a megacrysts-bearing mafic flow containing about 30% megacrysts, was duplicated as follows: sample n°151A1a is the unmodified rock, while megacrysts have been removed from sample n°151A1b prior to whole rock analysis.

The samples, duplicates and reference materials were analysed by ALS Laboratory Vancouver facility. After lithium borate fusion and aqua regia dissolution,

the samples were subjected to whole rock analysis using an induced coupled plasma (ICP) atomic emission spectrometer (ICP-AES) for major elements, and an ICP mass spectrometer (ICP-MS) for trace elements. Base metals and Ag were analysed using ICP-AES following four-acids digestion. Chlorine and F were analysed by ion chromatography after KOH fusion. Loss on ignition (LOI) was measured after heating at 1000°C. Carbon and S were analysed by combustion using a Leco furnace. Structural water ( $\text{H}_2\text{O}^+$ ) was analysed using a Leco furnace and an infrared spectrometer. Detection limits are 0.002-0.01 wt% for major elements, C, S and  $\text{H}_2\text{O}^+$ , 0.005-10 ppm for trace elements, base metals and Ag as well as 50 and 20 ppm for Cl and F, respectively. Analytical results are provided in the electronic supplemental material S1-1.

Seventeen whole rock analyses were compiled from the SIGÉOM geodatabase of the MERN (SIGÉOM 2019) in order to complete the dataset. The compiled samples comprise a felsic volcanic rock and several mafic flows with undocumented megacrysts content (Fig. 2a). In order to compare the SIGÉOM data with the collected samples, this dataset was filtered for the samples with major elements, LOI (loss on ignition) as well as the trace elements used for whole rock analyses investigation, which includes REE (rare earth elements), and Ni, Cr, Zr, Y, Ta, Nb, Th, Hf.

### **Processing of whole rock analyses**

The studied rocks are classified using major element chemistry. However, according to field relationships, the studied rocks have been altered by hydrothermal and

metamorphic fluids. For this reason, rocks are also classified using trace elements reputed immobile in most hydrothermal systems (Pearce 1975, Edwards 1978). The Zr/TiO<sub>2</sub> vs Nb/Y (Winchester and Floyd 1977) and the Th/Yb vs Zr/Y (Ross and Bédard 2009) diagrams are used to confirm the rock classification established using major elements.

The chemical composition of the studied lava flows is investigated along stratigraphy in an attempt to track changes in volcanic dynamics. The stratigraphic level assigned to each sample corresponds to the horizontal distance between the sample and a gabbro sill located in the lower part of the studied profile (Fig. 2a). The Zr/TiO<sub>2</sub> ratio is used as a proxy for magmatic differentiation (Winchester and Floyd 1977). The magmatic affinity is deduced by displaying the fields of the Th/Yb vs Zr/Y binary diagram of Ross and Bédard (2009) along stratigraphy ([eq. 1]; supplemental material S1-2).

$$[1] \log_{10}(\text{Th/Yb}) + 1.7424 \times \log_{10}(\text{Zr/Y}) = b$$

where b corresponds to the limits of the magmatic affinity fields, as displayed on the Th/Yb vs Zr/Y diagram, with tholeiitic field < 0.3233 < transitional field < 1.0412 < calc-alkaline field.

Trace element spidergrams (multielement diagrams) and REE patterns normalised to the primitive mantle (Hofmann 1988) are used to comment on source and

differentiation processes. As the rocks may have been altered, only immobile elements are considered on the spidergram (Pearce 2008). Europium, Ti, Nb and Ta anomalies are calculated as follows:  $\text{Eu/Eu}^* = \text{Eu}_{\text{N}} / (\text{Sm}_{\text{N}} \times \text{GD}_{\text{N}})^{0.5}$ ,  $\text{Ti/Ti}^* = \text{Ti}_{\text{N}} / (\text{Sm}_{\text{N}} \times \text{GD}_{\text{N}})^{0.5}$ ,  $\text{Nb/Nb}^* = \text{Nb}_{\text{N}} / (\text{Th}_{\text{N}} \times \text{La}_{\text{N}})^{0.5}$  and  $\text{Ta/Ta}^* = \text{Ta}_{\text{N}} / (\text{Th}_{\text{N}} \times \text{La}_{\text{N}})^{0.5}$ .

The intensity of hydrothermal alteration is quantified using a neural network-based method (Trépanier et al. 2016), which does mass balance calculations after modeling the composition of the precursor (pre-alteration fresh rock). This method has the advantage of not requiring the sampling of a fresh rock and to assign a precursor to each sample. However, this method uses the results of a neural network trained on the Georoc web database (GEOROC 2011), which contains mostly post-Archean lava samples, and it may not perform well on Archean volcanic rocks. In addition, carbonate alteration is estimated using the carbonate saturation index of Kishida and Kerrich (1987), which is calculated for rocks with CO<sub>2</sub> analyzed. Detailed results of the mass balance calculations and carbonate saturation index are provided as electronic supplemental material S2-1.

Magmatic differentiation modeling is done using the MELTS thermodynamic model (Ghiorso and Sack 1995) implemented in the alphaMELTS 1.9 software (Smith and Asimow 2005). Sample 05C2 (Table 1) is selected as starting composition (parental magma) because of its elevated MgO content and because of its low alteration according to the method of Trépanier et al. (2016). The water content of sample 05C2 has been modified during metamorphism and a modelled value of 0.2 wt% H<sub>2</sub>O is assigned to this

sample, as this is a realistic value for mafic tholeiitic lavas (Moore 1970). The alphaMELTS software performs a 100% recalculation prior computing the effect of fractional crystallisation on the major elements, Ni, Cr, Zr, Y, Ta, Nb, Th, Hf and REE content of the residual melt. Calculations are made at a set pressure of 500 bars with an incremented temperature decrease at each step ( $\delta T$ ) of 3°C and oxygen fugacity ( $\log fO_2$ ) values buffered at one log unit below and at the fayalite-magnetite-quartz buffer (FMQ -1 and FMQ). Starting temperatures (liquidus temperature) of 1205.75 °C (at FMQ) and 1210.38 °C (at FMQ -1) are estimated using the phase-diagram mode of the software and the chemical composition of the residual melt is recorded at each temperature increment (electronic supplemental material S2-2 and S2-3).

## Mineral chemistry

Petrographic observations were done on a total of 23 regular and 20 polished thin sections (30 µm thick), using a conventional polarized light microscope. In addition, XRF (X-rays fluorescence) mapping was carried on 9 polished thin sections for the following elements: K, Na, Ca, Mg, Fe, Mn, Al, Ti and Si. These data were obtained with a Bruker M4 Tornado XRF microprobe equipped with a rhodium X-ray tube and two energy dispersive spectroscopy (EDS) XFlash silicon drift detectors, located at the Laval University Laboratoire de Microanalyse (LMA). A step and beam size of 20 µm were used, with an acquisition time of 5 ms/pixel, an amperage of 600 µA and a tension of 50 Kv. The Fiji software (Schindelin et al. 2012) was used to produce composite

maps and unprocessed elemental maps are provided as electronic supplemental material S3-1.

Amphiboles were analyses were obtained using a scanning electron microprobe (SEM).. Analyses were done at the IOS Services Géoscientifiques facility using a Zeiss Sigma 300 VP field emission gun SEM equipped with a Ultim-Max EDS-SDD silicon drift detector and a 5 sectors HDBSD backscattered electron (BSE) detector. Acquisition was achieved at a working distance of ~ 10 mm with a tension and amperage of 20 kV and ~ 3.17 nA, respectively. Two million effective counts were acquired per analysis and calibration was done using a MAC-9783 standard (Micro-Analysis Consultants Ltd.). Beam current was also calibrated on a copper wire to correct for current variation. Detailed analytical results are provided in the electronic supplemental material S4-1, S4-2 and S4-3.

Amphibole structural formula was calculated on a 24 (OH, F, Cl, O) basis using the spreadsheet of Locock (2014), which implements the recommendations of Hawthorne et al. (2012). Estimation of Fe<sup>2+</sup> and Fe<sup>3+</sup> is based on a sum of cations, from Si to Mg, of 13 (Locock 2014), which is equivalent to the sum of cations (Ca, Na and K excluded) proposed by other authors (13eCNK; Gualda and Vlach 2005). Thermobarometry calculation was done using the empirical equations of Zenk and Schulz (2004), modified from Gerya et al. (1997). These equations rely partly on temperature to estimate pressure. Because of high Archean mantle temperature and related high geothermal gradients (Herzberg et al. 2010, Herzberg and Rudnick 2012), these equations may

provide imprecise pressure estimates in the study area. Chlorite formula was then calculated using the WinCcac program (Yavuz et al. 2015). Temperature was estimated using the geothermometer of Xie et al. (1997), which was developed using chlorite-bearing volcanic rocks of the Archean Barberton greenstone belt. Detailed results of these calculations are provided in the electronic supplemental material S4-1 and S4-2.

### **U-Pb geochronology**

The felsic unit of outcrop n°57 (Fig. 2a and 4b) was sampled (10 kg) for geochronological investigation. The sample was processed and analyzed at the Jack Satterly Geochronology Laboratory at the University of Toronto. Zircons grains were hand picked after crushing and grinding the sample using conventional methods followed by Wilfley table heavy mineral concentration. Uranium and Pb isotopes were analyzed using isotope dilution methods and thermal ionization mass spectrometry (ID-TIMS) after chemical abrasion of the grains. Uranium-Pb data are presented graphically using the Isoplot 3.71 Add-In for MS Excel (Ludwig 2009). Details of sample preparation, analytical procedures and data processing are provided by Appendix A1. Pictures of the zircon population and the grains selected for analysis are provided in the electronic supplemental material S3-2.

## Results

### Whole rock chemistry

The volcanic rocks identified as mafic units in the field are mostly mafic to intermediate according to their anhydrous Si-content, which ranges from 43.81 wt% to 57.93 wt% SiO<sub>2</sub> (hydrous Si-content of 39.8-57.12 wt% SiO<sub>2</sub>). These rocks contain more Fe than Mg (8.61-19.20 wt% Fe<sub>2</sub>O<sub>3</sub>t, 2.28-9.56 wt% MgO). They have relatively elevated Ca contents (4.58-17.15 wt% CaO) and contain a limited amount of K and Na (0.25-4.55 wt% Na<sub>2</sub>O, K<sub>2</sub>O ranging from below detection limits to 2.54 wt%). Their Al and Ti contents are 10.96-20.00 wt% Al<sub>2</sub>O<sub>3</sub> and 0.56-1.62 wt% TiO<sub>2</sub>. Most of the mafic rocks are basalt and basalt-andesite according to the total alkali silica (TAS; Le Bas et al. 1986) diagram (Fig. 5a), with one analyse falling in the field of andesites (sample n°F981). The felsic rocks (Table 1) fall into the rhyolite field of the TAS diagram. Data scattering is likely due to hydrothermal alteration, as the samples falling in the alkaline field of the TAS diagram correspond to flows showing intense phyllosilicate alteration in the field. The studied rocks are sub-alkaline and, on the AFM diagram (Fig. 5b; Irvine and Baragar 1971), the mafic and felsic rocks have tholeiitic and calc-alkaline affinities, respectively. Except for one sample of felsic rock (sample n°B600), the modified AFM diagram, or Jensen Cation Plot (Jensen 1976), confirms the classification obtained with the TAS and AFM diagrams. Most mafic rocks fall into the Fe-rich tholeiitic basalt field (Fig. 5c).

Representative trace elements compositions are listed in Table 1. The mafic rocks are basaltic and basaltic-andesite rocks according to their Zr/TiO<sub>2</sub> ratio (SiO<sub>2</sub> proxy, Fig. 6a). Three analyses (samples n°F362, F727 and n°F94A) have slightly more elevated Zr/TiO<sub>2</sub> ratio than the bulk of mafic rocks, while andesite sample n°F981 exhibits a slightly higher Nb/Y ratio. The felsic rocks fall into the rhyodacitic field of the diagram. The Zr/Ti ratio is generally not modified by hydrothermal alteration, while the relative amount of Zr and Ti increases and decreases as a consequence of, respectively, mass losses and gains induced by hydrothermal alteration. The Ti vs Zr diagram (Fig. 6b) confirms that the mafic rocks display a narrow range of Zr/Ti ratios and that hydrothermal alteration affected most of the studied rocks. The Th/Yb vs Zr/Y diagram (Ross and Bédard 2009) confirms that most mafic flows have a tholeiitic affinity, that the rocks with intermediate chemistry are transitional, and that felsic rocks are calc-alkaline (Fig. 6c). Also, no significant chemical difference between aphyric mafic rocks and megacrysts-bearing mafic flows is observed on the diagrams described here.

Multielement and REE patterns for samples n°151A1a (megacrysts-bearing mafic flow) and 151A1b (same rock from which megacrysts were removed prior to analysis) are studied to evaluate the impact of feldspar megacrysts on whole rock analyses (Fig. 8). The compositional difference between these two samples is negligible, except for the Eu anomaly (Eu/Eu\*), which is equal to 1.1662 and 0.9067 for samples 151A1b and 151A1b, respectively. Abundant feldspar megacrysts (around 30%) may also induce a limited dilution of HREE.

The Zr/TiO<sub>2</sub> ratio and the modified diagram / equation deduced of the diagram from Ross and Bédard (2009) are displayed along a NE-SW profile to evaluate along stratigraphy chemical variations (Fig. 7). Except for sample n°F94A, chemical variations are limited along stratigraphy. The SiO<sub>2</sub>-richest lava flow units, which also have the highest Zr/TiO<sub>2</sub> ratio, are located at the top of the sequence, where the Obatogamau Formation is interdigitated with lithologies (volcanic tuffs) typical of the Waconichi Formation. Again, no sequence duplication can be deduced from the data.

Most mafic rocks display relatively flat multielement and REE patterns (Fig. 9a and 9b). On the multielement diagram, most samples exhibit slight Nb and Th depletion relative to HREE. Six samples (two megacrysts-bearing rocks, samples n°28D1 and 29A1, as well as four analyses from the MERN) display large positive Ta anomalies (Fig. 9a and Table 1). Also, small negative Eu anomalies are displayed by some aphyric mafic rocks, while megacrysts-bearing mafic rocks lack negative Eu anomalies (Fig. 9b and Table 1).

Two samples with elevated values of the Zr/TiO<sub>2</sub> ratio (samples n°F94A and F362) display fractionated multielement and REE patterns, as well as small negative Ti anomalies (Fig. 9). The REE patterns of the other samples of intermediate rocks (samples n°F727 and F981) are not as fractionated but are enriched in most trace elements. Intermediate rocks also display negative Nb anomalies (Table 1).

Felsic rocks display contrasting patterns on trace elements spidergrams (Fig. 9). Sample n°B600 has fractionated patterns on the multielement and REE diagrams, is enriched in the most incompatible elements, and has negative Nb, Ta, Ti, and Eu anomalies. The felsic unit of outcrop n°57 (samples n°57B1 and 57B2) has fractionated multielement and REE patterns with negative Nb, Ti and Eu anomalies, as well as positive Zr and Hf anomalies. These samples have lower trace elements abundances than sample n°B600 and are HREE-depleted compared to mafic rocks (Fig. 9).

### **Hydrothermal alteration**

Results of mass balance calculations (Fig. 10) obtained using the method of Trépanier et al. (2016) indicate that hydrothermal alteration, in most mafic rocks display, is negligible, with  $\pm 1\text{g}$  and  $\pm 10\text{g}$  (per 100 g of precursor) mass changes obtained for K and Si, respectively. Sodium and Ca mass changes display more variation, which is likely due to feldspar destruction in rocks that interacted with sea water on the sea floor. Felsic rocks show limited chemical variations beside K losses, Na gains and silicification for sample n°B600. Some samples display more intense alteration with, for example, K gains and losses of the other elements, which could indicate sericitic alteration. Mafic rocks tend to display noticeable Fe gains and Mg losses (Fig. 10c) that could be due to chloritisation. The carbonate saturation index (Table 2) indicates that carbonatisation is generally weak, with mean values of 0.03-0.15 and median values of 0.01-0.08 for an index that takes values comprised between 0 (fresh rock) and 1 ( $\text{CO}_2$ -saturated rock). However, carbonatisation is locally intense, with the carbonate alteration

index taking values up to 0.71 for mafic rocks, and 0.29 for the felsic unit of outcrop n°57 (Table 2, electronic supplemental material S2-1).

### **Magmatic differentiation modelling**

The results of magmatic differentiation modelling, for mafic and intermediate rocks, are displayed using MgO and Ni vs Zr/TiO<sub>2</sub> (SiO<sub>2</sub> proxy) binary diagrams showing the evolution of residual melt composition (Fig. 11). According to the model, the main phases crystallizing during the first steps of differentiation, are plagioclase and clinopyroxene with minor olivine and orthopyroxene. At first, Zr/TiO<sub>2</sub> slightly decreases and then increases, i.e., this modelled chemical evolution of the residual melt is typical of the first stages of differentiation of ferro-basalts (Toplis and Carroll 1995; Toplis and Carroll, 1996). This evolution consists of a steady decrease of compatible elements content and of an increase of iron content at constant Zr/TiO<sub>2</sub> value, until 70% crystallization is reached. Then, the Zr/TiO<sub>2</sub> ratio increases and the Fe-content decreases as Fe-Ti oxides (titanomagnetite) crystallize. The modelled liquid has a composition similar to that of the sampled rocks. The mafic samples with the highest Zr/TiO<sub>2</sub> ratio (samples n°F94A, F362 and F727) fall off-trend at given Ni, MgO and Fe<sub>2</sub>O<sub>3T</sub> values. Degree of fractional crystallisation is limited between the most and least differentiated samples, and most mafic lava flows did not reach iron oxides saturation.

## Petrography and Thermobarometry

The matrix of the mafic rocks is made of >90% of amphibole and epidote (mostly zoisite), with minor calcite, albite, muscovite, quartz, sphene and sulfides (Fig. 12). The two samples with the largest amounts of sphene correspond to megacrysts-bearing mafic flows that display the largest positive Ta anomalies. Sulfides are mostly pyrrhotite, with some pyrite, chalcopyrite, sphalerite and galena observed. Chlorite forms thin-grained aggregates in the matrix and can locally form mm-long clusters, as well as indentations in feldspar megacrysts (Fig. 13). Feldspar megacrysts are either large ( $\geq 1$  cm) or smaller isolated euhedral cm-long minerals or clusters of small ( $\leq 0.5$  cm) euhedral minerals (phenocrysts). Feldspar megacrysts and phenocrysts are replaced by epidote (again mostly zoisite) as the main phase, and albite. These feldspars also show signs of hydrothermal alteration and are replaced by muscovite (sericitization), chlorite, calcite and quartz. Also, sulfides are locally observed in the cracks of feldspar megacrysts.

Amphiboles are either zoned or un-zoned. Most un-zoned amphiboles, as well as the cores of zoned amphiboles, are tremolite (Fig. 14a). The rim of zoned amphibole is made of Mg-hornblende, pargasite and tschermakite (Fig. 14b). The temperature and pressure calculated with the method of Zenk and Schulz (2004) range from 403.79 to 677.16 °C, and from 0.91 to 8.57 kbar, respectively. Most un-zoned amphiboles and amphibole cores display temperature and pressure of, respectively, ~500 °C and 4 kbar or less. With the exception of one amphibole with reverse zoning, all amphibole rims record higher temperature and pressure conditions than their cores. The un-zoned

amphiboles that record high temperatures and pressures are mostly located around the Presqu'Île Pluton and the gabbro sill located in the central part of the studied profile (Fig. 2). The temperatures obtained from chlorite, using the method of Xie et al. (1997), range from 238 °C to 311 °C (Table 3).

### **U-Pb geochronology**

Results of U-Pb geochronology analyses carried on the felsic unit of outcrop n°57 (Table 4) are shown on Fig. 15. Four high-quality, clear and faceted zircon grains have been analyzed, each of which yielded different concordant ages of  $2726.2 \pm 1.6$  Ma,  $2741.9 \pm 1.6$  Ma,  $2758.2 \pm 1.6$ , and  $2791.8 \pm 1.8$  Ma (all errors  $2\sigma$ ). The youngest age is statistically within error of the  $2728.7 \pm 1.0$  Ma age obtained for the Waconichi Formation (Leclerc et al. 2011). The ages of  $2758.2 \pm 1.6$  Ma and  $2791.8 \pm 1.8$  Ma are similar to these reported for the Des Vents and Chrissie formations, respectively (Mortensen 1993, Davis et al. 2014). There is no known volcanic or plutonic unit with an age close to 2742 Ma in the Chibougamau region.

## **Interpretation and Discussion**

The Obatogamau Formation makes up most of volcanic cycle 1 and is the most voluminous volcanic unit of the Chibougamau area. As discussed in this section, the

Obatogamau Formation is essential to our understanding of the early evolution and economic potential of the Chibougamau area.

### Fractional crystallisation

The Obatogamau Formation is a chemically homogeneous pile of mafic to intermediate lava flows. The magmatic affinity and source of these units is discussed in the next section, while the chemical modifications induced by differentiation are addressed here.

The Obatogamau Formation has a relatively homogeneous major and trace elements content (Fig. 5 to 9). The studied lavas are mostly mafic (Fig. 5a, 5c and 6a) and modelling using the alphaMELTS software shows that most samples of mafic lavas didn't reach Fe-Ti-oxide saturation. This points to limited fractional crystallisation for the mafic lavas. The bulk of the studied lavas displays near constant Zr/TiO<sub>2</sub> ratio, which is also a consequence of limited differentiation throughout the eruption process of the lava pile. However, and according to MELT modelling, the studied lavas differentiated prior the onset of eruption. Fractionation of Fe-Ti-oxides induced Ti-depletion in the residual melt and modified the Zr/TiO<sub>2</sub> ratio. Fractionation of a single parental magma fails to explain the high Zr/TiO<sub>2</sub> values of samples n°F94A, F362 and F727, as these samples didn't reach Fe-Ti-oxide saturation. These samples may have a distinct parental magma compared to the other rocks of the study area.

The main trace elements anomalies observed on multielement spidergrams are the Ti, Ta and Nb anomalies (Fig. 9a). In modern subduction settings, Ti-Nb-Ta (TNT) negative anomaly is a consequence of metasomatism of the mantle wedge and can be related to the presence of a Ti-bearing phase (rutile) in the source of arc magmas (Arculus and Powell 1986, Pearce and Peate 1995). In the study area however, the amplitude of these anomalies varies and they may be a consequence of the differentiation process. For example, a part of the megacrysts-bearing mafic flows (e.g. samples n°28D1 and 29A1) displays positive Ta anomalies. These rocks contain large amounts of sphene (metamorphosed Fe-Ti-oxides) that may explain the Ta anomaly, as Ta has an affinity for Ti-bearing phases (Green and Pearson 1987).

The feldspar megacrysts observed in some of the mafic lava flows are commonly interpreted as cumulates broken-up and remobilised by the magma on its way to the surface (Midra 1989, Phinney 1990, Ashwal and Bybee 2017, Polat et al. 2018a). This interpretation is based on the large size of the feldspars, their calcic composition, as well as the proximity between the megacrysts-bearing lavas and anorthosite-bearing layered intrusions. These layered intrusions have tholeiitic affinities with differentiation trends characterised by Fe-enrichment, as indicated by differentiated magnetite- and ilmenite-bearing Fe-rich units such as those observed in the LDIS (Allard 1976, Arguin et al. 2018, Mathieu 2019). The cumulate, or mush, remobilised and erupted by the mafic magma was dominated by feldspar and likely contained Fe-Ti-oxides, which may have induced positive Ta anomalies in a part of the flows.

Feldspar megacryst-bearing flows are a defining characteristic of the Obatogamau Formation. The magmatic system that produced these lava flows is poorly exposed and its evolution is speculative. However, the feldspar megacrysts may indicate large volumes of magmas accumulated at different levels of the crust, which ponded long enough to crystallise large feldspars. The Obatogamau Formation may result from the emptying of the shallowest magma bodies. Feldspar megacrysts are common at the base of the lava flow pile, abundant in the central part and almost absent at the top (Cimon 1977, Leclerc et al. 2011, 2017), as is confirmed by this study. This may indicate that eruption rates decreased toward the top of the lava flow pile, forming flows that become progressively unable to carry feldspar megacrysts. This may also indicate that the megacrysts supply decreased in the magma chamber through time or that the architecture of the magmatic system changed, and that erupted lava had no longer access to feldspar-dominated mush.

In the main study area, felsic and intermediate volcanic rocks display negative Ti, Nb and Ta anomalies. Such TNT anomalies are also observed in the rocks of the Queylus Member of the Waconichi Formation (Leclerc et al. 2011). In modern subduction settings, this is known as an ‘arc signature’. In Archean greenstone belts, the main magmas that display TNT anomalies are the TTG suites that result from deep partial melting of a metamorphosed (sphene, amphibole and garnet bearing) hydrated basalt (Moyen and Martin 2012). Beside large intrusive TTG bodies, the deep partial melting of basalts may also produce felsic volcanic rocks that display the TNT anomalies and may be considered as the volcanic equivalent of the TTG intrusive

bodies. Alternatively, felsic volcanic units, in greenstone belts, may correspond to anatexis induced by mafic magma accumulation in the mafic crust (Mathieu et al. 2020). In both scenarios, the source is a sphene-bearing mafic rocks that may produce Ta-Nb-Ti-depleted magma.

### **Age and eruption rate**

The chemical homogeneity of the Obatogamau Formation and modelling achieved using the alphaMELTS software suggest that, between the first and last lava flows, the magma chamber(s) emptied without significant differentiation. This suggests a relatively high eruption rate and a lava pile that formed rapidly. The apparent waning of megacrysts supply in the flows and the onset of more felsic facies may reflect a decline in the activity of the largest magma chambers, possibly once the magma supply decreased, and replenishment have been limited. The thickness of the sequence in the study area may also indicate the proximity to an emission center if no sequence duplication affects the lava pile. One should also keep in mind that such duplication coupled with outcrop scarcity in the upper part of the studied profile could also distort the observation of feldspar distribution and its evolution.

The geochronological investigation provides a possible crystallisation age of  $2726.2 \pm 1.6$  Ma for the felsic unit of outcrop n°57 possibly located in the core of the lava flow pile. This unit also contains several inherited zircons as old as 2792 Ma. The abundance of inherited zircons induced positive Zr and Hf anomalies (whole rock

chemistry). In the field, the dated unit is massive and may correspond to a tuff, i.e., ash fall deposit, a thin-grained pyroclastic flow, a lava flow, or some aphanitic sill. The inherited zircons may be accidentals (xenocrysts) torn from the magmatic conduit during magma ascent or an explosive eruptive event. Alternatively, inherited zircons are abundant and may indicate that the dated unit has a volcanoclastic origin and contains rocks eroded from outcropping rocks of the ca 2.79 Ga and 2.76 Ga Des Vents and Chrissie formations (Mortensen 1993, David et al. 2011), as well as an undocumented 2.74 Ga unit.

The origin of the unit of outcrop n°57, dated at  $2726.2 \pm 1.6$  Ma remains uncertain. The age obtained is similar to the age of the ca 2726-2730 Ma Waconichi Formation (Mortensen 1993, Leclerc et al. 2011). Thus, there are two possibilities, either this unit is a sill related to the Waconichi Formation, or this unit is volcanic and provides a first direct age for the Obatogamau Formation. If this unit is of volcanic nature, and since it is located at an intermediate level in the Obatogamau Formation, in the core of the lava pile, the felsic unit and overlaying lava flows may have formed in a short time interval before the onset of Waconichi Formation volcanism. This is consistent with high eruption rates. Volcanic cycle 1, which comprises the Obatogamau and Waconichi formations, would have therefore formed in a few My, and its contact with older volcanic units (Chrissie and Des Vents formations) would probably be a hiatus.

## Magmatic sources

The Obatogamau Formation is a thick and spatially extensive pile of mafic flows. It is a good example of ca. 2.73 Ga volcanic activity in the Abitibi Subprovince. The studied lava flows make up most of volcanic cycle 1 and they are likely representative of the basaltic constituent of greenstone belts.

As shown by both major and trace element contents, the Obatogamau Formation is made of basalts and basaltic andesites, with a limited amount of intermediate to felsic rocks. The mafic rocks have tholeiitic affinities according to their major elements content (Fig. 5b and 5c). These rocks are also slightly depleted in the most incompatible elements, such as LILE (Fig. 9a). This was observed by previous authors (Ludden et al. 1984, Picard and Piboule 1986) who proposed a depleted mantle source for these lava flows. However, the Obatogamau Formation is not as depleted in incompatible elements as modern N-MORB (Viereck et al. 1989). For this reason, Picard and Piboule (1986) compared these lavas to modern E-MORB.

The studied rocks show no clear LREE depletion, pointing to a mantle source that is not as depleted as the source of modern N-MORB. The Obatogamau Formation has a typical Archean basalts chemistry and displays a trace element chemistry that is intermediary between these of modern arc basalts, N-MORB and E-MORB (Bédard 2018, Moyen and Laurent 2018). This is because Archean basalts have enriched mantle sources and are either the result of plume activity (Benn and Moyen 2008, Gerya et al.

2015) or come from high degree (30%) partial melting of a hot ambient mantle (Herzberg et al. 2010). The Obatogamau Formation is probably a typical constituent of normal Archean oceanic crust.

Felsic rocks have major elements contents akin to these of calc-alkaline rocks on the AFM diagram (Fig. 5b). According to the Th/Yb vs Zr/Y diagram (Fig. 6c) of Ross and Bédard (2009), the felsic and intermediate rocks have calc-alkaline and transitional affinities, respectively. Sample B600 is a HREE-undepleted felsic rock that is more enriched in REE, and especially LREE, than the mafic samples, and may correspond to a differentiated tholeiitic magma. The other felsic units, such as this of outcrop n°57, are HREE-depleted and cannot be explained by the magmatic differentiation of tholeiitic magmas. Such rocks likely have a distinct source. This is confirmed by magmatic differentiation modelling that indicates that intermediate rocks with high Zr/TiO<sub>2</sub> values (samples n°F94A, F362 and F727), negative TNT anomalies and transitional affinities (Fig. 11) have a distinct parental magma compared to the other rocks of the study area.

In the Obatogamau (this study) and Waconichi (Leclerc et al. 2011) formations, the only volcanic rocks with calc-alkaline affinities are Si-rich (intermediate to felsic rocks). In modern settings, mafic magmas may accumulate in the crust, causing local temperature increase. This may induce anatexis and produce felsic magma (Blum-Oeste and Wörner 2016, Wörner et al. 2018). During volcanic cycle 1, the crust may have been mostly mafic. Magma accumulation in the lower crust may have induced partial melting of buried (amphibole- and, possibly, garnet-bearing) hydrated basalts. The partial

melting of such a source is known to produce HREE-depleted melt (Moyen and Martin 2012). Anatexis of mafic crust may have produced magmas with fractionated REE patterns and HREE-depletion. Mixing of these felsic anatexis melts with mantle-derived magmas, as proposed before (Bédard 2018, Mathieu et al. 2020), could produce the hybrid magmas with intermediate compositions and transitional affinities observed in the study area.

In the main study area (Fig. 2a), and except for sample n°F94A, felsic and intermediate rocks with transitional to calc-alkaline affinities are located in the upper part of the lava flow pile. These rocks are close to the Waconichi Formation, which contains mafic, intermediate and felsic rocks with tholeiitic and calc-alkaline affinities (Daigneault and Allard 1990, Leclerc et al. 2011, 2017). The rest of the Obatogamau Formation is chemically homogeneous and has a tholeiitic affinity (Fig. 6b and 7).

The chemical homogeneity of the Obatogamau Formation, as well as the results of magmatic differentiation modelling, point to high effusion rates and to limited magmatic differentiation during most of the emplacement of the thick lava pile. The mantle-derived melt likely differentiated in the lower crust, where the crystallisation of feldspar megacrysts may have initiated. The magma then ascended in the crust, possibly as a feldspar-laden melt, to accumulate at mid- to upper-crust levels. Eruptions then emptied these magma accumulations to form the thick lava pile of the Obatogamau Formation. By this time, the mafic magma accumulated at depth had warmed the mafic crust and induced anatexis, producing limited volumes of felsic melts with fractionated

REE patterns and negative TNT anomalies. Other mantle-derived magma pounded and differentiated to form layered intrusion that comprise limited volumes of felsic tholeiitic magmas. Eruption of felsic melts started once about half of the Obatogamau Formation had formed and continuous eruptions later formed the Waconichi Formation. At the same time, mixing between anatexis melts and mantle-derived magmas produced some intermediate lava flows with transitional affinities.

### **Economic potential**

According to field data, sedimentary horizons are rare in the Obatogamau Formation. This is consistent with high eruption rates and limited time lapses between eruptions. During the few episodes of volcanic quiescence, hydrothermal systems developed and induced moderate sericitisation, as observed on two outcrops. The studied rocks also display moderate chloritisation according to mass balance calculations (Trépanier et al. 2016), which point to  $\text{Fe}_2\text{O}_{3T}$  gains and  $\text{MgO}$  losses.

However, these limited mass gains and losses, in mafic rocks, mostly fall within the error of the mass balance method of Trépanier et al. (2016). Indeed, this method relies on a neural network trained using the whole rock composition of post-Archean lava flows and it may not be able to detect moderate chloritisation in Archean rocks. This is because Archean tholeiites have higher Fe/Mg ratios than modern tholeiites (Condie 1985, Cattell and Taylor 1990, Hamilton 2007, Condie et al. 2016). This method, however, has demonstrated that it could detect intense chloritisation in Archean

rocks (Mathieu et al. 2016). Chloritisation, in the study area, is likely moderate or absent.

Sericitisation and chloritisation are typical alteration styles in VMS systems (Franklin et al. 2005, Galley et al. 2007). However, the weak alteration observed in the study area is likely a surface process that affected mafic lavas in contact with sea water. No evidences of vigorous hydrothermal activity and VMS-style of mineralisation is observed in the studied part of the Obatogamau Formation. The lack of VMS systems may be due to an absence of synvolcanic faults able to efficiently canalise fluids or could be due to a weak heat source unable to sustain hydrothermal cells. However, the accumulation of hot mafic magma in the crust is expected to produce temperature anomalies. More likely, the eruption rate was too high and the episodes of volcanic quiescence too short to allow for the accumulation of a significant amount of sulphides. Moreover, sustained lava flow eruptions may have buried magma bodies and potential heat sources and separated them from sub-surface hydrothermal systems. This may also explain the paucity of VMS-style alteration and associated sulfide accumulation in the study area.

In the study area, the Obatogamau Formation may not be a favorable environment for VMS mineralisation. It may have been nevertheless mineralised later, during the syntectonic period. Evidence for orogenic gold-style of mineralisation are the carbonatisation and quartz-carbonate veins observed in the study area, as well as the gold showings observed in the Obatogamau Formation (MERN dataset, SIGÉOM 2019).

Critical parameters, for orogenic gold deposits, are metamorphic grade (with fluids released at the greenschist to amphibolite facies transition), major fault systems (to canalise the fluids) and a source of gold (Phillips and Powell 2010).

According to petrographic observations, the mineral assemblages of the studied lava are compatible with upper greenschists facies metamorphic conditions (Spear 1993). The temperatures measured from most amphibole cores and from un-zoned amphiboles point to upper greenschists to lower amphibolite grades. Some amphibole rims indicate higher grades of metamorphism (intermediate amphibolite facies) that partially overprint the greenschists assemblage. Most high temperature data (amphibole rims and high temperature unzoned amphiboles) are proximal to the Presqu'Île Pluton. These amphibole overgrowths likely formed within aureoles of contact metamorphism and can be viewed as anecdotal. Away from intrusions, the main metamorphic grade is ranging between upper greenschists and lower amphibolite.

The pressures obtained from amphiboles were calculated using empirical temperature-dependant equations developed from rocks with Barovian metamorphic evolution (Zenk and Schulz 2004). Therefore, pressure is likely overestimated in the study area, where metamorphism was likely characterised by higher temperature/pressure ratio than Barovian metamorphism. The temperatures calculated from chlorite are much lower than the temperatures obtained from amphibole. However, these temperatures were calculated from mm-long clusters of chlorite that are located in the matrix of the lava or that replace feldspar megacrysts. These chlorite-clusters may

correspond to retrograde chlorite. In any case, temperatures obtained from such chlorites are not representative of the conditions of peak regional metamorphism.

The peak of regional metamorphism was likely upper greenschist to lower amphibolite facies in the study area. This is in the upper range of the regional metamorphism observed in most of the Abitibi Subprovince (Powell et al. 1995). Peak metamorphism is related to terrane assembly and cratonisation, with rocks burial occurring during the shortening of the Abitibi Subprovince, which is associated with the formation of orogenic gold systems in the greenstone belt (Dallmeyer et al. 1975, Daigneault et al. 1990, Gosselin and Dubé 2005). The Obatogamau Formation has reached sufficiently elevated temperatures high enough to induce the release of large amounts of potentially Au-bearing fluids. These fluids may have been channelized by faults systems, acting as conduits, and leading to the mineralisation of rocks located at or near present-day erosion level. Such faults were not mapped during the work conducted here, but exploration efforts have already shown several gold mineralisations in the studied rocks, such as the Joe Mann mine (Pilote 1998) as well as many gold showings (Dion and Simard 1999). The gold-potential of the Obatogamau Formation likely remains underestimated.

## Conclusions

The Obatogamau Formation is a chemically homogeneous pile of Fe-rich basalts and basaltic andesites that potentially emplaced at ca 2.73 Ga or slightly before. In the Chibougamau area, the Obatogamau and Waconichi formations of volcanic cycle 1 would have thus likely erupted within a few My, possibly less than 10 m.a.. The mafic flows are mantle-derived magmas and are typical tholeiitic Archean basalts. Once eruption initiated, magmatic differentiation was limited, and eruption rate was elevated. Isolated magma pockets differentiated to produce a limited amount of tholeiitic felsic lavas. Most felsic lava units have a calc-alkaline affinity and are likely derived from the anatexis of the mafic crust heated by the accumulation of mafic melts. Rocks with intermediate chemistry may correspond to hybrid magmas formed by mixing between mantle-derived and anatetic melts.

High eruption rates, in the studied part of the Obatogamau Formation, likely prevented prolonged episodes of volcanic quiescence, which limited the the accumulation of significant amounts of sulfides within VMS systems. Subsequent eruption of the Waconichi Formation volcanic rocks occurred as magmatic activity declined, and magma became dominantly intermediate to felsic in composition. At this time, lower effusion rates allowed for VMS mineralising systems to form in the uppermost part of volcanic cycle 1 (i.e. the Waconichi Formation). In the study area, the Obatogamau Formation was then metamorphosed to relatively high grades (upper

greenschist to lower amphibolite facies) during the Kenoran orogeny and has therefore reached pressure-temperature conditions favorable for the release of metamorphic fluids that may be favorable to the onset of orogenic gold mineralisation.

## Acknowledgements

This study was undertaken as one of the M.Sc. projects of the Metal Earth project (Laurentian University) and was conducted in the Chibougamau area. The Metal Earth project is funded by Canada First Research Excellence Funds, as well as public and industry partners (<http://merc.laurentian.ca/research/metal-earth/>). The authors warmly thank the many collaborators from the Metal Earth project for the precious scientific discussions which allowed the reasoning behind this study to take shape. They acknowledge the Laurentian University for the training and logistical support provided throughout the project as well as Patrick Houle (MERN) constant help during summer work in the Chibougamau area. Professors from the Université du Québec at Chicoutimi (UQAC) Pierre A. Cousineau, Sarah-Jane Barnes, Edward W. Sawyer and Michael D. Higgins are thanked for sharing their expertise during the project. The first author wants to thank the field assistants for the work done and the dedication they put into it. This paper is Metal Earth contribution number MERC-ME-2020-054.

## References

- Allard, G.O. 1976. The Doré Lake Complex and its importance to Chibougamau Geology and Metallogeny. Ministère de l'Énergie et des Ressources Naturelles du Québec; DPV 368.
- Allard, G.O., and Gobeil, A. 1984. General geology of the Chibougamau region. In Chibougamau, stratigraphy and mineraliaztion. Edited by J. Guha and E.H. Chown. pp. 5–19.
- Arculus, R.J., and Powell, R. 1986. Source component mixing in the regions of arc magma generation. Journal of Geophysical Research, **91**: 5913. Wiley Online Library. doi:10.1029/JB091iB06p05913.
- Arguin, J.-P., Pagé, P., Barnes, S.-J., Girard, R., and Duran, C. 2018. An Integrated Model for Ilmenite, Al-Spinel, and Corundum Exsolutions in Titanomagnetite from Oxide-Rich Layers of the Lac Doré Complex (Québec, Canada). Minerals, **8**: 476. doi:10.3390/min8110476.
- Ashwal, L.D., and Bybee, G.M. 2017. Crustal evolution and the temporality of anorthosites. Earth-Science Reviews, **173**: 307–330. Elsevier. doi:10.1016/j.earscirev.2017.09.002.
- Ayer, J., Amelin, Y., Corfu, F., Kamo, S., Ketchum, J., Kwok, K., and Trowell, N. 2002. Evolution of the southern Abitibi greenstone belt based on U–Pb geochronology: autochthonous volcanic construction followed by plutonism, regional deformation and sedimentation. Precambrian Research, **115**: 63–95. doi:10.1016/S0301-

9268(02)00006-2.

Le Bas, M.J., Le Maître, R.W., Streckeisen, A., and Zanettin, B. 1986. A Chemical Classification of Volcanic Rocks Based on the Total Alkali-Silica Diagram. *Journal of Petrology*, **27**: 745–750. doi:10.1093/petrology/27.3.745.

Bateman, R., Ayer, J.A., and Dube, B. 2008. The Timmins-Porcupine Gold Camp, Ontario: Anatomy of an Archean Greenstone Belt and Ontogeny of Gold Mineralization. *Economic Geology*, **103**: 1285–1308. doi:10.2113/gsecongeo.103.6.1285.

Beakhouse, G.P., Lin, S., and Kamo, S.L. 2011. Magmatic and tectonic emplacement of the Pukaskwa batholith, Superior Province, Ontario, CanadaThis article is one of a series of papers published in this Special Issue on the theme of Geochronology in honour of Tom Krogh. *Canadian Journal of Earth Sciences*, **48**: 187–204. doi:10.1139/E10-048.

Bédard, J.H. 2018. Stagnant lids and mantle overturns: Implications for Archaean tectonics, magmagenesis, crustal growth, mantle evolution, and the start of plate tectonics. *Geoscience Frontiers*, **9**: 19–49. Elsevier Ltd. doi:10.1016/j.gsf.2017.01.005.

Bédard, J.H., Leclerc, F., Harris, L.B., and Goulet, N. 2009. Intra-sill magmatic evolution in the Cummings Complex, Abitibi greenstone belt: Tholeiitic to calc-alkaline magmatism recorded in an Archaean subvolcanic conduit system. *Lithos*, **111**: 47–71. Elsevier B.V. doi:10.1016/j.lithos.2009.03.013.

Benn, K., and Moyen, J.-F. 2008. The Late Archean Abitibi-Opatica terrane, Superior Province: A modified oceanic plateau. When Did Plate Tectonics Begin on Planet

- Earth?, **440**: 173. Geological Society of America.
- Blum-Oeste, M., and Wörner, G. 2016. Central Andean magmatism can be constrained by three ubiquitous end-members. *Terra Nova*, **28**: 434–440. Wiley Online Library. doi:10.1111/ter.12237.
- Card, K.D. 1990. A review of the Superior Province of the Canadian Shield, a product of Archean accretion. *Precambrian Research*, **48**: 99–156. doi:10.1016/0301-9268(90)90059-Y.
- Cattell, A.C., and Taylor, R.N. 1990. Archaean basic magmas. In *Early Precambrian Basic Magmatism*. Edited by R.P. Hall and D.J. Hughes. Springer Netherlands, Dordrecht. pp. 11–39. doi:10.1007/978-94-009-0399-9\_2.
- Charbonneau, J.M., Picard, C., and Dupuis-Hébert, L. 1991. Synthèse géologique de la région de Chapais-Branssat (Abitibi). Ministère de l'Énergie et des Ressources Naturelles du Québec; MM 88-01.
- Chown, E.H., Daigneault, R., Mueller, W., and Mortensen, J.K. 1992. Tectonic evolution of the Northern Volcanic Zone, Abitibi belt, Quebec. *Canadian Journal of Earth Sciences*, **29**: 2211–2225. doi:10.1139/e92-175.
- Chown, E.H., Harrap, R., and Moukhsil, A. 2002. The role of granitic intrusions in the evolution of the Abitibi Belt, Canada. *Precambrian Research*, **115**: 291–310. doi:10.1016/S0301-9268(02)00013-X.
- Cimon, J. 1977. Quart Sud-Est du Canton de Queylus. Ministère de l'Énergie et des Ressources Naturelles du Québec; DPV 448.
- Condie, K.C. 1985. Secular Variation in the Composition of Basalts: an Index to Mantle Evolution. *Journal of Petrology*, **26**: 545–563. doi:10.1093/petrology/26.3.545.

- Condie, K.C. 2005. High field strength element ratios in Archean basalts: a window to evolving sources of mantle plumes? *Lithos*, **79**: 491–504. doi:10.1016/j.lithos.2004.09.014.
- Condie, K.C., Aster, R.C., and Van Hunen, J. 2016. A great thermal divergence in the mantle beginning 2.5 Ga: Geochemical constraints from greenstone basalts and komatiites. *Geoscience Frontiers*, **7**: 543–553. Elsevier Ltd. doi:10.1016/j.gsf.2016.01.006.
- Daigneault, R., and Allard, G.O. 1990. Le Complexe du lac Doré et son environnement géologique (région de Chibougamau – Sous-province de l’Abitibi). Ministère de l’Énergie et des Ressources Naturelles du Québec; MM 89-03.
- Daigneault, R., Mueller, W.U., and Chown, E.H. 2002. Oblique Archean subduction: Accretion and exhumation of an oceanic arc during dextral transpression, Southern Volcanic Zone, Abitibi Subprovince Canada. *Precambrian Research*, **115**: 261–290. doi:10.1016/S0301-9268(02)00012-8.
- Daigneault, R., Mueller, W.U., and Chown, E.H. 2004. Abitibi greenstone belt plate tectonics: the diachronous history of arc development, accretion and collision. *Developments in Precambrian Geology*, **12**: 88–103.
- Daigneault, R., St-Julien, P., and Allard, G.O. 1990. Tectonic evolution of the northeast portion of the Archean Abitibi greenstone belt, Chibougamau area, Quebec. *Canadian Journal of Earth Sciences*, **27**: 1714–1736. doi:10.1139/e90-178.
- Dallmeyer, R.D., Maybin, A.H., and Durocher, M.E. 1975. Timing of Kenoran Metamorphism in the Eastern Abitibi Greenstone Belt, Quebec: Evidence From  $^{40}\text{Ar}/^{39}\text{Ar}$  Ages of Hornblende and Biotite From Post-Kinematic Plutons. *Canadian*

- Journal of Earth Sciences, **12**: 1864–1873. NRC Research Press. doi:10.1139/e75-165.
- David, J., Davis, D.W., Dion, C., Goutier, J., Legault, M., and Roy, P. 2007. Datations U-Pb effectuées dans la Sous-province de l’Abitibi en 2005-2006. Ministère de l’Énergie et des Ressources Naturelles du Québec; RP 2007-01.
- David, J., Mcnicoll, V.J., Simard, M., Bandyayera, D., Hammouche, H., Goutier, J., Pilote, P., Rhéaume, P., Leclerc, F., and Dion, C. 2011. Datations U-Pb effectuées dans les provinces du Supérieur et de Churchill en 2009-2010. Ministère de l’Énergie et des Ressources Naturelles du Québec; RP 2011-02.
- David, J., Simard, M., Bandyayera, D., Goutier, J., Hammouche, H., Pilote, P., Leclerc, F., and Dion, C. 2012. Datations U-Pb effectuées dans les provinces du Supérieur et de Churchill en 2010-2011. Ministère de l’Énergie et des Ressources Naturelles du Québec; RP 2012-01.
- Davis, D.W., Simard, M., Hammouche, H., Bandyayera, D., Goutier, J., Pilote, P., Leclerc, F., and DION, C. 2014. Datations U-Pb effectuées dans les provinces du Supérieur et de Churchill en 2011-2012. Ministère de l’Énergie et des Ressources Naturelles du Québec; RP 2014-05.
- Dimroth, E., Imreh, L., Rocheleau, M., and Goulet, N. 1982. Evolution of the south-central part of the Archean Abitibi Belt, Quebec. Part I: Stratigraphy and paleogeographic model. Canadian Journal of Earth Sciences, **19**: 1729–1758. doi:10.1139/e82-154.
- Dion, C., and Simard, M. 1999. Compilation et synthèse géologique et métallogénique du Segment de Caopatina, région de Chibougamau. Ministère de l’Énergie et des

- Ressources Naturelles du Québec; MB 99-33.
- Duquette, G. 1976. North half of McKenzie and Roy townships and Northwest quarter of McCorkill township. Ministère de l'Énergie et des Ressources Naturelles du Québec; DPV 368.
- Durocher, M. 1979. Dp 611. Ministère de l'Énergie et des Ressources Naturelles du Québec; DP 611.
- Edwards, A.C. 1978. Tectonic implications of the immobile trace-element geochemistry of mafic rocks bounding the Wonaminta Block. *Journal of the Geological Society of Australia*, **25**: 459–465. doi:10.1080/00167617808729054.
- Franklin, J.M., Gibson, H.L., Jonasson, I.R., and Galley, A.G. 2005. Volcanogenic Massive Sulfide Deposits. *In* One Hundredth Anniversary Volume. Edited by J.W. Hedenquist, J.F.H. Thompson, R.J. Goldfarb, and J.P. Richards. Society of Economic Geologists, Littleton, Colorado, USA. pp. 523–560.
- Galley, A.G., Hannington, M.D., and Jonasson, I.R. 2007. Volcanogenic massive sulphide deposits. *In* Mineral deposits of Canada: A synthesis of major deposit types, district metallogeny, the evolution of geological provinces, and exploration methods. Geological Association of Canada, Mineral Deposits Division: St. John's, NL, Canada. pp. 141–161.
- GEOROC. 2011. Geochemistry of Rocks of the Oceans and Continents. Max-Planck-Institut für Chemie. Available online: <http://georoc.mpch-mainz.gwdg.de/georoc/Start.asp> (accessed on 30 November 2011).
- Gerstenberger, H., and Haase, G. 1997. A highly effective emitter substance for mass spectrometric Pb isotope ratio determinations. *Chemical Geology*, **136**: 309–312.

doi:10.1016/S0009-2541(96)00033-2.

Gerya, T., Stern, R.J., Baes, M., Fischer, R., Sizova, E., Sobolev, S. V, and Whattam, S.A. 2015. Plume tectonics and cratons formation in the early Earth. *In AGU Fall Meeting Abstracts.*

Gerya, T. V, Perchuk, L.L., Triboulet, C., Audren, C., and Sez'Ko, A.I. 1997. Petrology of the Tumanshet zonal metamorphic complex, eastern Sayan. *Petrology*, **5**: 563–595.

Ghiorso, M.S., and Sack, R.O. 1995. Chemical mass transfer in magmatic processes IV. A revised and internally consistent thermodynamic model for the interpolation and extrapolation of liquid-solid equilibria in magmatic systems at elevated temperatures and pressures. *Contributions to Mineralogy and Petrology*, **119**: 197–212. doi:10.1007/BF00307281.

Gibson, H.L., Allen, R.L., Riverin, G., and Lane, T.E. 2007. The VMS Model : Advances and Application to Exploration Targeting. *Proceedings of Exploration*, **7**: 713-730 pp.

Gosselin, P., and Dubé, B. 2005. Gold deposits of the world: distribution, geological parameters and gold content. *Geological Survey of Canada Open File 4895*.

Green, T.H., and Pearson, N.J. 1987. An experimental study of Nb and Ta partitioning between Ti-rich minerals and silicate liquids at high pressure and temperature. *Geochimica et Cosmochimica Acta*, **51**: 55–62. Elsevier. doi:10.1016/0016-7037(87)90006-8.

Gualda, G.A.R., and Vlach, S.R.F. 2005. Stoichiometry-based estimates of ferric iron in calcic, sodic-calcic and sodic amphiboles: A comparison of various methods. *Anais*

- da Academia Brasileira de Ciencias, **77**: 521–534. doi:10.1590/s0001-37652005000300012.
- Hamilton, W.B. 2007. Earth's first two billion years – The era of internally mobile crust. In 4-D Framework of Continental Crust. Edited by R.D. Hatcher, J.H. Carlson, J.H. McBride, and J.R. Martínez Catalán. Geological Society of America Memoir. pp. 233–296. doi:10.1130/2007.1200(13).
- Hannington, M.D., Santaguida, F., Kjarsgaard, I.M., and Cathles, L.M. 2003. Regional-scale hydrothermal alteration in the Central Blake River Group, western Abitibi subprovince, Canada: implications for VMS prospectivity. Mineralium Deposita, **38**: 393–422. doi:10.1007/s00126-002-0298-z.
- Hawthorne, F.C., Oberti, R., Harlow, G.E., Maresch, W. V., Martin, R.F., Schumacher, J.C., and Welch, M.D. 2012. Nomenclature of the amphibole supergroup. American Mineralogist, **97**: 2031–2048. doi:10.2138/am.2012.4276.
- Herzberg, C., Condie, K., and Korenaga, J. 2010. Thermal history of the Earth and its petrological expression. Earth and Planetary Science Letters, **292**: 79–88. Elsevier B.V. doi:10.1016/j.epsl.2010.01.022.
- Herzberg, C., and Rudnick, R. 2012. Formation of cratonic lithosphere: An integrated thermal and petrological model. Lithos, **149**: 4–15. Elsevier. doi:10.1016/j.lithos.2012.01.010.
- Hofmann, A.W. 1988. Chemical differentiation of the Earth: the relationship between mantle, continental crust, and oceanic crust. Earth and Planetary Science Letters, **90**: 297–314. doi:10.1016/0012-821X(88)90132-X.
- Irvine, T.N., and Baragar, W.R.A. 1971. A Guide to the Chemical Classification of the

- Common Volcanic Rocks. Canadian Journal of Earth Sciences, **8**: 523–548.  
doi:10.1139/e71-055.
- Jaffey, A.H., Flynn, K.F., Glendenin, L.E., Bentley, W.C., and Essling, A.M. 1971. Precision Measurement of Half-Lives and Specific Activities of  $^{235}\text{U}$  and  $^{238}\text{U}$ . Physical Review C, **4**: 1889–1906. doi:10.1103/PhysRevC.4.1889.
- Jensen, L.S. 1976. New Cation Plot for Classifying Subalkalic Volcanic Rocks. Ontario Division of Mines Miscellaneous Papers, **66**: 1–22.
- Kerrich, R., Polat, A., and Xie, Q. 2008. Geochemical systematics of 2.7 Ga Kinojevis Group (Abitibi), and Manitouwadge and Winston Lake (Wawa) Fe-rich basalt–rhyolite associations: Backarc rift oceanic crust? Lithos, **101**: 1–23. doi:10.1016/j.lithos.2007.07.009.
- Kishida, A., and Kerrich, R. 1987. Hydrothermal alteration zoning and gold concentration at the Kerr- Addison Archean lode gold deposit, Kirkland Lake, Ontario (Canada). Economic Geology, **82**: 649–690. doi:10.2113/gsecongeo.82.3.649.
- Krogh, T.. 1973. A low-contamination method for hydrothermal decomposition of zircon and extraction of U and Pb for isotopic age determinations. Geochimica et Cosmochimica Acta, **37**: 485–494. doi:10.1016/0016-7037(73)90213-5.
- Laurent, O., Martin, H., Moyen, J.F., and Doucelance, R. 2014. The diversity and evolution of late-Archean granitoids: Evidence for the onset of “modern-style” plate tectonics between 3.0 and 2.5Ga. Lithos, **205**: 208–235. Elsevier B.V. doi:10.1016/j.lithos.2014.06.012.
- Leclerc, F., Bédard, J.H., Harris, L.B., McNicoll, V.J., Goulet, N., Roy, P., and Houle, P.

2011. Tholeiitic to calc-alkaline cyclic volcanism in the Roy Group, Chibougamau area, Abitibi Greenstone Belt — revised stratigraphy and implications for VHMS exploration. *Canadian Journal of Earth Sciences*, **48**: 661–694. doi:10.1139/E10-088.
- Leclerc, F., Harris, L.B., Bedard, J.H., van Breemen, O., and Goulet, N. 2012. Structural and Stratigraphic Controls on Magmatic, Volcanogenic, and Shear Zone-Hosted Mineralization in the Chapais-Chibougamau Mining Camp, Northeastern Abitibi, Canada. *Economic Geology*, **107**: 963–989. doi:10.2113/econgeo.107.5.963.
- Leclerc, F., Roy, P., Houle, P., Pilote, P., Bédard, J.H., Harris, L.B., Mcnicoll, V.J., Breemen, O. Van, and David, J. 2017. Géologie de la région de Chibougamau. Ministère de l'Énergie et des Ressources Naturelles du Québec; RG 2015-03.
- Legault, M. 2003. Environnement métallogénique du couloir de Fancamp avec emphase sur les gisements aurifères de Chevrier, région de Chibougamau, Québec. Université du Québec à Chicoutimi.
- Locock, A.J. 2014. An Excel spreadsheet to classify chemical analyses of amphiboles following the IMA 2012 recommendations. *Computers & Geosciences*, **62**: 1–11. Elsevier. doi:10.1016/j.cageo.2013.09.011.
- Ludden, J., Francis, D., and Allard, G.O. 1984. The geochemistry and evolution of the volcanic rocks of the Chibougamau region of the Abitibi metavolcanic belt. In Chibougamau, stratigraphy and mineraliaztion. Edited by J. Guha and E.H. Chown. pp. 20–34.
- Ludden, J., Hubert, C., and Gariépy, C. 1986. The tectonic evolution of the Abitibi greenstone belt of Canada. *Geological Magazine*, **123**: 153–166.

- doi:10.1017/S0016756800029800.
- Ludwig, K.R. 2009. User's manual for Isoplot 3.71 a geochronological toolkit for Excel. Berkeley Geochronology Center, Special Publication, **4**: 72.
- Maier, W.D., Barnes, S.-J., and Pellet, T. 1996. The economic significance of the Bell River Complex, Abitibi subprovince, Quebec. Canadian Journal of Earth Sciences, **33**: 967–980. doi:10.1139/e96-073.
- Mathieu, L. 2019. Origin of the Vanadiferous Serpentine–Magnetite Rocks of the Mt. Sorcerer Area, Lac Doré Layered Intrusion, Chibougamau, Québec. Geosciences, **9**: 110. doi:10.3390/geosciences9030110.
- Mathieu, L., Bouchard, R., Pearson, V., and Daigneault, R. 2016. The Coulon deposit: quantifying alteration in volcanogenic massive sulphide systems modified by amphibolite-facies metamorphism. Canadian Journal of Earth Sciences, **53**: 1443–1457. doi:10.1139/cjes-2016-0017.
- Mathieu, L., Snyder, D.B., Bedeaux, P., Cheraghi, S., Lafrance, B., Thurston, P.C., and Sherlock, R. 2020. Deep into the Chibougamau area, Abitibi Subprovince: structure of a Neoarchean crust revealed by seismic reflection profiling. Earth and Space Science Open Archive,. doi:10.1002/essoar.10501539.1.
- Mattinson, J.M. 2005. Zircon U–Pb chemical abrasion (“CA-TIMS”) method: Combined annealing and multi-step partial dissolution analysis for improved precision and accuracy of zircon ages. Chemical Geology, **220**: 47–66. doi:10.1016/j.chemgeo.2005.03.011.
- Mercier-Langevin, P., Lafrance, B., Becu, V., Dube, B., Kjarsgaard, I., and Guha, J. 2014. The Lemoine Auriferous Volcanogenic Massive Sulfide Deposit,

- Chibougamau Camp, Abitibi Greenstone Belt, Quebec, Canada: Geology and Genesis. *Economic Geology*, **109**: 231–269. doi:10.2113/econgeo.109.1.231.
- Midra, R. 1989. Géochimie des Laves de la Formation d'Obatogamau (bande sud de la ceinture archéenne Chibougamau-Matagami) Québec, Canada. Université du Québec à Chicoutimi. Available from <https://constellation.uqac.ca/1616/>.
- Mints, M. V. 2017. The composite North American Craton, Superior Province: Deep crustal structure and mantle-plume model of Neoarchaean evolution. *Precambrian Research*, **302**: 94–121. Elsevier. doi:10.1016/j.precamres.2017.08.025.
- Moore, J.G. 1970. Water Content of Basalt Erupted on the ocean floor. Contributions to Mineralogy and Petrology, **28**: 272–279. doi:10.1007/BF00388949.
- Mortensen, J.K. 1993. U–Pb geochronology of the eastern Abitibi Subprovince. Part 1: Chibougamau–Matagami–Joutel region. *Canadian Journal of Earth Sciences*, **30**: 11–28. doi:10.1139/e93-002.
- Moyen, J.-F., and Laurent, O. 2018. Archaean tectonic systems: A view from igneous rocks. *Lithos*, **302–303**: 99–125. Elsevier B.V. doi:10.1016/j.lithos.2017.11.038.
- Moyen, J.F., and Martin, H. 2012. Forty years of TTG research. *Lithos*, **148**: 312–336. Elsevier B.V. doi:10.1016/j.lithos.2012.06.010.
- Moyen, J.F., Martin, H., Jayananda, M., and Auvray, B. 2003. Late Archaean granites: A typology based on the Dharwar Craton (India). *Precambrian Research*, **127**: 103–123. doi:10.1016/S0301-9268(03)00183-9.
- Mueller, W., Chown, E.H., Sharma, K.N.M., Tait, L., and Rocheleau, M. 1989. Paleogeographic and Paleotectonic Evolution of a Basement-Controlled Archean Supracrustal Sequence, Chibougamau-Caopatina, Quebec. *The Journal of Geology*,

- 97: 399–420. doi:10.1086/629319.
- Mueller, W., and Donaldson, J.A. 1992. Development of sedimentary basins in the Archean Abitibi belt, Canada: an overview. Canadian Journal of Earth Sciences, 29: 2249–2265. doi:10.1139/e92-177.
- Pearce, J.A. 1975. Basalt geochemistry used to investigate past tectonic environments on Cyprus. Tectonophysics, 25: 41–67. doi:10.1016/0040-1951(75)90010-4.
- Pearce, J.A. 2008. Geochemical fingerprinting of oceanic basalts with applications to ophiolite classification and the search for Archean oceanic crust. Lithos, 100: 14–48. doi:10.1016/j.lithos.2007.06.016.
- Pearce, J.A., and Peate, D.W. 1995. Tectonic Implications of the Composition of Volcanic ARC Magmas. Annual Review of Earth and Planetary Sciences, 23: 251–285. Annual Reviews 4139 El Camino Way, PO Box 10139, Palo Alto, CA 94303-0139, USA. doi:10.1146/annurev.ea.23.050195.001343.
- Phillips, G.N., and Powell, R. 2010. Formation of gold deposits: a metamorphic devolatilization model. Journal of Metamorphic Geology, 28: 689–718. Wiley Online Library.
- Phinney, C. 1990. Open-system evolution versus source control in basaltic magmas : Matachewan-Hearst dike swarm , Superior Province , canadal.
- Picard, C., and Piboule, M. 1986. Pétrologie des roches volcaniques du sillon de roches vertes archéennes de Matagami – Chibougamau à l'ouest de Chapais (Abitibi est, Québec).1. Le groupe basal de Roy. Canadian Journal of Earth Sciences, 23: 561–578. doi:10.1139/e86-056.
- Pilote, P. 1998. Géologie et métallogénie du district minier de Chapais-Chibougamau :

nouvelle vision du potentiel de découverte. Ministère de l'Énergie et des Ressources Naturelles du Québec; DV 98-03.

Polat, A., Frei, R., Longstaffe, F.J., and Woods, R. 2018a. Petrogenetic and geodynamic origin of the Neoarchean Doré Lake Complex, Abitibi subprovince, Superior Province, Canada. *International Journal of Earth Sciences*, **107**: 811–843. Springer Berlin Heidelberg. doi:10.1007/s00531-017-1498-1.

Polat, A., and Kerrich, R. 2001. Geodynamic processes, continental growth, and mantle evolution recorded in late Archean greenstone belts of the southern Superior Province, Canada. *Precambrian Research*, **112**: 5–25. doi:10.1016/S0301-9268(01)00168-1.

Polat, A., Longstaffe, F.J., and Frei, R. 2018b. An overview of anorthosite-bearing layered intrusions in the Archean craton of southern West Greenland and the Superior Province of Canada: implications for Archean tectonics and the origin of megacrystic plagioclase. *Geodinamica Acta*, **30**: 84–99. Taylor & Francis. doi:10.1080/09853111.2018.1427408.

Potvin, R. 1991. Étude volcanologique du centre volcanique felsique du Lac des Vents, région de Chibougamau. University of Quebec at Chicoutimi.

Powell, W.G., Carmichael, D.M., and Hodgson, C.J. 1995. Conditions and timing of metamorphism in the southern Abitibi greenstone belt, Quebec. *Canadian Journal of Earth Sciences*, **32**: 787–805. doi:10.1139/e95-067.

Rey, P.F., Philippot, P., and Thébaud, N. 2003. Contribution of mantle plumes, crustal thickening and greenstone blanketing to the 2.75–2.65Ga global crisis. *Precambrian Research*, **127**: 43–60. Elsevier. doi:10.1016/S0301-9268(03)00179-7.

- Ross, P.-S., and Bédard, J.H. 2009. Magmatic affinity of modern and ancient subalkaline volcanic rocks determined from trace-element discriminant diagrams. *Canadian Journal of Earth Sciences*, **46**: 823–839. doi:10.1139/e09-054.
- Ross, P.S., McNicoll, V.J., Debreil, J.A., and Carr, P. 2014. Precise U-Pb Geochronology of the Matagami Mining Camp, Abitibi Greenstone Belt, Quebec: Stratigraphic Constraints and Implications for Volcanogenic Massive Sulfide Exploration. *Economic Geology*, **109**: 89–101. doi:10.2113/econgeo.109.1.89.
- Sage, R.P., Lightfoot, P.C., and Doherty, W. 1996. Geochemical characteristics of granitoid rocks from within the Archean Michipicoten Greenstone Belt, Wawa Subprovince, Superior Province, Canada: implications for source regions and tectonic evolution. *Precambrian Research*, **76**: 155–190. doi:10.1016/0301-9268(95)00021-6.
- Schindelin, J., Arganda-Carreras, I., Frise, E., Kaynig, V., Longair, M., Pietzsch, T., Preibisch, S., Rueden, C., Saalfeld, S., Schmid, B., Tinevez, J.-Y., White, D.J., Hartenstein, V., Eliceiri, K., Tomancak, P., and Cardona, A. 2012. Fiji: an open-source platform for biological-image analysis. *Nature Methods*, **9**: 676–682. doi:10.1038/nmeth.2019.
- Scott, C.R., Mueller, W.U., and Pilote, P. 2002. Physical volcanology, stratigraphy, and lithogeochemistry of an Archean volcanic arc: Evolution from plume-related volcanism to arc rifting of SE Abitibi Greenstone Belt, Val d'Or, Canada. *Precambrian Research*, **115**: 223–260. doi:10.1016/S0301-9268(02)00011-6.
- SIGÉOM. 2019. Système d'information géominière du Québec. Ministère de l'Énergie et des Ressources Naturelles. Available from <http://sigeom.mines.gouv.qc.ca>

(accessed on 15 May 2019).

- Smith, P.M., and Asimow, P.D. 2005. Adiabat\_1ph: A new public front-end to the MELTS, pMELTS, and pHMELTS models. *Geochemistry, Geophysics, Geosystems*, **6**: 1–8. doi:10.1029/2004GC000816.
- Spear, F.S. 1993. Metamorphic phase equilibria and pressure-temperature-time paths. Monograph series, Mineralogical Society of America, Washington DC, USA.
- Stacey, J.S., and Kramers, J.D. 1975. Approximation of terrestrial lead isotope evolution by a two-stage model. *Earth and Planetary Science Letters*, **26**: 207–221. doi:10.1016/0012-821X(75)90088-6.
- Taner, M.F., and Trudel, P. 1991. Gold distribution in the Val-d'Or Formation and a model for the formation of the Lamaque–Sigma mines, Val-d'Or, Quebec. *Canadian Journal of Earth Sciences*, **28**: 706–720. doi:10.1139/e91-061.
- Thurston, P.C., Ayer, J.A., Goutier, J., and Hamilton, M.A. 2008. Depositional Gaps in Abitibi Greenstone Belt Stratigraphy: A Key to Exploration for Syngenetic Mineralization. *Economic Geology*, **103**: 1097–1134. doi:10.2113/gsecongeo.103.6.1097.
- Toplis, M.J., and Carroll, M.R. 1995. An Experimental Study of the Influence of Oxygen Fugacity on Fe-Ti Oxide Stability, Phase Relations, and Mineral–Melt Equilibria in Ferro-Basaltic Systems. *Journal of Petrology*, **36**: 1137–1170. doi:10.1093/petrology/36.5.1137.
- Toplis, M.J., and Carroll, M.R. 1996. Differentiation of ferro-basaltic magmas under conditions open and closed to oxygen: Implications for the skaergaard intrusion and other natural systems. *Journal of Petrology*, **37**: 837–858.

- doi:10.1093/petrology/37.4.837.
- Trépanier, S., Mathieu, L., Daigneault, R., and Faure, S. 2016. Precursors predicted by artificial neural networks for mass balance calculations: Quantifying hydrothermal alteration in volcanic rocks. *Computers & Geosciences*, **89**: 32–43. Elsevier.  
doi:10.1016/j.cageo.2016.01.003.
- Viereck, L.G., Flower, M.F.J., Hertogen, J., Schmincke, H.-U., and Jenner, G.A. 1989. The genesis and significance of N-MORB sub-types. *Contributions to Mineralogy and Petrology*, **102**: 112–126. Springer. doi:10.1007/BF01160195.
- Whitney, D.L., and Evans, B.W. 2010. Abbreviations for names of rock-forming minerals. *American Mineralogist*, **95**: 185–187. doi:10.2138/am.2010.3371.
- Winchester, J.A., and Floyd, P.A. 1977. Geochemical discrimination of different magma series and their differentiation products using immobile elements. *Chemical Geology*, **20**: 325–343. doi:10.1016/0009-2541(77)90057-2.
- Wörner, G., Mamani, M., and Blum-Oeste, M. 2018. Magmatism in the Central Andes. *Elements*, **14**: 237–244. doi:10.2138/gselements.14.4.237.
- Wyman, D.A. 1999. A 2.7 Ga depleted tholeiite suite: Evidence of plume-arc interaction in the Abitibi Greenstone Belt, Canada. *Precambrian Research*, **97**: 27–42.  
doi:10.1016/S0301-9268(99)00018-2.
- Xie, X., Byerly, G.R., and Ferrell Jr., R.E. 1997. IIb trioctahedral chlorite from the Barberton greenstone belt: crystal structure and rock composition constraints with implications to geothermometry. *Contributions to Mineralogy and Petrology*, **126**: 275–291. doi:10.1007/s004100050250.
- Yavuz, F., Kumral, M., Karakaya, N., Karakaya, M.C., and Yıldırım, D.K. 2015. A

- Windows program for chlorite calculation and classification. *Computers & Geosciences*, **81**: 101–113. doi:10.1016/j.cageo.2015.04.011.
- York, D. 1968. Least squares fitting of a straight line with correlated errors. *Earth and Planetary Science Letters*, **5**: 320–324. doi:10.1016/S0012-821X(68)80059-7.
- Zenk, M., and Schulz, B. 2004. Zoned Ca-amphiboles and related P-T evolution in metabasites from the classical Barrovian metamorphic zones in Scotland. *Mineralogical Magazine*, **68**: 769–786. doi:10.1180/0026461046850218.

## Appendix

### A1

A sample for conventional U-Pb geochronological analysis (18UCB-0057B) was processed and analyzed at the Jack Satterly Geochronology Laboratory at the University of Toronto. The sample was crushed using a standard jaw crusher and underwent grinding using a Bico<sup>TM</sup> disk mill. Initial separation of heavy minerals was carried out by passing the ground sample and derived heavy concentrates over a shaking, riffled water (Wilfley<sup>TM</sup>) table multiple times. Further processing employed density separation with methylene iodide and paramagnetic separation with a Frantz isodynamic separator. Final sample selection was achieved by hand picking in alcohol under a binocular microscope, choosing the freshest, least cracked, core-and inclusion-free grains of zircon.

Analytical methods involved isotope dilution thermal ionization mass spectrometry (ID-TIMS) following a chemical abrasion pre-treatment (CA, modified after Mattinson, 2005). Zircon grains that underwent CA protocols were annealed in quartz crucibles at 900°C for 2 days. Annealed grains were subsequently leached in concentrated hydrofluoric (HF) acid for several hours in Teflon vessels at 200°C.

Weights of mineral fractions chosen for ID-TIMS analysis were estimated from scaled digital photomicrographs, using the density of zircon. Estimated weights should be accurate to about  $\pm$  20%. This affects only U and Pb concentrations, not age information, which depends only on isotope ratio measurements. Samples were washed prior to dissolution. A mixed  $^{205}\text{Pb}$ - $^{235}\text{U}$  isotopic spike was added to the dissolution capsules during sample loading. Zircon grains were dissolved using concentrated HF in Teflon bombs at 200°C for 4 days, then dried and re-dissolved in 3N HCl overnight (Krogh 1973). U and Pb were isolated using 50 microliter anion exchange columns using HCl elutions, dried down, and then loaded onto outgassed rhenium filaments with silica gel (Gerstenberger and Haase 1997).

Lead and  $\text{UO}_2$  were analyzed on a VG354 mass spectrometer using a Daly collector in pulse counting mode. The mass discrimination correction for this detector was constant at 0.07%/AMU. Thermal mass discrimination corrections are 0.10%/AMU for Pb and U. Dead time of the Daly system was 16 ns for Pb during the analytical period, monitored using the SRM982 Pb standard.

Mass spectrometer data was reduced using in-house software (UtilAge program) coded by D. Davis (University of Toronto). All common Pb was assigned to procedural blank. Initial Pb from geological sources above 1 picogram was corrected using the Pb evolution model of Stacey and Kramers (1975). Plotting of Concordia curves and averaging of age results were carried out using the Isoplot 3.71 Add-In for MS Excel, of Ludwig (2009). Ages calculated on the basis of a regression using a modified version of

the York (1968) algorithm, in which points are weighted proportional to the inverse of the square of the assigned errors, incorporating error correlations (see Ludwig, 2009); uncertainties in the U decay constants are shown in the Concordia diagram. Uranium decay constants are from Jaffey et al. (1971). All age errors and error ellipses are given at the 2 sigma or 95% level of confidence.

Total common Pb levels in the analyzed zircon fractions are generally very low, ranging from about 0.18–0.33 pg.

## Figures

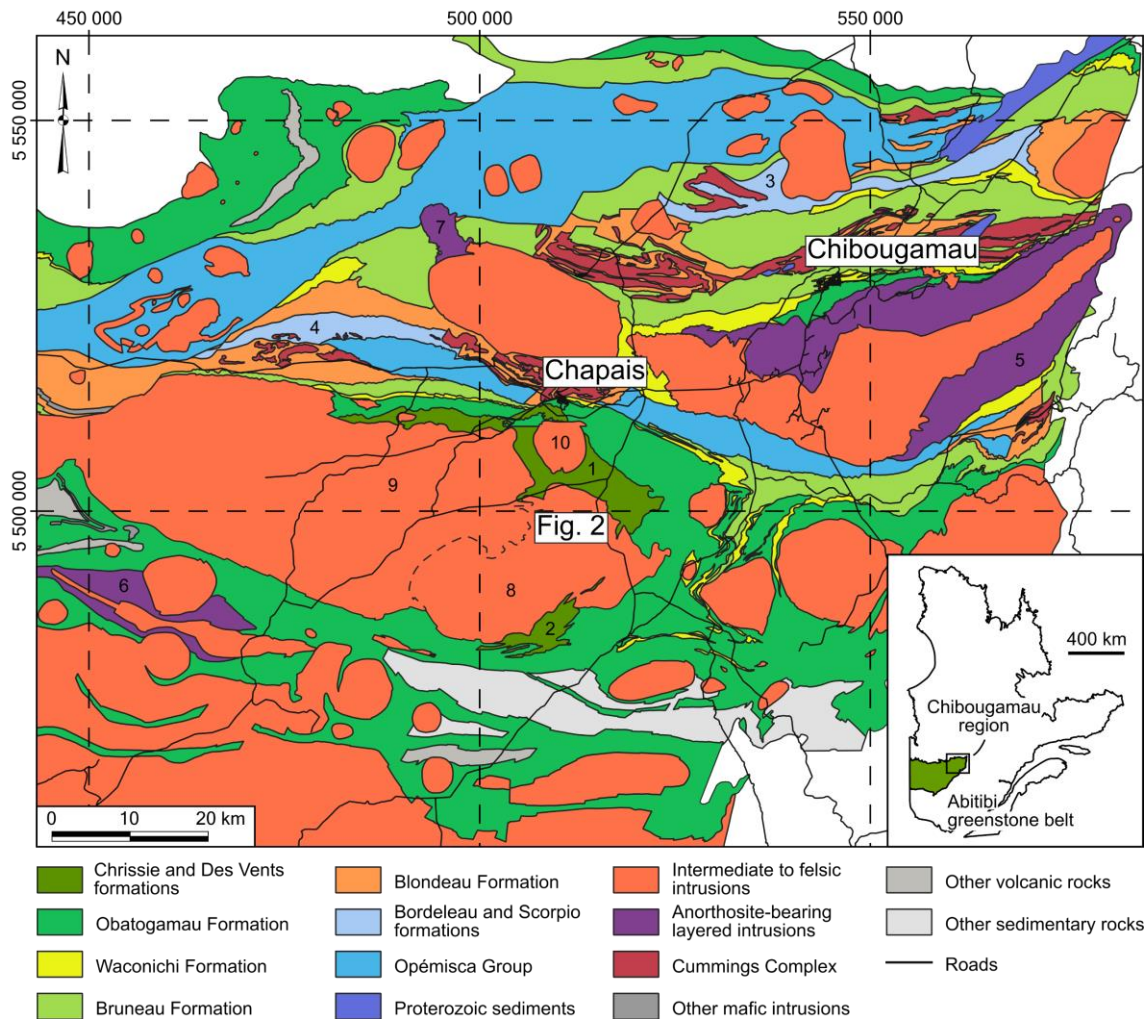


**Figure 1:** Simplified geological map of the Chibougamau area, modified from the MERN (SIGEOM 2019). Numbers 1 to 13 correspond to: Chrissie Formation (1), Des Vents Formation (2), Bordeleau Formation (3), Scorpio Formation (4), Lac Doré Intrusive Suite (5), Rivière Opawica Intrusive Suite (6), Lac de la Chaleur Intrusive Suite (7), Eau Jaune Complex (8), Lapparent Intrusive Suite (9), and Presqu'Île Pluton

(10). Map projection system is UTM NAD83 and coordinate system corresponds to zone 18 N.

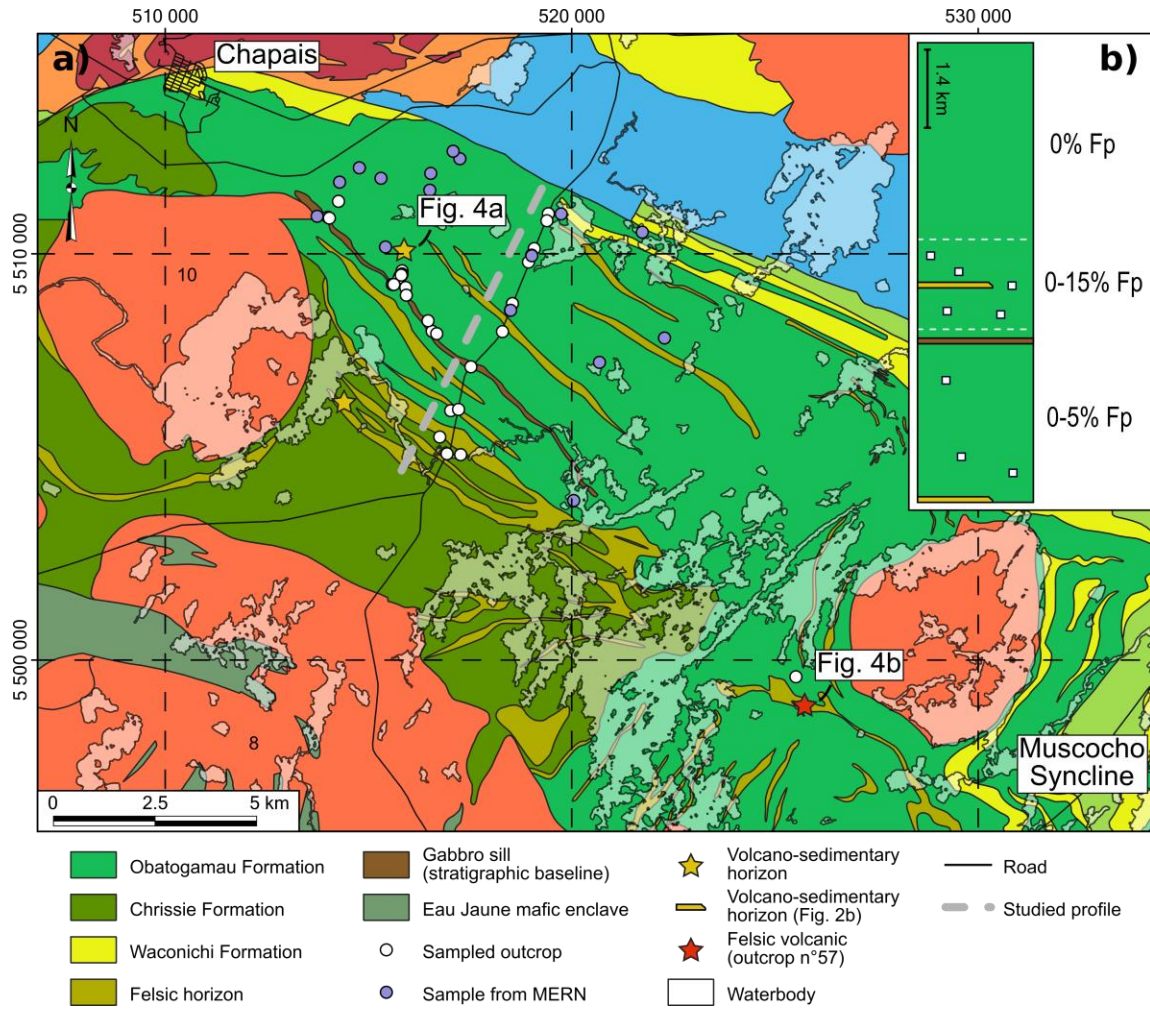


**Figure 2:** (a) Simplified geological map of the main study area, modified from the MERN (SIGEOM 2019), locating the samples, episodes of volcanic quiescence and felsic units observed in the field. Complete legend is available in Fig. 1. The gabbro sill, the felsic horizons shown on this map are tentatively interpreted by the MERN from drill core and magnetic data mostly. Map projection system is UTM NAD83 zone 18N. (b) Schematic stratigraphic column showing general feldspar megacrysts abundance, with 14 outcrops visited in both the base and central parts (12 outcrops sampled in each part)

of the profile, as well as 5 visited in the upper part (4 outcrops sampled). One of the observed mafic flows in the central part of the profile contains about 30% feldspar megacrysts.

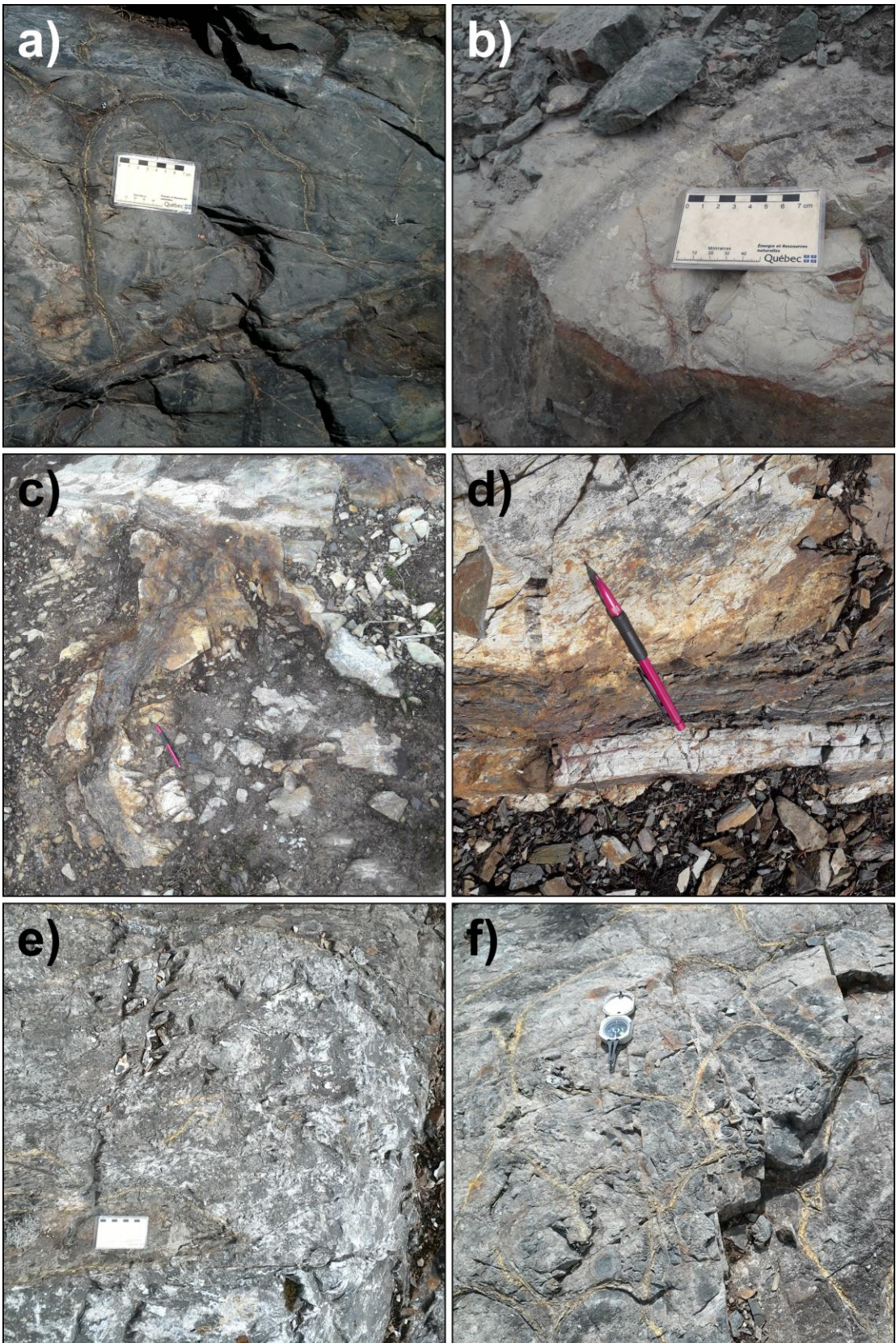


**Figure 3:** Field photographs showing (a) feldspar megacrysts bearing pillow basalts; (b) megacrysts bearing mafic flow; (c) sedimentary horizon (folded) formed during an episode of volcanic quiescence (from the outcrop shown by Fig. 4a); (d) zoom on the sedimentary horizon with, from top to bottom, siltstone, claystone, and chert; (e) felsic unit (light grey) and mafic flow (darker grey) transposed in a shear zone (outcrop n°57, see figure Fig. 2 for location); (f) slightly deformed pillow lavas observed on outcrop n°57. Yellow chalk lines highlight the rims of pillows (a, f), as well as the contact between the felsic and mafic units (e). The pencils point toward the north (c, d).

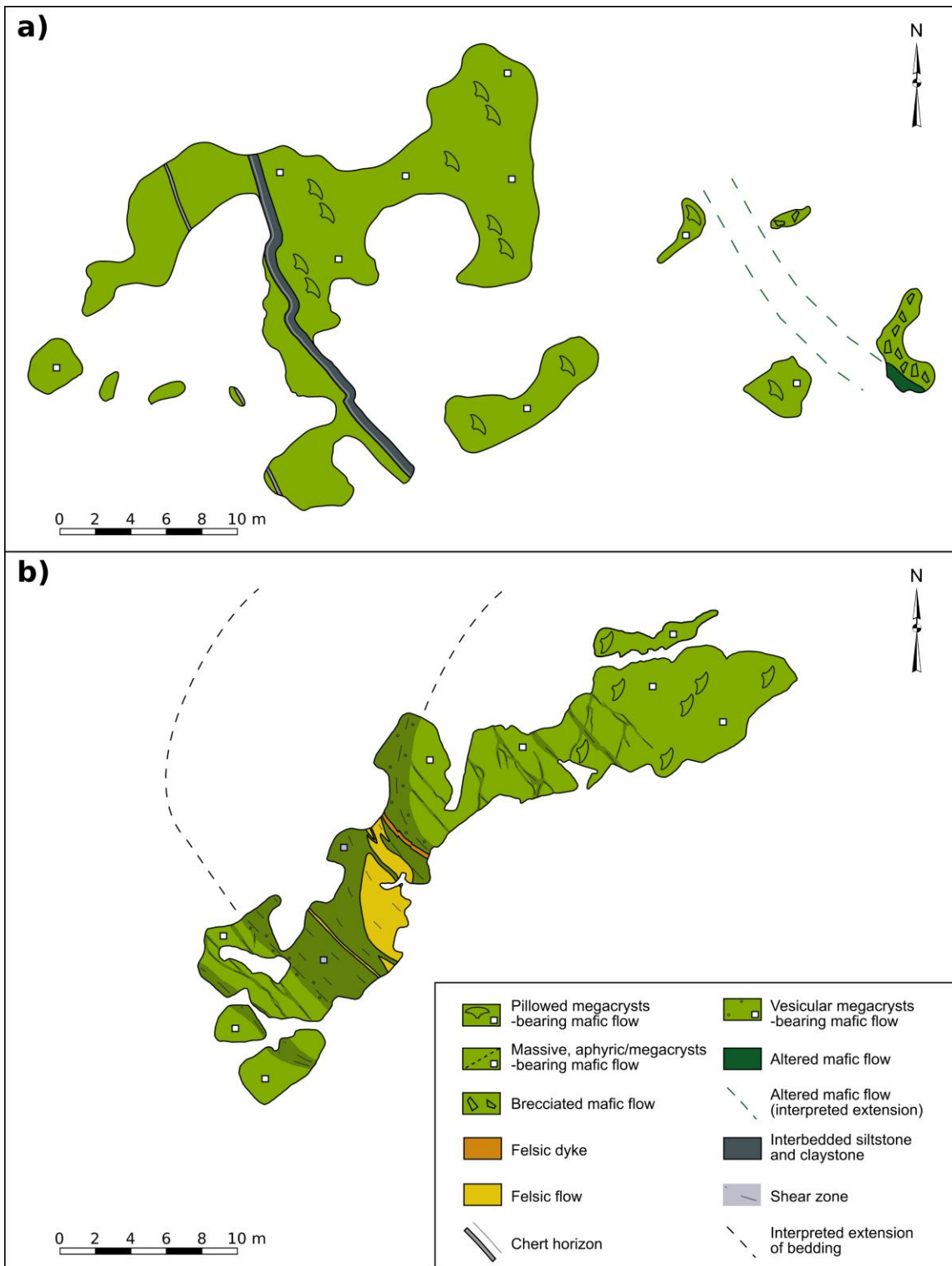


**Figure 4:** (a) Detailed map of an outcrop showing a sedimentary unit (episode of volcanic quiescence) interbedded with moderately altered lava flow. The stratigraphic top, as indicated by the shape of pillows, is to the NE. (b) Detailed map of outcrop n°57 showing a felsic unit interbedded with feldspar megacrysts-bearing mafic flows. These rocks are partly transposed in a shear zone that folded the bedding planes (refer to vesicles distribution). See Fig. 2 for location of these outcrops.

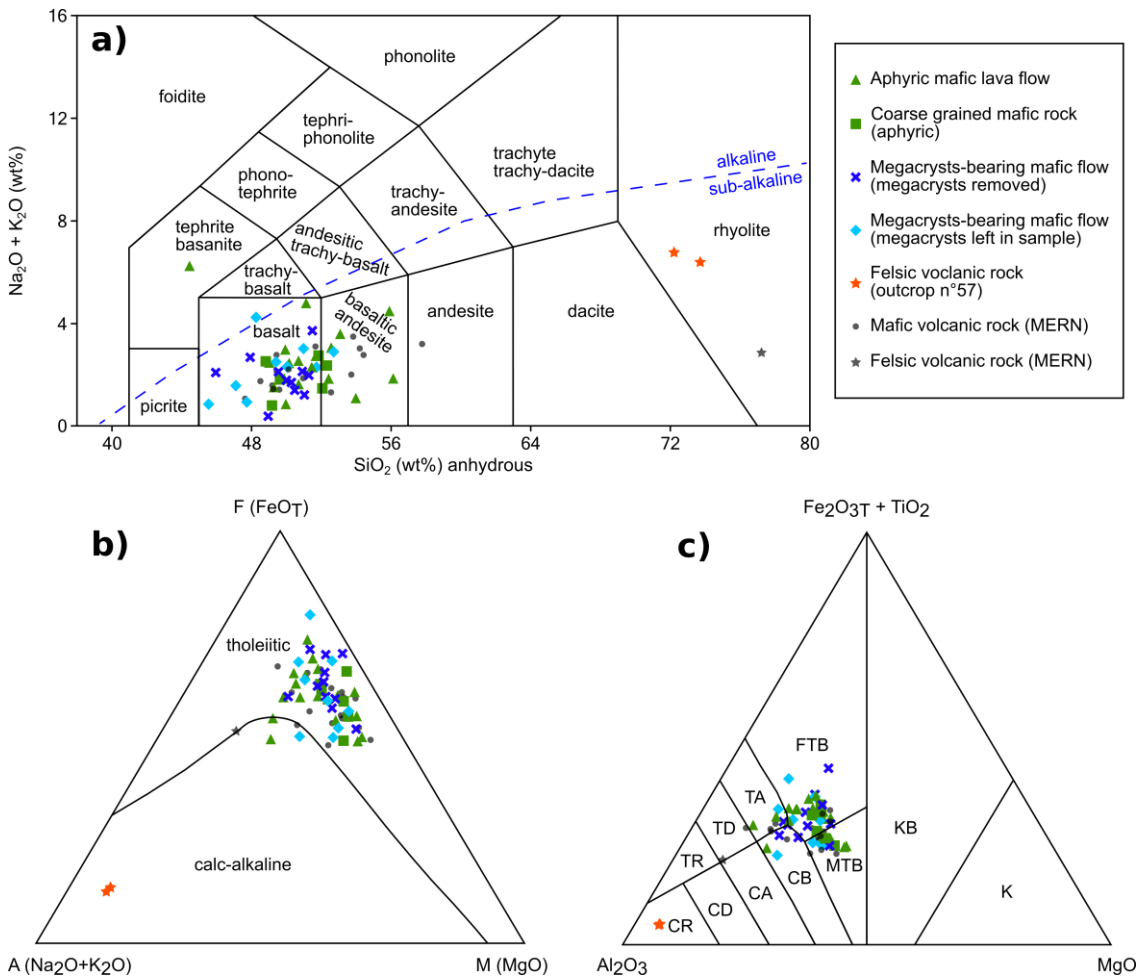


**Figure 5:** Major elements diagrams displaying the rocks analysed as part of this study (in color) and analyses compiled from the SIGEOM geodatabase (in grey); (a) total alkali vs silica (TAS) diagram (Le Bas et al. 1986); (b) Alkali-iron-magnesium (AFM) diagram (Irvine and Baragar 1971); and (c) Modified AFM diagram or Jensen cation plot (Jensen 1976). Letters C and T in the acronyms of the Jensen cation plot stand for calc-alkaline and tholeiitic, respectively. Letters F and M stand for Fe-rich and Mg-rich, respectively. Letters R, D, A, and B stand for rhyolite, dacite, andesite and basalt, respectively. Letter K stand for komatiite (when alone) or komatiitic. Note that aphyric and megacrysts-bearing mafic flows have similar major elements contents.

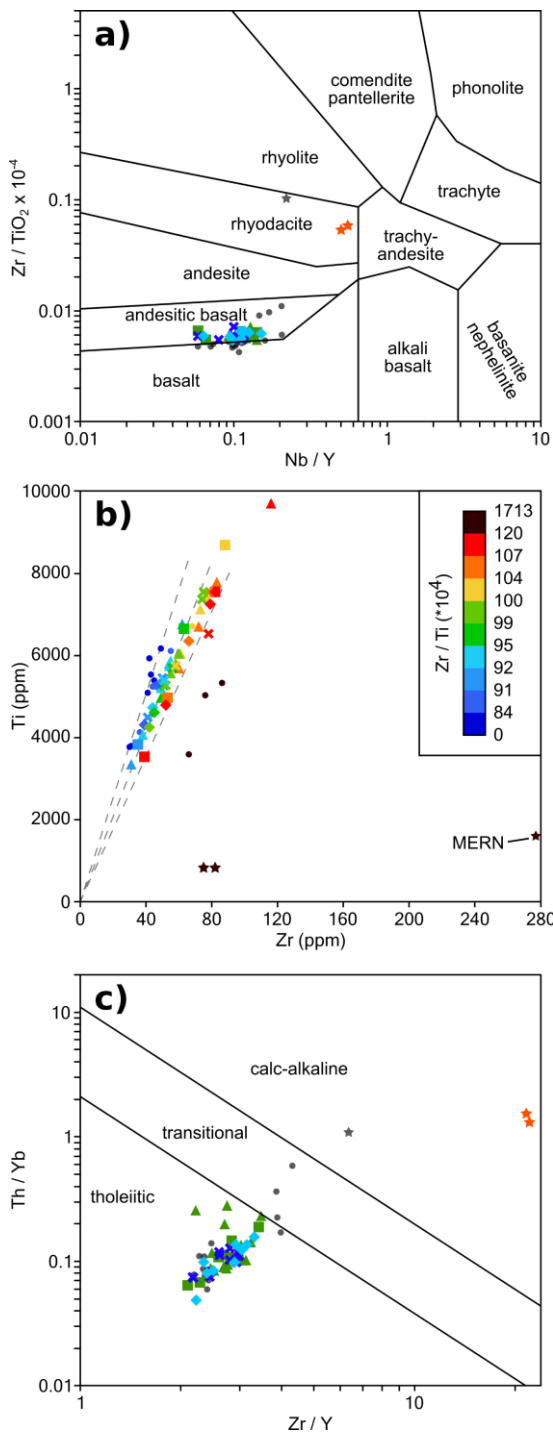


**Figure 6:** Rocks displayed on (a) Zr/TiO<sub>2</sub> vs Nb/Y diagram (Winchester and Floyd (1977). Except for three samples, including andesite sample n°981, mafic units have homogeneous Zr/TiO<sub>2</sub> ratio. (b) Ti vs Zr diagram, with a color code that enhances the Zr/Ti ratio. The dashed lines locate arbitrary values of the Zr/Ti ratio, data alignment along these lines points to hydrothermal alteration. (c) Th/Yb vs Zr/Y diagram (Ross and Bédard 2009) showing that mafic and felsic rocks have tholeiitic and calc-alkaline affinities, respectively. Most of the samples with intermediate Zr/TiO<sub>2</sub> ratios or high Nb/Y ratio have transitional affinities. Legend (a, c) as in Fig. 5.

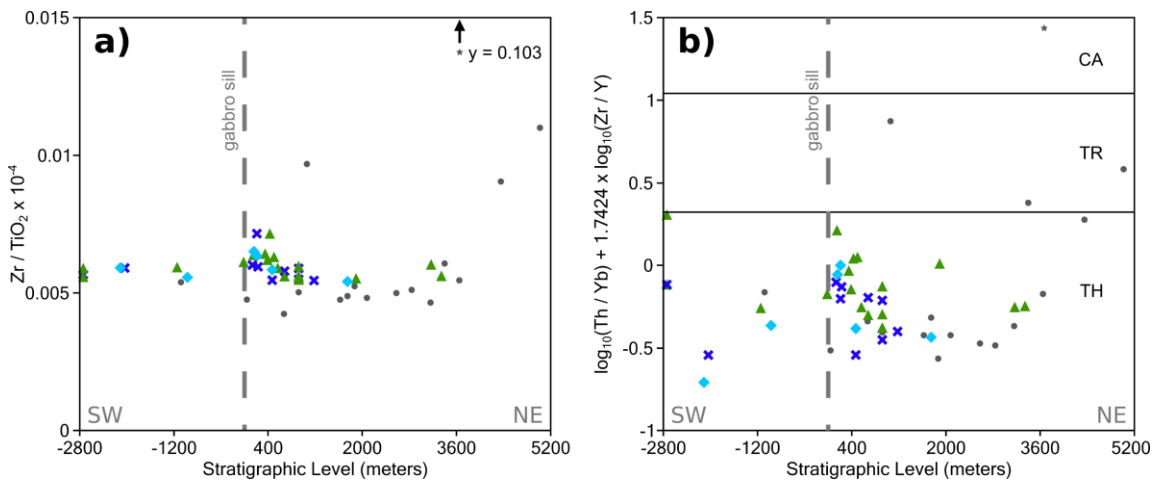


**Figure 7:** Chemical variations along the studied profile (Fig. 2) displayed using the (a)  $Zr/TiO_2$  and (b) the fields of the  $Th/Yb$  vs  $Zr/Y$  diagram (Ross and Bédard 2009). Legend as in Fig. 5.

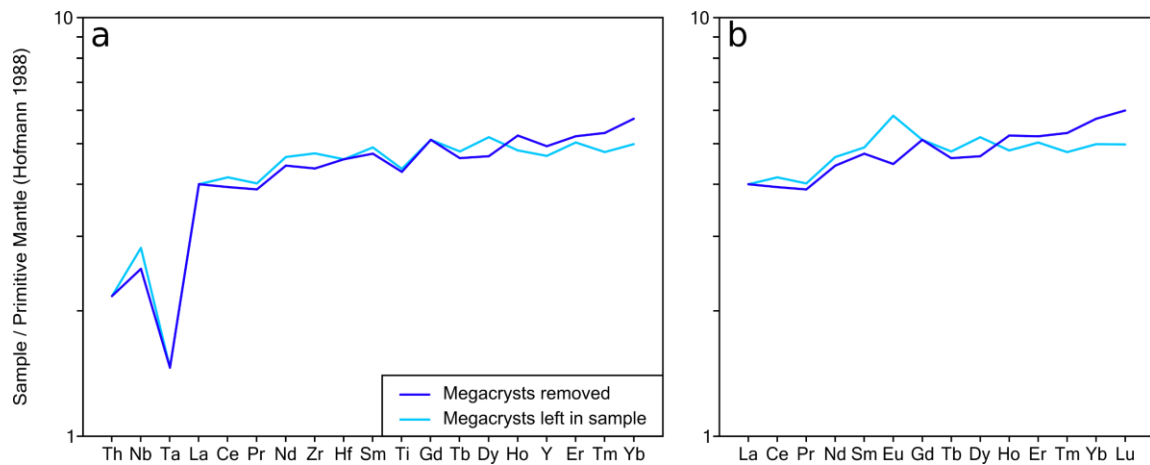


**Figure 8:** Multielement (Pearce 2008) (a) and REE (b) diagrams normalized to the primitive mantle (Hofmann 1988), used to compare the chemistry of a megacrysts-bearing mafic rock (sample n°151A1a) and its megacrysts-free matrix (sample n°151A1b). The profiles are similar, except for Eu that concentrates in feldspars and for HREE, which are probably diluted by the large amount of feldspar megacrysts (~30%) observed in sample n°151A1a.

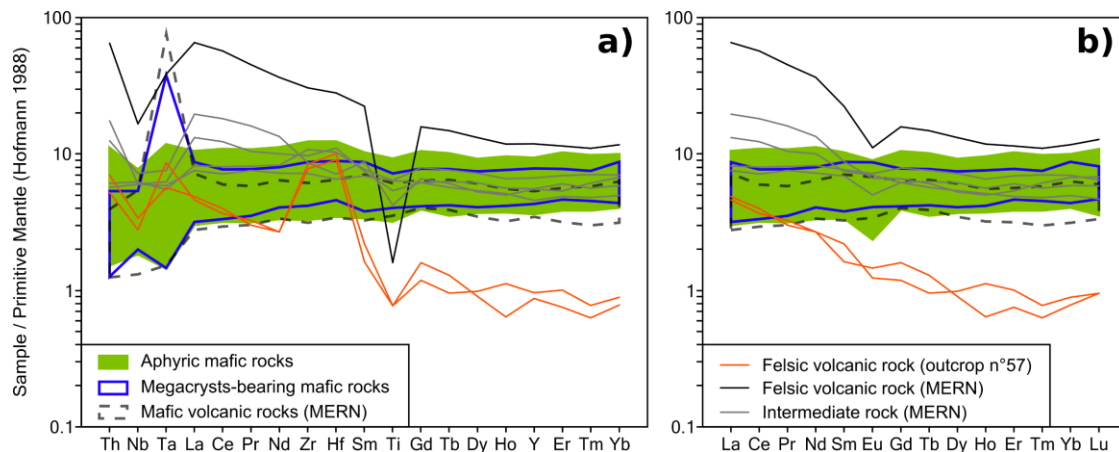


**Figure 9:** Multielement (Pearce 2008) (a) and REE (b) diagrams normalized to the primitive mantle (Hofmann 1988). Mafic rocks are characterised by flat patterns while felsic rocks have more fractionated profiles. Rocks with intermediate chemistry (samples n°F727, F362, F981 and F94A) are more enriched in incompatible elements than mafic rocks. Two megacrysts-bearing mafic flows and four mafic rocks from the MERN dataset display large positive Ta anomalies. The felsic unit of outcrop n°57 (Fig. 4b) has the lowest HREE abundance.

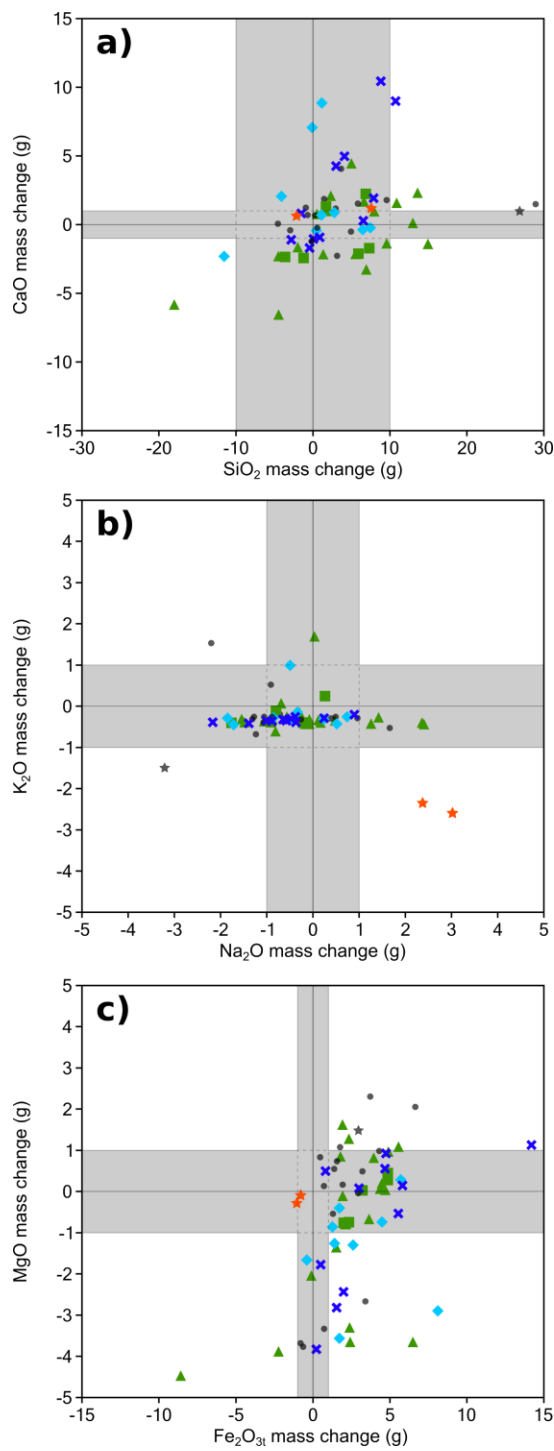


**Figure 10:** Results of mass balance calculations achieved using the method of Trépanier et al. (2016). The results are shown as absolute mass changes, in g per 100g of precursor, for (a) CaO vs SiO<sub>2</sub>; (b) K<sub>2</sub>O vs Na<sub>2</sub>O; and (c) MgO vs Fe<sub>2</sub>O<sub>3</sub>T. Grey areas and dashed lines correspond to negligible mass changes that fall within the error of the method. Legend as in Fig. 5.

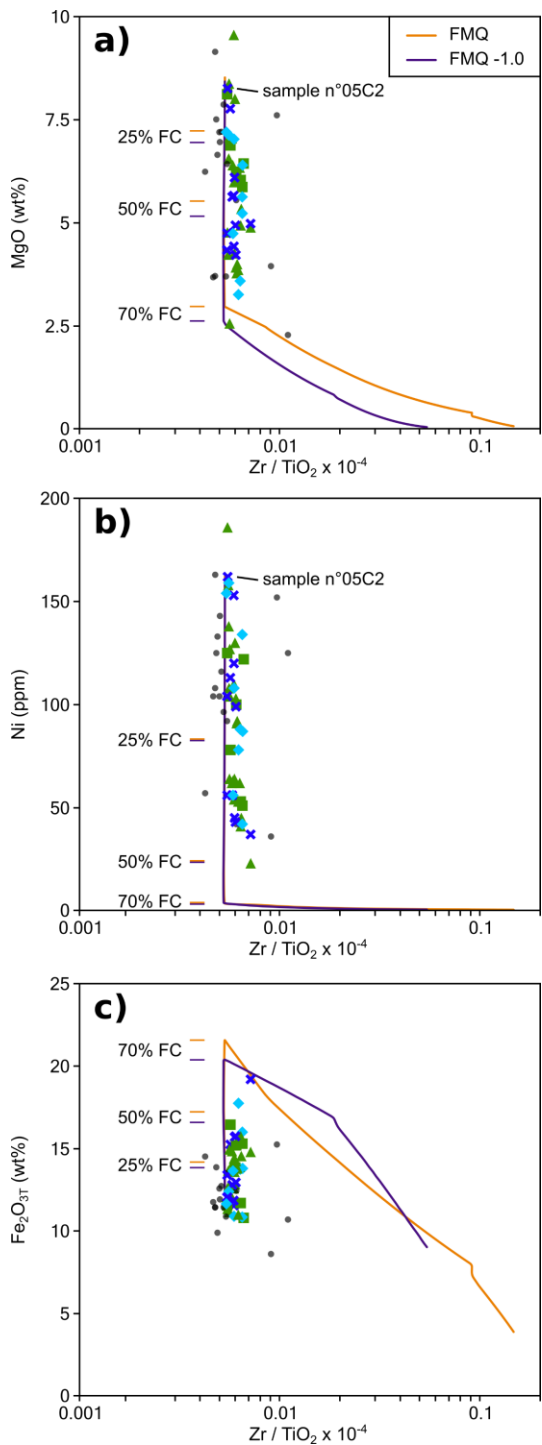


**Figure 11:** Results of magmatic differentiation modelling calculated for two  $\log fO_2$  values (FMQ and FMQ -1) using the MELTS thermodynamic model (Ghiorso and Sack 1995) implemented in the alphaMELTS 1.9 software (Smith and Asimow 2005). The binary diagrams also display the mafic and intermediate rocks of the Obatogamau Formation. Results are shown on the  $MgO$  vs  $Zr/TiO_2$  (a),  $Ni$  vs  $Zr/TiO_2$  (b), and  $Fe_{2}O_{3T}$  vs  $Zr/TiO_2$  (c) diagrams. Percentage of fractional crystallization (FC) is indicated on the left of data. Sample n°05C2 is one of the least altered and most mafic rocks and is used as the starting composition. Legend as in Fig. 5.

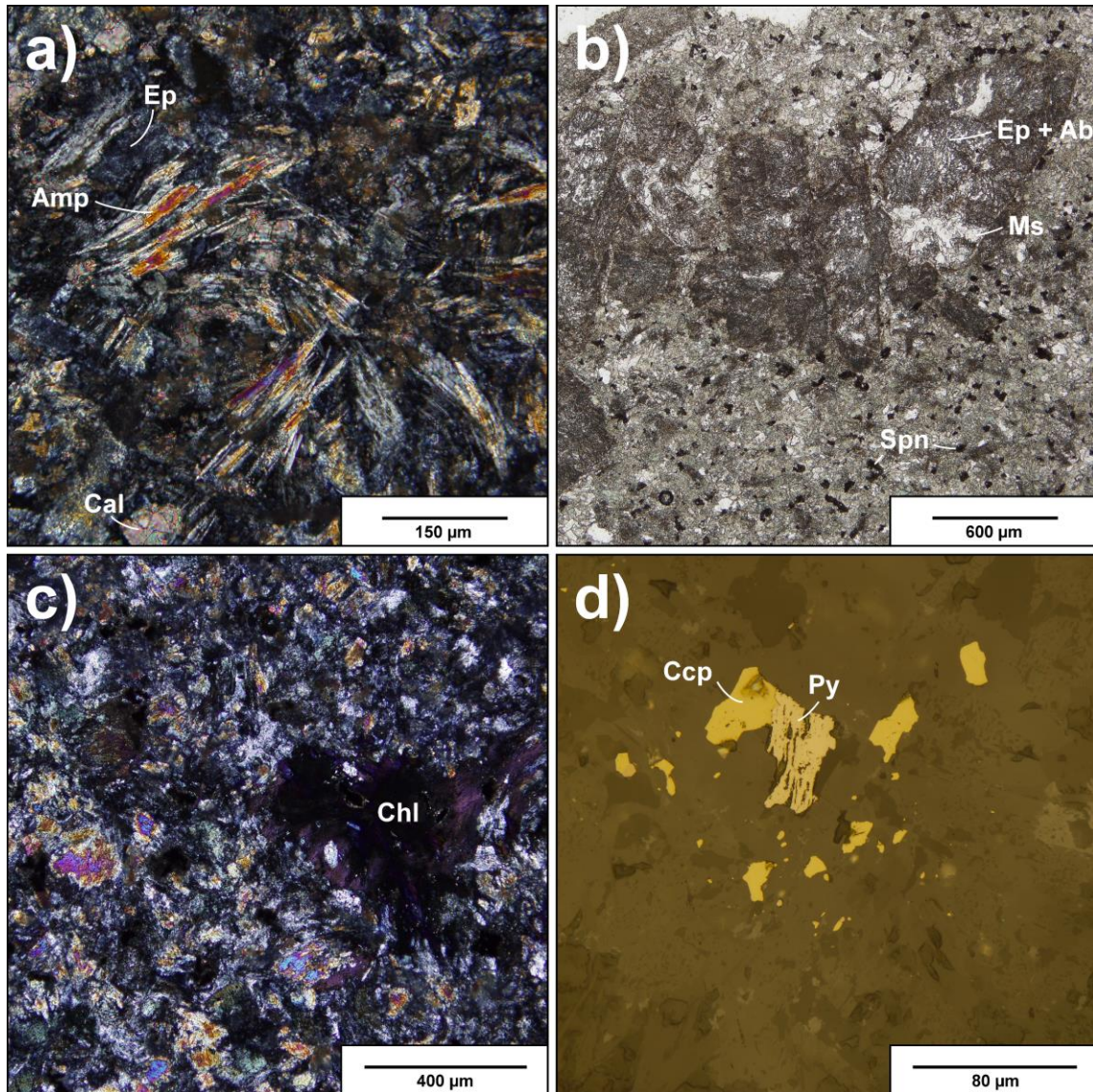


**Figure 12:** Polarized (a, c), transmitted (b) and reflected light (d) images of mafic rocks showing (a) the metamorphic assemblage of the matrix (sample 17A1); (b) feldspar phenocrysts bearing rock rich in sphene (sample 29A1); (c) chloritised matrix (sample 19A1); (d) mineralized matrix (sample 05C2). Mineral abbreviations are from Whitney and Evans (2010).

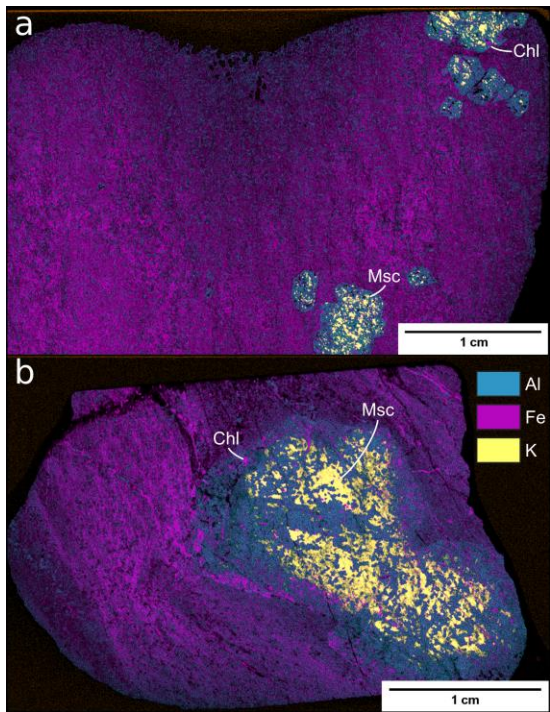


**Figure 13:** False color chemical maps (micro-XRF) of (a) sample 17A1 showing a cluster of feldspar phenocryst in a thin-grained matrix; and (b) sample 27A1 showing large euhedral megacrysts. The feldspar megacrysts are replaced by muscovite, chlorite and epidote with minor albite and calcite during hydrothermal alteration and subsequent metamorphism. Mineral abbreviations are from Whitney and Evans (2010).

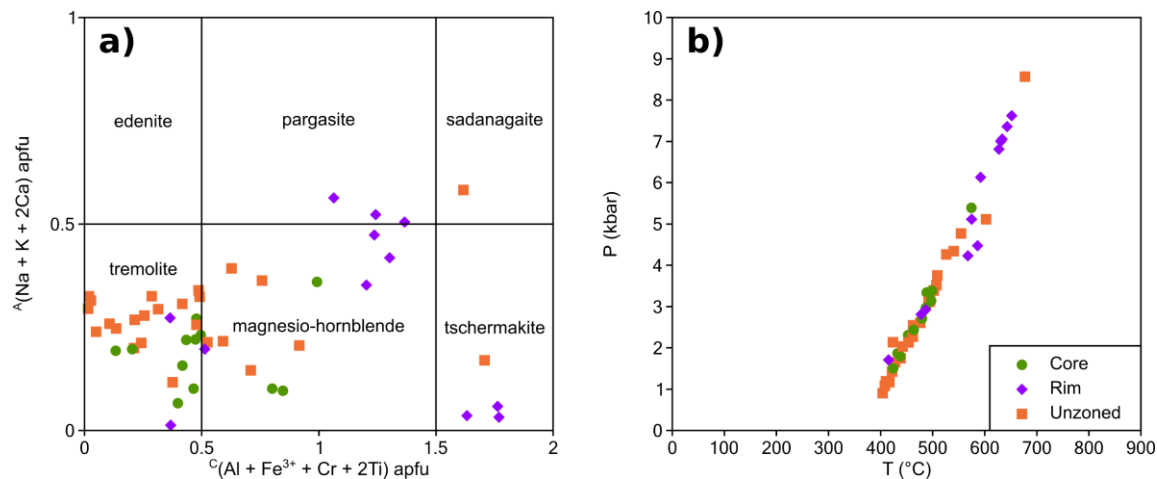


**Figure 14:** (a) Amphiboles displayed on the diagram for Ca amphiboles of Hawthorne et al. (2012); (b) Pressure vs temperature diagram showing the results of calculation achieved using amphibole chemistry and the method of Zenk and Schulz (2004).

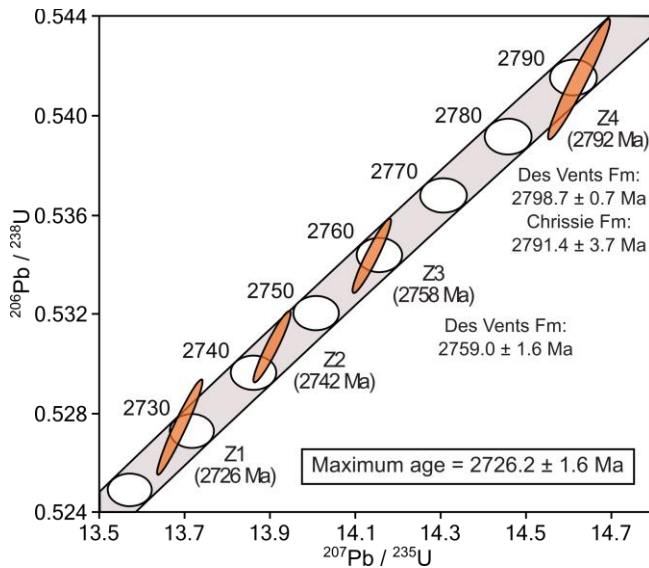


**Figure 15:** Results of ID-TIMS analyses achieved on zircon of Sample 18UCB-0057B from the felsic volcanic unit of outcrop n°57 (Fig. 4b) and displayed on the Concordia diagram. Four zircon grains (Z1, Z2, Z3 and Z4) were analysed, and the obtained values were four ages of  $2726.2 \pm 1.6$  Ma,  $2741.9 \pm 1.6$  Ma,  $2758.2 \pm 1.6$ , and  $2791.8 \pm 1.8$  Ma. The age of  $2726.2 \pm 1.6$  Ma obtained for zircon Z1 is considered as the potential crystallisation age of the unit, while older ages may correspond to inherited zircon grains (see text for detail). The age errors and error ellipses are at the 2 sigma and 95% level of confidence, respectively.

## Tables

**Table 1:** Representative analyses for the volcanic rocks of the Obatogamau Formation.

Sample	152A1 AMF <sup>a</sup>	33B1 AMF <sup>a</sup>	12B1 CGMR- a <sup>b</sup>	13B1 CGMR- a <sup>b</sup>	05C2 MBMF- r <sup>c</sup>	151A1b MBMF- r <sup>c</sup>	28D1 MBMF- r <sup>c</sup>	29A1 MBMF- r <sup>c</sup>	151A1a MBMF- l <sup>d</sup>	18A1 MBMF- l <sup>d</sup>
<b>Major element (wt%)</b>										
SiO <sub>2</sub>	50.4	55	47.3	47.5	48.9	47.3	46.8	48.2	46.6	50
Al <sub>2</sub> O <sub>3</sub>	13.5	13.2	15.15	15.45	15.65	13	15.05	12.6	15.1	15.1
CaO	10.3	9.33	8.18	8.66	10.05	16.7	8.96	10.1	15.5	10.35
Fe <sub>2</sub> O <sub>3T</sub>	13.9	11	16.45	15.2	12.05	13.4	15.25	15.75	13.65	13.75
K <sub>2</sub> O	0.1	0.07	0.01	0.04	0.02	0.03	0.07	0.08	0.04	0.1
MgO	6.34	3.86	6.88	6.24	8.26	4.75	7.77	4.94	4.74	3.59
MnO	0.24	0.24	0.27	0.22	0.18	0.3	0.23	0.4	0.29	0.31
Na <sub>2</sub> O	2.15	4.34	0.76	2.41	1.72	0.33	2.54	1.06	0.87	2.11
TiO <sub>2</sub>	0.95	1.24	1.11	1.45	0.91	0.75	0.9	1.23	0.77	1.26
P <sub>2</sub> O <sub>5</sub>	0.09	0.11	0.08	0.12	0.06	0.05	0.08	0.1	0.05	0.09
Total (anhydrous)	97.97	98.39	96.19	97.29	97.8	96.61	97.65	94.46	97.61	96.66
LOI	2.18	1.73	4.28	2.98	3.32	3.09	2.32	4.85	3	3.31
C	0.09	0.26	0.1	0.01	0.03	0.49	0.01	0.67	0.34	0.37
S	0.01	0.03	0.02	0.01	0.02	0.02	0.03	0.12	0.02	0.08
H <sub>2</sub> O <sup>+</sup>	2.92	1.53	5.38	4.26	4.29	1.98	3.55	3.9	2.6	3.19
<b>Trace element (ppm)</b>										
Ba	46.3	27.1	8.2	21.1	8.7	11.2	20.9	34.7	21.5	42.6
Rb	1.9	0.6	0.2	0.6	0.5	0.3	0.5	1.8	0.8	1.5
Sr	133	105.5	105	139	103.5	226	79.6	102	225	127
Cr	220	150	200	210	300	150	270	90	140	240
Ni	62	53	78	100	162	56	113	43	56	88
Th	0.48	0.3	0.29	0.4	0.19	0.17	0.28	0.35	0.17	0.36
Nb	2.3	2.9	2.9	4.2	2.2	1.5	1.9	2.9	1.7	3.2
Ta	0.3	0.4	0.3	0.4	0.4	<0.1	1.3	1	<0.1	0.3
Zr	60	77	63	88	50	41	51	74	45	80
Hf	1.6	2	1.8	2.5	1.4	1.2	1.3	2	1.2	2.1
Y	22.2	25.1	24.3	32.8	20.5	18.8	18.2	24.9	18	25.4
La	4.1	4.6	3.8	5.4	2.7	2.4	2.5	3.8	2.4	4
Ce	9.8	11.1	9.6	14.7	7.4	6.1	6.8	10.4	6.5	11.1
Pr	1.48	1.81	1.52	2.31	1.21	0.91	1.16	1.52	0.95	1.72
Nd	7.8	9.5	7.6	12.4	6.4	5.1	5.9	8	5.4	8.7
Sm	2.2	2.93	2.38	3.51	2.15	1.77	1.88	2.87	1.85	2.92
Eu	0.87	0.94	0.91	1.27	0.78	0.63	0.75	1.02	0.83	0.9
Gd	3.26	4.08	3.35	4.91	2.92	2.55	2.87	3.55	2.56	3.54
Tb	0.54	0.67	0.58	0.83	0.5	0.42	0.46	0.69	0.44	0.65

Dy	3.83	4.43	4.31	5.25	3.47	2.88	3.31	4.44	3.23	4.26
Ho	0.81	0.95	0.91	1.26	0.78	0.72	0.69	0.96	0.67	0.93
Er	2.34	3.12	2.82	3.69	2.38	2.1	2.25	3.07	2.05	2.94
Tm	0.36	0.42	0.4	0.51	0.34	0.33	0.35	0.43	0.3	0.4
Yb	2.41	2.94	2.68	3.55	2.53	2.3	2.2	2.95	2.02	2.65
Lu	0.36	0.44	0.4	0.5	0.34	0.37	0.34	0.47	0.31	0.43
<b>Ratio</b>										
Zr/TiO <sub>2</sub> x 10 <sup>-4</sup>	0.006	0.006	0.006	0.006	0.005	0.005	0.006	0.006	0.006	0.006
(La/Yb) <sub>N</sub>	1.15	1.06	0.96	1.03	0.72	0.70	0.77	0.87	0.80	1.02
Eu/Eu*	0.99	0.83	0.99	0.94	0.95	0.91	0.99	0.98	1.17	0.86
Ta/Ta*	1.36	2.17	1.82	1.73	3.55	-	9.89	5.52	-	1.59
Ti/Ti*	0.87	0.88	0.97	0.86	0.89	0.87	0.95	0.95	0.87	0.96
Nb/Nb*	0.59	0.89	1.00	1.03	1.11	0.85	0.82	0.91	0.96	0.96

(continued)

Sample	23A1 MBMF- 1 <sup>d</sup>	57B1 FV <sup>e</sup>	57B2 FV <sup>e</sup>	M169 MV-M <sup>f</sup>	F001 MV-M <sup>f</sup>	F981 MV-M <sup>f</sup>	F94A MV-M <sup>f</sup>	F362 MV-M <sup>f</sup>	F727 MV-M <sup>f</sup>	B600 FV-M <sup>g</sup>
<b>Major element (wt%)</b>										
SiO <sub>2</sub>	46.4	72.4	72.9	44.96	46.21	57.12	46.13	47.8	45.4	74.45
Al <sub>2</sub> O <sub>3</sub>	16.5	16.5	14.9	14.93	15.49	10.96	14.69	15.5	12.7	10.77
CaO	13.5	2.3	2.78	7.83	11.75	8.26	8.62	8.04	9.69	2
Fe <sub>2</sub> O <sub>3T</sub>	12.4	1.32	1.12	11.92	13.87	12.44	15.25	10.7	8.61	4.75
K <sub>2</sub> O	0.05	0.99	0.54	1.73	0.01	0.02	0.09	0.6	1.2	1.81
MgO	7.13	0.74	0.65	6.96	7.51	5.55	7.61	2.28	3.95	1.26
MnO	0.2	0.01	0.01	0.155	0.25	0.18	0.16	0.35	0.18	0.06
Na <sub>2</sub> O	1.5	5.81	5.8	0.25	1.02	3.14	1.57	1.83	1.74	0.96
TiO <sub>2</sub>	0.79	0.14	0.14	0.875	0.85	1.12	0.89	0.6	0.84	0.27
P <sub>2</sub> O <sub>5</sub>	0.05	0.04	0.05	0.08	0.05	0.07	0.09	0.13	0.03	0.07
Total (anhydrous)	98.52	100.25	93.89	89.69	97.01	98.86	95.1	87.83	84.34	96.4
LOI	2.59	1.08	1.39	10.54	3.67	1.4	4.2	11.6	15.8	3.39
C	0.07	0.1	0.25	-	-	-	0.05	-	-	-
S	0.03	<0.01	<0.01	0.01	0.09	0.08	1.76	0.09	0.1	0.05
H <sub>2</sub> O <sup>+</sup>	3.35	0.81	0.64	-	-	-	-	-	-	-
<b>Trace element (ppm)</b>										
Ba	13.5	170.5	89.2	252	12	19	23	168	167	350
Rb	0.8	22.1	14.7	50	<1	<1	2.6	20	35	52
Sr	174	385	331	48	218	78	120.2	210	164	40
Cr	350	30	30	209	250	50	205	141	22	<5
Ni	159	4	3	143	125	42	152	125	36	4
Th	0.2	0.57	0.42	0.17	0.17	0.45	1.3	0.8	0.36	4.92

Nb	2.1	2.1	1.7	1.9	1.8	3.6	3.4	3.5	2.8	9.6
Ta	0.2	0.2	0.3	0.12	0.13	0.2	0.2	0.21	0.14	1.26
Zr	44	82	75	44	41	68	86.2	66	76	277
Hf	1.3	2.7	2.4	1.4	1.1	1.7	2.7	1.5	2	7
Y	18.8	3.8	3.4	18.3	17.6	17.5	20	17.1	19.1	43.6
La	2.4	3	2.8	1.68	2.19	4.51	7.4	9.47	3.66	37.6
Ce	6.9	6.4	5.8	4.69	5.91	11.1	18	22.9	9.36	85.1
Pr	1.1	0.73	0.78	0.76	0.94	1.78	2.31	3.06	1.43	10.2
Nd	5.5	3.2	3.2	3.9	5.1	8.36	10.9	12.6	7.14	40.5
Sm	1.76	0.85	0.62	1.5	1.72	2.59	2.63	2.68	2.16	8.08
Eu	0.76	0.18	0.21	0.66	0.69	0.71	0.93	0.76	0.76	1.51
Gd	2.5	0.61	0.81	2.31	2.29	3.08	2.89	2.66	2.95	7.57
Tb	0.46	0.09	0.12	0.46	0.45	0.52	0.54	0.45	0.52	1.3
Dy	3.07	0.63	0.57	3.11	2.95	3.34	3.58	2.65	3.35	7.85
Ho	0.68	0.16	0.09	0.66	0.62	0.71	0.73	0.56	0.68	1.57
Er	2.14	0.42	0.31	1.96	1.88	1.98	2.3	1.76	2.1	4.45
Tm	0.31	0.05	0.04	0.3	0.3	0.3	0.33	0.31	0.33	0.66
Yb	2.03	0.37	0.32	1.99	1.96	2	2.22	2.2	2.11	4.52
Lu	0.31	0.06	0.06	0.33	0.28	0.29	0.34	0.34	0.3	0.76
<b>Ratio</b>										
Zr/TiO <sub>2</sub> x 10 <sup>-4</sup>	0.006	0.059	0.054	0.005	0.005	0.006	0.01	0.011	0.009	0.103
(La/Yb) <sup>h</sup>	0.80	5.47	5.91	0.57	0.75	1.52	2.25	2.91	1.17	5.62
Eu/Eu* <sup>i</sup>	1.11	0.76	0.91	1.08	1.06	0.77	1.03	0.87	0.92	0.59
Ta/Ta* <sup>i</sup>	1.84	0.97	1.76	1.43	1.36	0.89	0.41	0.49	0.78	0.59
Ti/Ti* <sup>i</sup>	0.93	0.48	0.49	1.16	1.05	0.98	0.79	0.55	0.82	0.08
Nb/Nb* <sup>i</sup>	1.10	0.58	0.57	1.29	1.07	0.91	0.40	0.46	0.88	0.26

**Note:** ‘<’ indicates values below detection limit.

<sup>a</sup>Aphyric mafic flow.

<sup>b</sup>Coarse grained mafic rock (aphyric).

<sup>c</sup>Megacrysts-bearing mafic flow (megacrysts removed from the sample).

<sup>d</sup>Megacrysts-bearing mafic flow (megacrysts left in sample).

<sup>e</sup>Felsic volcanic (outcrop n°57).

<sup>f</sup>Mafic volcanic (MERN).

<sup>g</sup>Felsic volcanic (MERN).

<sup>h</sup>Ratio of La and Yb concentrations (after normalization to the primitive mantle (Hofmann 1988).

<sup>i</sup>Trace element anomalies for Eu, Ta, Ti and Nb using the geometric mean of neighbour elements after normalization to the primitive mantle (Hofmann 1988).

**Table 2:** Carbonate saturation index (Kishida and Kerrich 1987).

Lithology	AMF	MV-	CGMR-	FV	MBMF-	MBMF-
Number of samples	18	4	6	2	11	9
Min value	0	0.01	0	0.01	0	0.12
Max value	0.45	0.08	0.71	0.29	0.17	0.09
Mean value	0.12	0.03	0.15		0.08	0.04
Median value	0.08	0.01	0.02		0.06	0.04

**Note:** Lithology abbreviations are the same as for table 1.

**Table 3:** Chlorite thermometry (method of Xie et al. 1997).

<b>Sample</b>	<b>151A1a</b>	<b>57A1</b>	<b>19A1</b>	<b>29A1</b>	<b>28D1</b>	<b>27A1</b>	<b>17A1</b>	<b>05C2</b>	<b>IMG</b>
Min value	252	252	266	238	274	272	248	281	292
Max value	272	257	284	244	288	296	253	311	295
Mean value	260		278.17	241.40	280.67	285	249.60	296.25	293.33
Median value	259		280.50	242	280	290	249	296.50	293

**Table 4:** Zircon U-Pb isotopic data for Obatogamau rhyolite sample 18UCB-0057B.

Fraction	U (ppm)	Pb <sub>T</sub> <sup>a</sup> (pg)	Pbc <sup>b</sup> (pg)	Th/U <sup>c</sup>	<sup>206</sup> Pb/ <sup>204</sup> Pb	<sup>206</sup> Pb/ <sup>238</sup> U	± 2σ	<sup>207</sup> Pb/ <sup>235</sup> U	± 2σ
Z1	46.75	27.33	0.28	0.36	5667.28	0.53	0.00	13.68	0.04
Z2	87.18	50.23	0.18	0.26	16587.34	0.53	0.00	13.90	0.03
Z3	85.72	50.58	0.30	0.34	9699.10	0.53	0.00	14.14	0.04
Z4	32.54	20.43	0.33	0.55	3471.40	0.54	0.00	14.62	0.06

(continued)

Fraction	<sup>207</sup> Pb/ <sup>206</sup> Pb	± 2σ	<sup>206</sup> Pb/ <sup>238</sup> U	± 2σ	Age (Ma)				
					<sup>207</sup> Pb/ <sup>235</sup> U	± 2σ	<sup>207</sup> Pb/ <sup>206</sup> Pb	± 2σ	Disc (%) <sup>d</sup>
Z1	0.19	0.00	2730.67	6.55	2728.11	3.10	2726.21	1.6	-0.2
Z2	0.19	0.00	2744.34	4.86	2742.96	2.38	2741.94	1.5	-0.1
Z3	0.19	0.00	2759.77	5.24	2758.85	2.53	2758.18	1.6	-0.1
Z4	0.20	0.00	2789.78	8.34	2790.94	3.81	2791.78	1.9	0.1

**Note:** Pb/U atomic ratios are corrected for spike, fractionation, blank, and, where necessary, initial common Pb;  $^{206}\text{Pb}/^{204}\text{Pb}$  is corrected for spike and fractionation.

<sup>a</sup>Total amount (in picograms) of Pb.

<sup>b</sup>Total measured common Pb (in picograms) assuming the isotopic composition of laboratory blank:  $^{206}/^{204}$  - 18.221;  $^{207}/^{204}$  - 15.612;  $^{208}/^{204}$  - 39.360 (errors of 2%).

<sup>c</sup>Model value calculated from radiogenic  $^{208}\text{Pb}/^{206}\text{Pb}$  ratio and  $^{207}\text{Pb}/^{206}\text{Pb}$  age, assuming concordance.

<sup>d</sup>Per cent discordance for the given  $^{207}\text{Pb}/^{206}\text{Pb}$  age.

## CONCLUSION GÉNÉRALE

Le présent mémoire de maîtrise porte sur l'étude de la Formation d'Obatogamau dans la région de Chibougamau. La Formation d'Obatogamau a été principalement étudiée le long d'un profil orienté SO-NE situé à l'ouest du Synclinal de Muscocho. Ce secteur a été choisi en raison des facilités d'accès routier et de l'exposition relativement complète de la séquence volcanique depuis sa base jusqu'à son sommet stratigraphique. Une partie des données de type roche totale utilisées provient de la base de données SIGÉOM du Ministère de l'Énergie et des Ressources Naturelles du Québec (MERN). Les objectifs du projet étaient de 1) documenter l'hétérogénéité chimique et pétrologique des laves de la Formation d'Obatogamau et leur variation spatiale dans le secteur d'études ; 2) caractériser la source mantellique des laves ; 3) documenter les conditions de formation des mégacristaux présents dans les coulées et tenter de déterminer un lien potentiel avec les complexes lités associés spatialement à la Formation d'Obatogamau ; 4) tenter de dater la mise en place de la Formation ; et 5) évaluer, dans la mesure du possible et pour le secteur d'étude sélectionné, le potentiel économique de la Formation d'Obatogamau pour les minéralisations de types SMV et or orogénique.

Le premier objectif est traité dans les sous-parties *Whole rock chemistry* et *Magmatic differentiation modelling* de la partie *Results* ainsi que dans les parties *Fieldwork and Sampling* et *Interpretation and Discussion* de l'étude. Il a été rempli par l'analyse de la chimie des éléments majeurs et traces des laves, par la modélisation de

leur niveau de différenciation et par un essai de quantification du contenu de la quantité de mégacristaux de plagioclases dans la séquence.

Le second objectif (traité dans la sous-partie *Whole rock chemistry* de la partie *Results* et dans la partie *Interpretation and Discussion* de l'étude) a été rempli par l'analyse des contenus en éléments traces des échantillons collectés.

Le troisième objectif est appréhendé dans les sous-parties *Whole rock chemistry* et *Petrography and Thermobarometry* de la partie *Results* et dans la partie *Interpretation and Discussion* de l'étude. L'importante recristallisation des mégacristaux de plagioclase a fortement limité l'étude de leurs conditions de formation. Il n'a pu être rempli complètement.

Le quatrième objectif (traité dans la sous-partie *U-Pb geochronology* de la partie *Results* ainsi que dans les parties *Fieldwork and Sampling* et *Interpretation and Discussion* de l'étude) a été potentiellement rempli avec la datation d'une unité felsique située au cœur de la séquence de laves mafiques a pu être datée et a donné un âge de  $2726,2 \pm 1,6$  Ma.

Enfin, le cinquième objectif a été traité dans les sous-partie *Petrography and Thermobarometry* et *Petrography and Thermobarometry* de la partie *Results* ainsi que dans les parties *Fieldwork and Sampling* et *Interpretation and Discussion* de l'étude. L'approche utilisée correspond à l'observation et la quantification de l'altération

hydrothermale ainsi que par l'évaluation du faciès métamorphique de la zone d'étude principale.

Les principaux résultats obtenus pour cette étude correspondent majoritairement aux réponses apportées aux objectifs du projet. Ils sont détaillés ci-après :

- L'étude a montré une mise en place rapide la Formation d'Obatogamau dans le secteur d'étude. Ceci est indiqué par la grande homogénéité chimique de l'empilement de coulées de lave (à l'exception des roches situées au sommet de l'empilement), ce qui indique un dynamisme éruptif vigoureux, sans temps de pause important. Cela aurait limité les possibilités de différenciation du magma accumulé dans la croûte supérieure par des processus de cristallisation fractionnée prolongés et expliquerait la rareté des niveaux intermédiaires et felsiques à distance du sommet stratigraphique de la séquence. Les modélisations des processus de différenciation magmatique qui ont été effectuées avec l'algorithme MELTS corroborent les hypothèses énumérées ci-dessus en montrant que la plupart des roches échantillonnées n'ont pas subi de différenciation magmatique importante ; en effet, le point de saturation en oxydes de Fe-Ti (tardif dans le cas de la différenciation des magmas tholéïitiques) n'a pas été atteint. De même, l'apparente évolution de la quantité de mégacristaux dans les coulées (qui augmente, plafonne, puis s'essouffle depuis la base vers le sommet stratigraphique de l'empilement de coulées de lave) semble indiquer un système volcanique volcanique très dynamique qui s'éteint progressivement. On notera que la section étudiée présente une épaisseur nettement plus importante dans la zone d'étude que les 3-4 km habituellement considérés pour la

Formation d'Obatogamau, ce qui pourrait indiquer des répétitions structurales liées à des failles, et introduire un biais (en combinaison avec la faible densité d'affleurements) dans l'observation de la distribution de ces mégacristaux ainsi que l'évolution de cette distribution. Aucune répétition structurale n'a cependant pu être mise en évidence lors de l'étude de terrain, et cette épaisseur importante pourrait alternativement indiquer la proximité d'un centre d'émission actif.

- La composition en éléments traces de la majorité des laves mafiques indique une source mantellique plus faiblement appauvrie en éléments incompatibles que les N-MORB, ce qui indique un manteau plus enrichi que le manteau actuel. La source des coulées de lave étudiées est probablement le manteau. La composition en éléments traces des laves felsiques et intermédiaires indique qu'elles proviennent d'une source différente, probablement non mantellique et qui pourrait correspondre à la croûte mafique affectée par un processus d'anatexie. En effet, l'accumulation de magma mafique dans la croûte aurait pu faire augmenter la température localement et ainsi entraîner la fusion partielle de cette croûte.

- Les mégacristaux de plagioclase ont recristallisé en raison de l'altération et du métamorphisme que les roches ont subie sur le fond marin et du métamorphisme régional qui a suivi. Les anomalies en Ta mesurées dans une partie des coulées de lave contenant des mégacristaux de feldspaths et riches en grains de sphène (interprété comme étant des xénocristaux ou des antécristaux d'oxydes de Fe-Ti recristallisés en sphène pendant le métamorphisme) donne toutefois des indications sur le système magmatique.

En effet, ceci pourrait indiquer que les chambres magmatiques d'où proviennent les mégacristaux de plagioclase ont cristallisé des oxydes de Fe-Ti et des plagioclase qui pourraient s'être accumulés avant d'être remobilisés par les éruptions successives de laves basaltiques. Ces cumulats se notamment communs dans les suites intrusives anorthositiques comme la Suite Intrusive du Lac Doré (Daigneault et Allard 1990, Polat 2018a, 2018b).

- Un âge U-Pb sur zircon de  $2726,2 \pm 1,6$  Ma a pu être obtenu sur une unité felsique située à un niveau stratigraphique intermédiaire de la séquence de coulées de lave. Cet âge est similaire à celui de la Formation de Waconichi, sus-jacente, datée à environ 2726-2730 Ma (David et al. 2012, Mortensen 1993, Leclerc et al. 2011). Ceci semble indiquer une mise en place rapide de la partie supérieure de la Formation d'Obatogamau et corrobore les hypothèses énumérées ci-dessus. Il reste toutefois un doute quant à la nature extrusive ou intrusive de l'unité datée, et si l'hypothèse d'un faciès volcanique est privilégiée, l'hypothèse d'un filon-couche lié à la Formation de Waconichi ne peut être exclue définitivement.

- D'un point de vue économique, la mise en place rapide de l'ensemble de la séquence de coulées de lave dans le secteur d'étude, et l'intensité relativement faible de l'altération hydrothermale observée sur le terrain, indique un environnement probablement non favorable au développement des minéralisations de type SMV dans la zone d'étude. Les données obtenues sur le métamorphisme régional par thermobarométrie sur amphibole, ainsi que l'observation d'altération potentiellement associée

aux systèmes aurifères orogéniques, telle qu'une carbonatation locale des laves, semblent indiquer un contexte favorable pour la formation de minéralisations de type or orogénique dans le secteur d'étude. Cependant la présence de conduits structuraux adéquats est également nécessaire pour la formation de tels gisements. En effet, ces réseaux de failles, non observés sur le terrain, sont indispensables à la circulation, la canalisation et enfin la concentration de ces fluides permettant la formation des gisements d'or.

Cette maîtrise apporte des éléments de réponse quant à la mise en place de la Formation d'Obatogamau, notamment sur le dynamisme éruptif important et sa durée probablement assez courte. Elle apporte potentiellement un âge direct pour cette formation à l'étendue très importante dans la Sous-province de l'Abitibi. La maîtrise vient conforter, de façon légère, le possible lien entre les laves à mégacristaux de plagioclase et les intrusions contenant des cumulats de plagioclase et d'oxydes de fer-titane comme les suites intrusives anorthositiques, déjà proposé dans la littérature. Enfin elle apporte quelques éléments quant au potentiel prospectif de la Formation d'Obatogamau pour les minéralisations économiques dans le secteur d'étude principal.

De nombreux points restent cependant sujet à amélioration, tel que l'âge présenté qui doit nécessairement être confronté à un autre âge obtenu sur un échantillon pour lequel la nature volcanique ne fait aucun doute (par exemple une datation U-Pb sur baddeleyite à partir d'un échantillon de lave mafique). Afin de lever des incertitudes quant à l'épaisseur réelle de la formation et la distribution des mégacristaux de

plagioclase il pourrait également être nécessaire d'identifier clairement la position des limites géographiques entre la Formation de Chrissie et la Formation d'Obatogamau ainsi que d'éventuelles répétitions structurales dans l'empilement. De plus, seule une petite partie de la Formation d'Obatogamau a été étudiée dans le détail dans le cadre de ce projet. Des études similaires devraient être menées dans d'autres secteurs afin de confirmer l'homogénéité chimique de la Formation d'Obatogamau, de préciser l'architecture volcanique et l'évolution du système magmatique associé et d'obtenir plus de données quant au potentiel économique de la formation.

## RÉFÉRENCES

- Allard, G.O. 1976. The Lac Doré Complex and its importance to Chibougamau Geology and Metallogeny. Ministère de l'Énergie et des Ressources Naturelles du Québec; DPV 368.
- Allard, G.O., et Gobeil, A. 1984. General geology of the Chibougamau region. *Dans Chibougamau, stratigraphy and mineralization*. Édité par J. Guha et E.H. Chown. pp. 5–19.
- Ashwal, L.D. 2010. The temporality of anorthosites. *The Canadian Mineralogist*, **48**(4): 711-728. doi: 10.3749/canmin.48.4.711.
- Ashwal, L.D., et Bybee, G.M. 2017. Crustal evolution and the temporality of anorthosites. *Earth-Science Reviews*, **173**: 307-330. Elsevier B.V. doi: 10.1016/j.earscirev.2017.09.002.
- Bédard, J.H. 2006. A catalytic delamination-driven model for coupled genesis of Archaean crust and sub-continental lithospheric mantle. *Geochimica et Cosmochimica Acta*, **70**(5): 1188-1214. doi: 10.1016/j.gca.2005.11.008.
- Bédard, J.H., Leclerc, F., Harris, L.B., et Goulet, N. 2009. Intra-sill magmatic evolution in the Cummings Complex, Abitibi greenstone belt: Tholeiitic to calc-alkaline magmatism recorded in an Archaean subvolcanic conduit system. *Lithos*, **111**: 47–71. Elsevier B.V. doi:10.1016/j.lithos.2009.03.013.
- Bédard, J.H., Harris, L.B., et Thurston, P.C. 2013. The hunting of the snArc. *Precambrian Research*, **229**: 20-48. doi: 10.1016/j.precamres.2012.04.001.

- Card, K.D. 1990. A review of the Superior Province of the Canadian Shield, a product of Archean accretion. *Precambrian Research*, **48**: 99–156. doi:10.1016/0301-9268(90)90059-Y.
- Cattell, A.C., et Taylor, R.N. 1990. Archaean basic magmas. *Dans Early Precambrian Basic Magmatism. Édité par R.P. Hall et D.J. Hughes*. Springer Netherlands, Dordrecht. pp. 11–39. doi:10.1007/978-94-009-0399-9\_2.
- Charbonneau, J.M., Picard, C., et Dupuis-Hébert, L. 1991. Synthèse géologique de la région de Chapais-Branssat (Abitibi). Ministère de l’Énergie et des Ressources Naturelles du Québec; MM 88-01.
- Cimon, J. 1977. Quart Sud-Est du Canton de Queylus. Ministère de l’Énergie et des Ressources Naturelles du Québec; DPV 448.
- Condie, K.C. 1989. Geochemical changes in basalts and andesites across the Archean-Proterozoic boundary: Identification and significance. *Lithos*, **23**(1-2): 1-18. Elsevier B.V. doi: 10.1016/0024-4937(89)90020-0.
- Condie, K.C. 2005. High field strength element ratios in Archean basalts: A window to evolving sources of mantle plumes? *Lithos*, **79**: 491–504. Elsevier B.V. doi:10.1016/j.lithos.2004.09.014.
- Daigneault, R., et Allard, G.O. 1990. Le Complexe du lac Doré et son environnement géologique (région de Chibougamau – Sous-province de l’Abitibi). Ministère de l’Énergie et des Ressources Naturelles du Québec; MM 89-03.
- Daigneault, R., Mueller, W.U., et Chown, E.H. 2002. Oblique Archean subduction: Accretion and exhumation of an oceanic arc during dextral transpression, Southern

- Volcanic Zone, Abitibi Subprovince Canada. Precambrian Research, **115**: 261–290.  
doi:10.1016/S0301-9268(02)00012-8.
- David, J., Mcnicoll, V.J., Simard, M., Bandyayera, D., Hammouche, H., Goutier, J., Pilote, P., Rhéaume, P., Leclerc, F., et Dion, C. 2011. Datations U-Pb effectuées dans les provinces du Supérieur et de Churchill en 2009-2010. Ministère de l'Énergie et des Ressources Naturelles du Québec; RP 2011-02.
- David, J., Simard, M., Bandyayera, D., Goutier, J., Hammouche, H., Pilote, P., Leclerc, F., et Dion, C. 2012. Datations U-Pb effectuées dans les provinces du Supérieur et de Churchill en 2010-2011. Ministère de l'Énergie et des Ressources Naturelles du Québec; RP 2012-01.
- Davis, D.W., Simard, M., Hammouche, H., Bandyayera, D., Goutier, J., Pilote, P., Leclerc, F., et DION, C. 2014. Datations U-Pb effectuées dans les provinces du Supérieur et de Churchill en 2011-2012. Ministère de l'Énergie et des Ressources Naturelles du Québec; RP 2014-05.
- Dimroth, E., Imreh, L., Rocheleau, M., et Goulet, N. 1982. Evolution of the south-central part of the Archean Abitibi Belt, Quebec. Part I: Stratigraphy and paleogeographic model. Canadian Journal of Earth Sciences, **19**: 1729–1758.  
doi:10.1139/e82-154.
- Dion, C., and Simard, M. 1999. Compilation et synthèse géologique et métallogénique du Segment de Caopatina, région de Chibougamau. Ministère de l'Énergie et des Ressources Naturelles du Québec; MB 99-33.

- Hamilton, W.B. 1998. Archean magmatism and deformation were not products of plate tectonics. *Precambrian Research*, **91**(1-2): 143-179. doi: 10.1016/S0301-9268(98)00042-4.
- Hamilton, W.B. 2007. Earth's first two billion years – The era of internally mobile crust. *Dans 4-D Framework of Continental Crust. Édité par R.D. Hatcher, J.H. Carlson, J.H. McBride, et J.R. Martínez Catalán. Geological Society of America Memoir*. pp. 233–296. doi:10.1130/2007.1200(13).
- Herzberg, C., Condie, K., et Korenaga, J. 2010. Thermal history of the Earth and its petrological expression. *Earth and Planetary Science Letters*, **292**: 79–88. Elsevier B.V. doi:10.1016/j.epsl.2010.01.022.
- Laurent, O., Martin, H., Moyen, J.F., et Doucelance, R. 2014. The diversity and evolution of late-Archean granitoids: Evidence for the onset of “modern-style” plate tectonics between 3.0 and 2.5Ga. *Lithos*, **205**: 208–235. Elsevier B.V. doi:10.1016/j.lithos.2014.06.012.
- Leclerc, F., Bédard, J.H., Harris, L.B., Goulet, N., Houle, P., et Roy, P. 2008. Nouvelles subdivisions de la Formation de Gilman, Groupe de Roy, région de Chibougamau, sous-province de l'Abitibi, Québec: résultats préliminaires. *Recherches en cours, Commission géologique du Canada*, **7**: p. 20.
- Leclerc, F., Bédard, J.H., Harris, L.B., McNicoll, V.J., Goulet, N., Roy, P., et Houle, P. 2011. Tholeiitic to calc-alkaline cyclic volcanism in the Roy Group, Chibougamau area, Abitibi Greenstone Belt — revised stratigraphy and implications for VHMS exploration. *Canadian Journal of Earth Sciences*, **48**: 661–694. doi:10.1139/E10-

- 088.
- Leclerc, F., Roy, P., Houle, P., Pilote, P., Bédard, J.H., Harris, L.B., Mcnicoll, V.J., Breemen, O. Van, et David, J. 2017. Géologie de la région de Chibougamau. Ministère de l'Énergie et des Ressources Naturelles du Québec; RG 2015-03.
- Ludden, J., Francis, D., et Allard, G.O. 1984. The geochemistry and evolution of the volcanic rocks of the Chibougamau region of the Abitibi metavolcanic belt. *Dans Chibougamau, stratigraphy and mineraliaztion. Édité par J. Guha et E.H. Chown.* pp. 20–34.
- Midra, R. 1989. Géochimie des Laves de la Formation d'Obatogamau (bande sud de la ceinture archéenne Chibougamau-Matagami) Québec, Canada. Université du Québec à Chicoutimi. Disponible depuis <https://constellation.uqac.ca/1616/>.
- Mortensen, J.K. 1993. U–Pb geochronology of the eastern Abitibi Subprovince. Part 1: Chibougamau–Matagami–Joutel region. Canadian Journal of Earth Sciences, **30**: 11–28. doi:10.1139/e93-002.
- Moyen, J.-F., et Laurent, O. 2018. Archaean tectonic systems: A view from igneous rocks. Lithos, **302–303**: 99–125. Elsevier B.V. doi:10.1016/j.lithos.2017.11.038.
- Moyen, J.F., Martin, H., Jayananda, M., et Auvray, B. 2003. Late Archaean granites: A typology based on the Dharwar Craton (India). Precambrian Research, **127**: 103–123. doi:10.1016/S0301-9268(03)00183-9.
- Mueller, W., Chown, E.H., Sharma, K.N.M., Tait, L., et Rocheleau, M. 1989. Paleogeographic and Paleotectonic Evolution of a Basement-Controlled Archean Supracrustal Sequence, Chibougamau-Caopatina, Quebec. The Journal of Geology,

- 97: 399–420. doi:10.1086/629319.
- Namur, O., Charlier, B., Pirard, C., Hermann, J., Liégeois, J.P., et Vander Auwera, J. 2011. Anorthosite formation by plagioclase flotation in ferrobasalt and implications for the lunar crust. *Geochimica et Cosmochimica Acta*, **75**(17): 4998-5018. doi: 10.1016/j.gca.2011.06.013.
- Phinney, W.C., et Morrison, D.A. 1990. Partition coefficients for calcic plagioclase: Implications for Archean anorthosites. *Geochimica et Cosmochimica Acta*, **54**(6): 1639-1654. doi: 10.1016/0016-7037(90)90397-4.
- Phinney, W.C., Morrison, D.A., et Maczuga, D.E. 1988. Anorthosites and related megacrystic units in the evolution of Archean crust. *Journal of Petrology*, **29**(6): 1283-1323. doi: 10.1093/petrology/29.6.1283.
- Picard, C., et Piboule, M. 1986. Pétrologie des roches volcaniques du sillon de roches vertes archéennes de Matagami – Chibougamau à l’ouest de Chapais (Abitibi est, Québec). 1. Le groupe basal de Roy. *Canadian Journal of Earth Sciences*, **23**: 561–578. doi:10.1139/e86-056.
- Polat, A., et Kerrich, R. 2001. Geodynamic processes, continental growth, and mantle evolution recorded in late Archean greenstone belts of the southern Superior Province, Canada. *Precambrian Research*, **112**(1-2): 5-25. doi: 10.1016/S0301-9268(01)00168-1.
- Polat, A., Herzberg, C., Münker, C., Rodgers, R., Kusky, T., Li, J., Fryer, B., et Delaney, J. 2006. Geochemical and petrological evidence for a suprasubduction zone origin of Neoarchean (ca. 2.5 Ga) peridotites, central orogenic belt, North

- China craton. Geological Society of America Bulletin, **118**(7-8): 771–784. doi: 10.1130/B25845.1.
- Polat, A., Frei, R., Longstaffe, F.J., et Woods, R. 2018a. Petrogenetic and geodynamic origin of the Neoarchean Doré Lake Complex, Abitibi subprovince, Superior Province, Canada. International Journal of Earth Sciences, **107**: 811–843. Springer Berlin Heidelberg. doi:10.1007/s00531-017-1498-1.
- Polat, A., Longstaffe, F.J., et Frei, R. 2018b. An overview of anorthosite-bearing layered intrusions in the Archaean craton of southern West Greenland and the Superior Province of Canada: implications for Archaean tectonics and the origin of megacrystic plagioclase. Geodinamica Acta, **30**(1): 84–99. doi: 10.1080/09853111.2018.1427408.
- Potvin, R. 1991. Étude volcanologique du centre volcanique felsique du Lac des Vents, région de Chibougamau. University of Quebec at Chicoutimi.
- Sage, R.P., Lightfoot, P.C., et Doherty, W. 1996. Geochemical characteristics of granitoid rocks from within the Archean Michipicoten Greenstone Belt, Wawa Subprovince, Superior Province, Canada: implications for source regions and tectonic evolution. Precambrian Research, **76**: 155–190. doi:10.1016/0301-9268(95)00021-6.
- Scott, C.R., Mueller, W.U., et Pilote, P. 2002. Physical volcanology, stratigraphy, and lithogeochemistry of an Archean volcanic arc: Evolution from plume-related volcanism to arc rifting of SE Abitibi Greenstone Belt, Val d'Or, Canada. Precambrian Research, **115**: 223–260. doi:10.1016/S0301-9268(02)00011-6.

- Thurston, P.C. 2002. Autochthonous development of Superior Province greenstone belts? *Precambrian Research*, **115**(1-4): 11-36. doi: 10.1016/S0301-9268(02)00004-9.
- Warren, P.H. 1990. Lunar anorthosites and the magma-ocean plagioclase-flotation hypothesis: Importance of FeO enrichment in the parent magma. *American Mineralogist*, **75**: 46-58.
- Windley, B.F. 2017. Tectonic models for the geological evolution of crust, cratons and continents in the Archaean. *Revista Brasileira de Geociencias*, **28**(2): 183-188.
- Wyman, D.A. 1999. A 2.7 Ga depleted tholeiite suite: Evidence of plume-arc interaction in the Abitibi Greenstone Belt, Canada. *Precambrian Research*, **97**: 27-42. doi:10.1016/S0301-9268(99)00018-2.

## MATÉRIEL SUPPLÉMENTAIRE

Le matériel supplémentaire pour ce mémoire comprend les données non présentées sous forme de figure ou tableau dans le texte. Il est fourni sous forme de classeurs Microsoft Excel afin de faciliter l'éventuelle manipulation des données par le lecteur. Le contenu de ces classeurs est rédigé et formaté en anglais.

Le matériel supplémentaire est divisé en quatre fichiers nommés S1, S2, S3 et S4 tel que mentionné dans le corps de l'article présenté. Ces fichiers sont disponibles au téléchargement sur le site <https://constellation.uqac.ca/>, hébergeant les travaux présentés sous format électronique.

Les fichiers S1, S2, S3 et S4 contiennent les tables suivantes (titres traduits) :

### S1

- Table S1-1 : Chimie roche totale
- Table S1-2 : Variations le long de la stratigraphie pour les roches volcaniques échantillonnées

### S2

- Table S2-1 : Estimations de l'altération hydrothermale
- Table S2-2 : Modélisation de la différenciation magmatique (FMQ)
- Table S2-3 : Modélisation de la différenciation magmatique (FMQ -1)

**S3**

- Figure S3-1 : Cartes élémentaires brutes ( $\mu$ XRF) de lames minces de coulées mafiques à mégacristaux
- Figure S3-2 : Photographies de la population et des grains de zircon de l'échantillon 18UCB-0057B sélectionnés pour géochronologie U-Pb

**S4**

- Table S4-1 : Chimie et thermobarométrie de l'amphibole
- Table S4-2 : Chimie et thermométrie de la chlorite
- Table S4-3 : Calibration MEB